UC Irvine

UC Irvine Electronic Theses and Dissertations

Title

Novel strategies to inhibit the growth of enteropathogens and pathobionts

Permalink

https://escholarship.org/uc/item/53153932

Author

Sassone-Corsi, Martina

Publication Date

2016

Peer reviewed|Thesis/dissertation

eScholarship.org Powered by the California Digital Library
University of California

UNIVERSITY OF CALIFORNIA,
IRVINE

Novel strategies to inhibit the growth of enteropathogens and pathobionts

DISSERTATION

submitted in partial satisfaction of the requirements

for the degree of

DOCTOR OF PHILOSOPHY

in Biomedical Sciences

by

Martina Sassone-Corsi

Dissertation Committee:
Professor Manuela Raffatellu, Chair
Professor Celia Goulding
Professor Ming Tan
Professor Michael Demetriou
Professor Alan Barbour

2016

Portion of Chapter 1 © 2015 Sassone-Corsi and Raffatellu

Figure 1.1 © The America Association of Immunologists, Inc. Originally published in The Journal of Immunology Sassone-Corsi M. and Raffatellu M. No Vacancy: How Beneficial Microbes Cooperate with Immunity to Provide Colonization Resistance to Pathogens. J. Immunol. 2015;194:4081-4087

Chapter 3 Figures and material and methods for chemical synthesis 2016 © Dr. Phoom Chairatana and Dr. Elizabeth M. Nolan (MIT)

All other materials © 2016 Martina Sassone-Corsi

DEDICATION

To my parents Rosaria & Emilio and to my brother Andrea,
for their infinite support.

To my husband Alborz,
for everything and more.

TABLE OF CONTENTS

	Page
LIST OF FIGURES	vi
LIST OF TABLES	x
ACKNOWLEDGMENTS	xv
CURRICULUM VITAE	xiv
ABSTRACT OF DISSERTATION	xx
CHAPTER 1: Introduction	
1.1 Introduction to the Gut Microbiota	1
1.1.1 Mirobiota Mediated Colonization Resistance to Intestinal Pathogens	2
1.2 The Enterobacteriaceae Bacterial Family in the Gut During Health and Disease	8
1.2.1 The Probiotic Strain *Escherichia coli* Nissle 1917	9
1.2.1.1 Beneficial Effects of *Escherichia coli* Nissle 1917	11
1.2.2 *Salmonella enterica* and Non-typhoidal salmonellosis (NTS)	14
1.2.2.1 Molecular Pathogenesis of NTS-induced gastroenteritis	16

1.2.2.2 *Salmonella* Inflammation-adapted Gut Life Style 18

1.3 Nutritional Immunity and the Battle for Iron Acquisition 20
1.3.1 Microbial Mechanism for Iron Acquisition 21
1.3.2 Host Mechanism for Iron Sequestration 22
1.3.3 The Battle for Iron Acquisition in the Enterobacteriaceae Family 25
1.3.3.1 Antimicrobial Peptides of *Escherichia coli* Nissle 1917:Microcins of Class IIb 26
1.4 Objectives 32
1.5 References 35

CHAPTER 2: Microcins mediate interspecies and intraspecies competition among Enterobacteriaceae in the inflamed gut
2.1 Summary 42
2.2 Introduction 44
2.3 Results 46
2.4 Discussion 80
2.5 Material and methods 84
2.6 References 102

CHAPTER 3: A novel mucosal immunization strategy to reduce *Salmonella* gastroenteritis by targeting iron acquisition
3.1 Summary 105
3.2 Introduction 107
3.3 Results 110
3.4 Discussion 140
3.5 Material and methods 142
3.6 References 164

CHAPTER 4: Discussion and Future Directions

4.1 Summary and Conclusions 165

4.1.1 The probiotic strain *Escherichia coli* Nissle 1917 (EcN) microcins inhibit the growth of related commensals and pathogens in an inflamed gut and are essential for EcN survival 169

4.1.1.1 Future directions 171

4.1.2 Boosting nutritional immunity by immunization against bacterial siderophores inhibits the growth of enteric pathogens 181

4.1.2.1 Future Directions 184

4.2 References 189

LIST OF FIGURES

Page

Figure 1.1 Caption 6

Figure 1.1 Direct mechanisms of colonization resistance against enteropathogens. 7

Figure 1.2 Fitness factors of *E.coli* Nissle 1917. 13

Figure 1.3 Mechanism of iron acquisition by *Salmonella* in the inflamed intestine. 24

Figure 1.4 Mechanism of siderophores and microcin-siderophore conjugates uptake. 28

Figure 2.1 Representation of microcin gene cluster in *E. coli* Nissle. 47

Figure 2.2 Caption 50

Figure 2.2 *E. coli* Nissle wild-type and microcin mutant (*chef*) gut colonization during competition with commensally *E. coli* in the absence of intestinal inflammation. 51

Figure 2.3 Caption 52

Figure 2.3. Microcins are dispensable in the absence of intestinal inflammation. 53

Figure 2.4 Caption 55

Figure 2.4 Microcins enhance *E. coli* Nissle growth and competition against commensally *E. coli* for a niche in the inflamed gut. 56

Figure 2.5 Caption 57

Figure 2.5 Colonization and histopathology of EcN wild-type and microcin mutant (*chef*) in competition with commensally *E. coli*, in mice with DSS-colitis. 58

Figure 2.6 Colonization of wild-type EcN and microcin mutant (*mcmA mchB*) in competition with commensal *E. coli*, in mice with DSS-colitis. 59

Figure 2.7 *In vitro* competition growth curves between wild-type EcN and microcin mutants against commensally *E. coli.* 62

Figure 2.8 *In vitro* growth curves of wild-type EcN and microcin mutants alone or in competition. 63

Figure 2.9 *E. coli* Nissle wild-type and microcins mutant gut colonization during inflammation. 64

Figure 2.10 *E. coli* Nissle wild-type and microcins mutant gut colonization when in competition and in the presence of the commensally *E.coli* during DSS-colitis. 65

Figure 2.11 *E. coli* Nissle wild-type and microcins mutants gut colonization during competition with commensally *E. coli* post iron rich diet and in the presence of intestinal in inflammation. 66

Figure 2.12 Caption 69

Figure 2.12 *In vitro* activity of EcN microcins against enteric pathogens and pathobionts 70

Figure 2.13 Microcins reduce colonization of enteric pathogens in the inflamed gut. 71

Figure 2.14 Caption 72

Figure 2.14 STm infection in competition with wild-type EcN and EcN *mchDEF*. 73

Figure 2.15 Caption 74

Figure 2.15 AIEC administration post-DSS treatment in competition with wild-type EcN and EcN *mchDEF*. 75

Figure 2.16 Therapeutic administration of wild-type EcN but not EcN *chef* colonization of enteric pathogens in the inflamed gut 77

Figure 2.17 Caption 78

Figure 2.17 *In vitro* activity of microcin M (*mcmA*) and microcin H47 (*mchB*) against Stem, commensally *E.coli* and AIEC. 79

Figure 2.18 Microcins do not broadly impact composition of the gut microbiota during inflammation 82

Figure 2.19 EcN microcins selectively target specific competitors through their iron receptor 83

Figure 3.1 Caption 112

Figure 3.1 Detection of mucosal IgA anti-siderophores. 113

Figure 3.2. Characterization of CTB-Ent. 115

Figure 3.3 Synthesis of Ent-PEG_3-biotin conjugate 13. 116

Figure 3.4 Caption 118

Figure 3.4. Detection and characterization of antibodies in response to CTB/CTB-Ent immunization. 119

Figure 3.5. Intraperitoneal immunization with CTB-Ent induces the development anti-siderophores Inga antibodies. 120

Figure 3.6 Caption 122

Figure 3.6. Immunization of mice with CTB-Ent reduces *Salmonella* gut colonization and systemic dissemination. 123

Figure 3.7 Caption 125

Figure 3.7 (Related to Figure 3.6) Immunization with CTB-Ent reduces *Salmonella* gut colonization. 126

Figure 3.8. Mice immunized with CTB-Ent show similar pathology and inflammation as CTB-immunized mice. 129

Figure 3.9 Caption 133

Figure 3.9. Analysis of the gut microbiota in mice immunized with CTB or CTB-Ent before and after infection with *Salmonella.* 134

Figure 3.10. Analytical HPLC traces of Ent-PEG_3-CO_2H. 149

Figure 3.11. Analytical HPLC traces of Ent-PEG_3-biotin. 153

Figure 4.1. *In vitro* competition assay of EcN wild-type and mutants against *S*. Typhimurium. 174

Figure 4.2. Effects of EcN mono-colonization of Germ-Free mice on the gut mucosal barrier. 179

Figure 4.3. Effects of EcN mono-colonization of Germ-Free mice on the adaptive immune system. 180

Figure 4.4. Flow cytometry analysis to detect B cells producing anti-Ent antibodies. 187

LIST OF TABLES

Page

Table 2.1 Strains used in this study (Related to Chapter 2) 93

Table 2.2 Plasmids used in this study (Related to Chapter 2) 96

Table 2.3 Primers for targeted mutagenesis (Related to Chapter 2) 97

Table 2.4 Primers for quantitative Real-Time PCR (Related to Chapter 2) 101

Table 3.1 Caption 135

Table 3.1 Analysis of the microbiota of CTB-Ent/CTB immunized mice before and after *Salmonella* infection 136

Table 3.2 Bray Curtis dissimilarities test of the microbiota of CTB-Ent/CTB-immunized mice before and after *Salmonella* infection. 139

Table 3.3 Primers for quantitative Real-Time PCR (Related to Chapter 3) 159

ACKNOWLEDGMENTS

There are no words that can precisely summarize the past 5 years of my life, and I can't realize yet that I almost made it!

I still remember making the decision to come to UCI without hesitation, even though that meant leaving my family and close friends behind, 10,000 miles away. I now begin to understand why I was not hesitant at that time. I somehow knew deep inside that this huge sacrifice would allow me to cultivate my future career while also helping me to grow as a person. For some reason, being distant from your loved ones empowers you for the best. Although it was not simple for me to be physically close to my family only once a year, it gave me the strength to work as much as I could and to make the most of this experience. People kept telling me that all the effort, months of frustrations and all the sacrifice I was accumulating, were going to be paid off in the future. Although I'm not at that stage yet, I do realize how much I've already gained if I look at myself now compared to 5 years ago. This experience helped me to not only grow as a scientist, but also to finally place the last piece of the puzzle to complete my identity. I have discovered what I really enjoy to do, and I have also been able to narrow down my future goals. This path has helped me to identify what I believe is important in my life.

At the end of this long journey, that has deeply enriched me, I finally appreciate how much other people have contributed to all of this.

I'm so grateful to Dr. Manuela Raffatellu. I would like to thank Manuela for giving me the opportunity to carry out my thesis in her lab and for her belief in my

potential as a researcher. This work could not be possible without her great vision and her way of thinking “outside the box”. I’d like to thank her for guiding me throughout this time while giving me the freedom to make mistakes and, therefore, grow independently.

I’m also grateful to all the members of the Raffatellu lab. The entire Raffatellu lab crew has always been very helpful and supportive. I benefited greatly from their active participation and suggestions during lab meeting. In particular, I’d like to thank Dr. Stefan Jellbauer and Dr. Elisa Deriu, who trained me on animal husbandry and other techniques at the beginning of this experience. Although they are not part of this lab anymore, we are still in touch and we remain very good friends. I’m also grateful to Dr. Judith Behnsen, Dr. Janet Liu, Dr. Sean-Paul Nuccio, Suzi Klaus and Evelyn Hoover for being caring and ready to lend a hand during the past 5 years. In particular, Dr. Sean-Paul Nuccio was of great help for the analysis of the microbiota composition and he should get all the credit for analyzing data in figure 2.18. I will be always glad to for the opportunity to meet great colleagues and to have made such good friends with Dr. Araceli Perez-Lopez and Dr. Vladimir-Diaz Ochoa. I think these years would have been much more difficult without their friendship and constant support. I’m very thankful to Araceli for her great scientific guidance, and for her contributions with many ideas for the immunization project. I’m also grateful for her friendship and for our long conversations outside of the lab, and of course for making this journey more fun! Also, I have learned so much from Vlad. During these years, Vlad was always there when I needed support and he really helped me to grow

as a person. I also want to thank Dr. Maria Valeri, who joined the lab only recently but we became very good friends instantly, and I hope that our friendship will continue for years to come. I'm also grateful to our past lab managers, Milad and Thao. Their help in the maintenance and organization of the lab has been very helpful. Moreover, without all of my driven undergraduate students, this work would have taken much longer. In particular, I want to thank Henry Liu, Christine Vu, Amy Takahashi, and Dulcemaria Hernandez for their great help and also for being always interested and passionate on our projects.

The beauty of this job is that you have the opportunity to meet new people and to find very good friends that sometimes remain with you for the rest of your life.

I would also like to thank the all MMG department. Everybody has been extremely helpful. And of course, I'd like to thank my committee members for their great suggestions during these years that helped me think and improve as a scientist.

I will be eternally grateful to my family. My uncle, Paolo, and my aunt, Emiliana, have been a great source of inspiration for me. They have been a great example for me to follow, and without their support, all this would have been much more difficult. My parents, Emilio and Rosaria, together with my brother, Andrea, have also made an immense sacrifice to be so far away from me. However, they have always been there for me. They have supported all of my decisions and have helped me in difficult times. I would not be where I am now if it was not for their love and positivity.

Finally, I will always be glad to have made the decision to come here, because that is how I met my loving boyfriend and now husband. Without Alborz and his love and patience during these years, I truly believe I could not be here now. He is the reason why I kept going.

CURRICULUM VITAE

Martina Sassone-Corsi

Professional Summary

- Seven years experience in molecular biology, host response to bacterial infection (in particular, *Salmonella* gastrointestinal infection), microbiology, and immunology.
- Bachelor degree in Molecular and Cellular biology from the University of Rome, Torvergata. Bachelor's thesis in molecular virology in MG. Santoro's laboratory (2008-2009, University of Rome, Torvergata).
- Master's degree in Molecular and Cellular biology, with emphasis in proteomics and genomics, from the University of Rome, Torvergata (2009-2011). Master's thesis in Dr. Manuela Raffatellu's Lab at the University of California Irvine (2010-2011).
- Current position: PhD candidate at University of California, Irvine in Dr. Manuela Raffatellu Lab.
- Skills include cell culture, viral infection, protein quantification and expression, bacterial genetics, mouse vaccination, bacterial infection, mouse models, and maintenance of mouse colonies, including germ-free colonies.

Education

Qualification	Institution	Year	CGPA/Percentage
PhD student	University of California Irvine	2012-2016	4.0
M.S. Mol. and Cell Biology (honors)	Univ. of Rome Torvergata	2012	110/110
B.S. Mol. and Cell Biology	Univ. of Rome Torvergata	2009	110/110

Research Experience

University of California Irvine, Irvine, 2012-2016
Department of Microbiology and Molecular Genetics
Graduate Researcher; Advisor: Manuela Raffatellu, MD
Research focus:
Developing new therapeutic strategies against enteric pathogens. Bacterial antimicrobial peptides and their role against enteric pathogens and commensals.

- Conducted *in vivo* vaccination studies and developed ELISA, ELISPOT and DOTBLOT assays for detection of specific antibodies.
- Bacterial genetics, including molecular cloning and vector construction.
- Conducted *in vivo* studies of bacterial gastrointestinal infection, and employed methods such as microbiota analysis by 16S rRNA qPCR and gene expression analysis by real-time qPCR.
- Tissues cell isolation and flow cytometry for single cell sorting
- Maintained mouse colonies, including germ-free and gnotobiotic mice

University of California Irvine, Irvine, 2010-2011
Department of Microbiology and Molecular Genetics
Junior specialist; Advisor: Manuela Raffatellu, MD
Research focus:
Bacterial antimicrobial peptides and their role against enteric pathogens and commensals.

- Conducted *in vivo* studies of bacterial gastrointestinal infection and employed methods such as microbiota analysis by 16S rRNA qPCR, real time qPCR.
- Bacterial genetics, including molecular cloning and vector construction.
- Cell culture

University of Rome Torvergata, Rome, 2008-2009
Department of Biology
Undergraduate Researcher; Advisor: Maria G. Santoro, PhD
Research focus:
Host stress response during Rhabdovirus infection

- Cell culture and viral infection
- Protein quantification

Teaching Experience

University of California, Irvine
2015-2016 Mentor of Johnny Davoodifard, Master's in biotechnology program
2015-2016 Mentor of Dulcemaria Hernandez, undergraduate student
2014-2015 Mentor of Amy Takahashi, undergraduate student. Recipient of: Excellence in Research Dean's award
2013-2015 Mentor of Christine Vu, undergraduate student
2012-2014 Mentor of Henry Liu, undergraduate student
2015 Teaching assistant, Biochemistry Lecture (BIO98)
2014 Teaching assistant, Microbiology Lecture (M122)
2013 Teaching assistant, Immunology Lecture (M121)
2013 Teaching assistant, Molecular Biology Laboratory (M116L)
2015 Visiting teaching assistant at the Marine Biological Laboratory, advanced summer course titled "Frontiers in host pathogens interaction", Woodshole, MA, USA

Honors and Awards

2016 Recipient of Harris Moyer Award, Department of Microbiology and Molecular Genetics, University of California Irvine

2014 American Society for Microbiology (ASM) Student Travel Award to attend the ASM General Meeting

2012 University of Rome Torvergata MS program. Graduated with honors

2008 ERASMUS scholarship recipient, for a semester of study abroad at the University Autonomy, Barcelona, Spain.

Publications

Martina Sassone-Corsi, Sean-Paul Nuccio**,** Henry Liu, Dulcemaria Hernandez, Christine Vu, Amy Takahashi, Robert A. Edwards, and Manuela Raffatellu. Microcin production enables a robotic bacterium to limit the expansion of enteric pathogens and pathobionts in the inflamed gut. *Under revision* (2016)

Martina Sassone-Corsi, Phoom Chairatana, Araceli Perez-Lopez, Robert Edwards, Elizabeth M. Nolan, and Manuela Raffatellu. A novel siderophore-

based immunization strategy to inhibit growth of enteric pathogens. *Accepted* PNAS (2016)

Martina Sassone-Corsi and Manuela Raffatellu. No Vacancy: How Beneficial Microbes Cooperate with Immunity To Provide Colonization Resistance to Pathogens. ***Journal of Immunology***. Review. (2015) May 1;194(9):4081-7. doi: 10.4049/jimmunol.140316

Martina Sassone-Corsi and Manuela Raffatellu. A hydrogen boost for *Salmonella*. ***Cell Host and Microbe***. (Preview to Maier et al. 2013 Dec 11;14(6):641-51) (2013) Dec 11;14(6):603-4. doi: 10.1016/j.chom.2013.11.011

Judith Bentsen, Elisa Derik, **Martina Sassone-Corsi,** and Manuela Raffatellu Robotics: properties, examples, and specific applications. ***Cold Spring Harbor Perspectives in Medicine***. Review. (2013) Mar 1;3(3):a010074. doi: 10.1101/cshperspect.a010074

Patents

Martina Sassone-Corsi, Phoom Chairatana, Elizabeth M. Nolan, Manuela Raffatellu, Araceli Perez-Lopez. Siderophore-based immunization against Gram-negative bacteria. WO2015168380 A1. (2015)

Conference Presentations

Martina Sassone-Corsi, Henry Liu, Robert A. Edwards and Manuela Raffatellu. Mechanisms of colonization resistance: the robotic strain *Escherichia coli* Nissle 1917 secretes antimicrobial peptides to kill related pathogens and commensals. Poster presentation at Keystone symposium “Gut Microbiota Modulation of Host Physiology: The search for mechanism). Keystone, CO. (March 2015).

Martina Sassone-Corsi, Phoom Chairatana, Araceli Perez-Lopez, Elizabeth M. Nolan, Manuela Raffatellu. Inhibition of *Salmonella* Typhimurium growth by targeting its iron uptake system. Oral presentation at the Immunology Fair, University of California, Irvine, CA. (November 2014).

Martina Sassone-Corsi, Henry Liu, and Manuela Raffatellu. The probiotic strain *Escherichia coli* Nissle 1917 inhibits the growth of related Enterobacteriaceae through secretion of antimicrobial peptides. Poster presentation at the American Society for Microbiology General Meeting, Boston, MA. (May 2014).

Martina Sassone-Corsi, Phoom Chairatana, Araceli Perez-Lopez, Elizabeth M. Nolan, Manuela Raffatellu. Inhibition of *Salmonella* Typhimurium intestinal colonization by specific anti-siderophore antibodies. Poster presentation at the

Pacific Southwest Regional Center of Excellence meeting, Huntington Beach, CA. (November 2013).

Martina Sassone-Corsi, Henry Liu, and Manuela Raffatellu. The probiotic strain *Escherichia coli* Nissle 1917 inhibits the growth of *Salmonella* Typhimurium through secretion of antimicrobial peptides. Poster presentation at the Gordon Conference on "Antimicrobial Peptides", Ventura, CA. (February 2013).

Service

- 2015-2016 Graduate student representative, Department of Microbiology and Molecular Genetics, University of California, Irvine

Other Professional Experiences

- Visitor, CNRS- Inserm in Strasbourg, France (2005, 10 days)
- Visitor, UCI campus (2006, 1 month)
- Laboratory practice in Barcelona Autonoma University (2009, 2 months)
- Symposium, Lincei Academy in Rome: "Biotechnology for health" (2007)
- Joint symposium, Italy and Harvard Medical School, Rome: "The stress Response in Tumor Cell Signaling: New Perspectives in Anticancer therapy" (2008)
- 40th Annual Meeting of Society for Neuroscience at the San Diego Convention Center, California (2010)
- 2010 Immunology Fair, University California, Irvine (2010)
- Midwinter Conference of Immunologists, Asilomar, CA (2011)

ABSTRACT OF THE DISSERTATION

Novel strategies to inhibit the growth of enteropathogens and pathobionts

By

Martina Sassone-Corsi

Doctor of Philosophy in Biomedical Sciences

University of California, Irvine, 2016

Professor Manuela Raffatellu, Chair

Enterobacteriaceae are a family of Gram-negative bacteria that cause morbidity and mortality worldwide. Infections with these organisms may cause foodborne diarrheal illnesses, urinary tract infections, and sepsis. These pathogens pose a serious global public health threat that is exacerbated by the increase of antibiotic resistance, the dearth of new antibiotics in the drug pipeline, and the limited availability of vaccines. To slow the emergence of antibiotic resistance and reduce the incidence of secondary infections, narrow-spectrum therapeutic strategies that limit the disruption of the host microbiota, which comprises beneficial microbes that provide colonization resistance to pathogens, are needed.

Iron is an essential nutrient for almost all organisms, and bioavailability of iron is limited in the vertebrate host. Thus, scavenging iron from the host environment

using small molecule iron chelators called siderophores is an essential process for the pathogenesis of infection. Therefore, bacterial iron acquisition represents an appealing target for the development of new therapeutic approaches that are needed in the wake of antibiotic resistance. In this work, we have developed two new possible strategies to target pathogens belonging to the Enterobacteriaceae family that are siderophore-producers.

In particular, we provide the first evidence that antimicrobial proteins termed microcins are important for inter- and intraspecies competition among enterobacteria during intestinal inflammation. Indeed, we demonstrate that *E. coli* Nissle 1917, a prominent probiotic organism originally isolated from the human gut, utilizes microcins to inhibit a variety of competitors: commensal *E. coli*, the pathobiont (a commensal strain that can become pathogenic in certain conditions) adherent invasive *E. coli*, and the pathogen *Salmonella*. Microcins produced by *E. coli* Nissle 1917 are post-translationally modified at the C-terminus with a siderophore moiety. Therefore, these microcins can target competing bacteria through siderophore receptors, a mechanism described as a "Trojan horse" mode of action. In this work I show for the first time that this mechanism plays a role *in vivo*, as these microcins coupled to siderophores promote competition among enterobacteria in the inflamed gut, where iron is limited.

As a second way to target pathogens that utilize siderophore to acquire iron, we employed a novel immunization strategy to target siderophores with antibodies. Specifically, in collaboration with Dr. Elisabeth Nolan and Dr. Phoom Chariatana at MIT, we synthesized the enterobactin siderophore to be then linked to an immunogenic carrier protein. We found that our immunization strategy induced the development of specific anti-siderophore antibodies and successfully reduced *Salmoenlla* gut colonization. Moreover, we found that this siderophore-capture mechanism mediated by the adaptive immune system provided narrow-spectrum growth inhibitory activity, as other member of the microbiota were unaffected by our immunization.

Altogether, we demonstrated that microcins are a source of narrow-spectrum antimicrobials that target siderophore-producing Enterobacteriaceae in the inflamed gut. In addition, we provide first evidence of a successful immunization against bacterial siderophores in order to reduce pathogens' growth.

CHAPTER 1

Introduction

1.1 Introduction to the Gut Microbiota

The mammalian gastrointestinal (GI) tract is home to a community of trillions of microorganisms commonly known as the microbiota (1). The long co-existence of the microbiota and the host intestinal mucosa has established a mutual beneficial relationship: On the one hand, this complex community of bacteria protects the host from infection with pathogenic microorganisms and contributes to both nutrient metabolism as well as to the development and function of the GI immune system; on the other hand, the host provides nutrient-rich niches to ensure the survival of its resident bacterial communities.

The human gut microbiome consists of many different species of bacteria, some of which are non-culturable and therefore not well known or characterized. Indeed, it has only been through the advent of deep sequencing, genomics, and metagenomics in the last decade that the complexity of the microbiota has been fully appreciated. Remarkably, each individual presents a specific “bacterial fingerprint,” which is influenced by a variety of factors including the maternal environment, host genotype, diet, and antibiotic treatment (2). In particular, in healthy subjects, at least 1,000 different bacterial species contribute to intestinal homeostasis, with Firmicutes and

Bacteroidetes representing the most common intestinal phyla, followed by Actinobacteria and Proteobacteria (3, 4). Within these phyla, Gram-positive *Lactobacillus* (phylum Firmicutes) and *Bifidobacterium* (phylum Actinobacteria) as well as certain Gram-negative bacteria such as *Escherichia coli* Nissle 1917 (phylum Proteobacteria) have been shown to benefit the host by replacing harmful microorganisms; for this reason, they are referred to as "probiotics." In addition to the few known probiotics, the microbiota in general has beneficial effects on the host; for example, the absence of the microbiota renders GF mice more susceptible to infection in comparison to conventionally raised mice (1, 5). A brief summary of some of the mechanisms that certain members of the microbiota utilize to provide a barrier against pathogens will further highlight the objectives of this dissertation.

1.1.1 Microbiota-mediated colonization resistance to intestinal pathogens

Several studies have begun to elucidate the molecular mechanisms behind the beneficial role of commensal and probiotic strains. It is now becoming clear that beneficial bacteria provide colonization resistance to pathogens by two major mechanisms (6, 7). The first mechanism involves the direct competition between certain commensals and pathogens for nutrients or niche establishment. The second mechanism comprises indirect effects on pathogen colonization, deriving from the stimulation of the innate and adaptive immune system by commensal bacteria. One of the mechanisms by which commensal and probiotic bacteria provide colonization

resistance to pathogens is by directly competing for the same niche. Some beneficial microbes acquire similar nutrients as pathogens, often more efficiently, thus hindering the replication and colonization of infectious agents. In addition, some microbes produce antimicrobial proteins that can target pathogens. Numerous studies on the battle between commensals and pathogens belonging to the Enterobacteriaceae family have put forward the idea that competition for nutrients in the gut appears to occur primarily between metabolically related bacteria. For example, in germ-free mice, certain commensal *Escherichia coli* strains reduce cecal colonization of the enteric pathogen enterohemorrhagic *E. coli* (EHEC), a leading cause of bloody diarrhea in humans, by competing for the amino acid proline (8). Similarly, pre-colonization of streptomycin-treated mice with specific human commensal *E. coli* strains prevented the growth of EHEC (9). This latter effect was later reported to be linked to the capacity of the human commensal *E. coli* strain HS and of the probiotic strain *E. coli* Nissle 1917 to occupy a unique nutritional niche in the mouse gut. Indeed, utilization of multiple sugar molecules (6 by *E. coli* HS and 7 by *E. coli* Nissle 1917) limited the nutrient availability to pathogenic strains of *E. coli*, thereby impeding their successful colonization of the gut (10). It is worth noting that the competition for nutrients is not limited to bacteria within the same species. For instance, a commensal strain of *E. coli* was able to delay the intestinal colonization and translocation of the pathogen *Salmonella* Typhimurium in GF mice, possibly due to competition for nutrients (11). As competition for nutrients is one of the mechanisms by which commensals provide colonization resistance, it is not surprising that certain pathogens have evolved to evade this mechanism. This is, for instance, the case for certain pathogenic *E. coli* strains, which can utilize sugars that are

not used by commensal *E. coli* (12). Moreover, the types of nutrient sources available to both commensals and pathogens can vary if the intestinal environment is altered; e.g. because of inflammation or antibiotic treatment (13, 14). In such conditions, changes in nutrient type and availability enhance the growth of specific strains capable of exploiting the new nutrient sources; for example, the pathogen *Salmonella* Typhimurium, but not the microbiota, can utilize ethanolamine and fructose-asparagine in the inflamed intestine (15). Similarly, antibiotic treatment of mice induces substantial changes in the gut metabolome (the composition of metabolites present in the gut), resulting in an increase of specific carbon sources that support the germination and growth of *C. difficile* (14). Another means of direct competition between commensals and pathogens within the gut involves the secretion of toxins and antimicrobial peptides. Though originally described as a virulence trait of pathogens to kill their commensal competitors (16), new evidence suggests that the secretion of antibacterial toxins via phage-like machinery known as a "type VI secretion system" (T6SS) is also employed by commensals to attack competitors vying for the same ecological niche (17). Other mechanisms employed by bacteria to deliver toxins to their competitors (for instance, the contact-dependent growth inhibition system (18)) could also promote inter and intra-species competition as well as colonization resistance to pathogens. Moreover, some commensal Enterobacteriaceae, including the probiotic *E. coli* Nissle, secrete small antimicrobial peptides called microcins, which specifically target and kill related competitors, including pathogenic organisms (19, 20). Some microcins target competitors expressing the same nutrient receptors as the microcin producers, and are

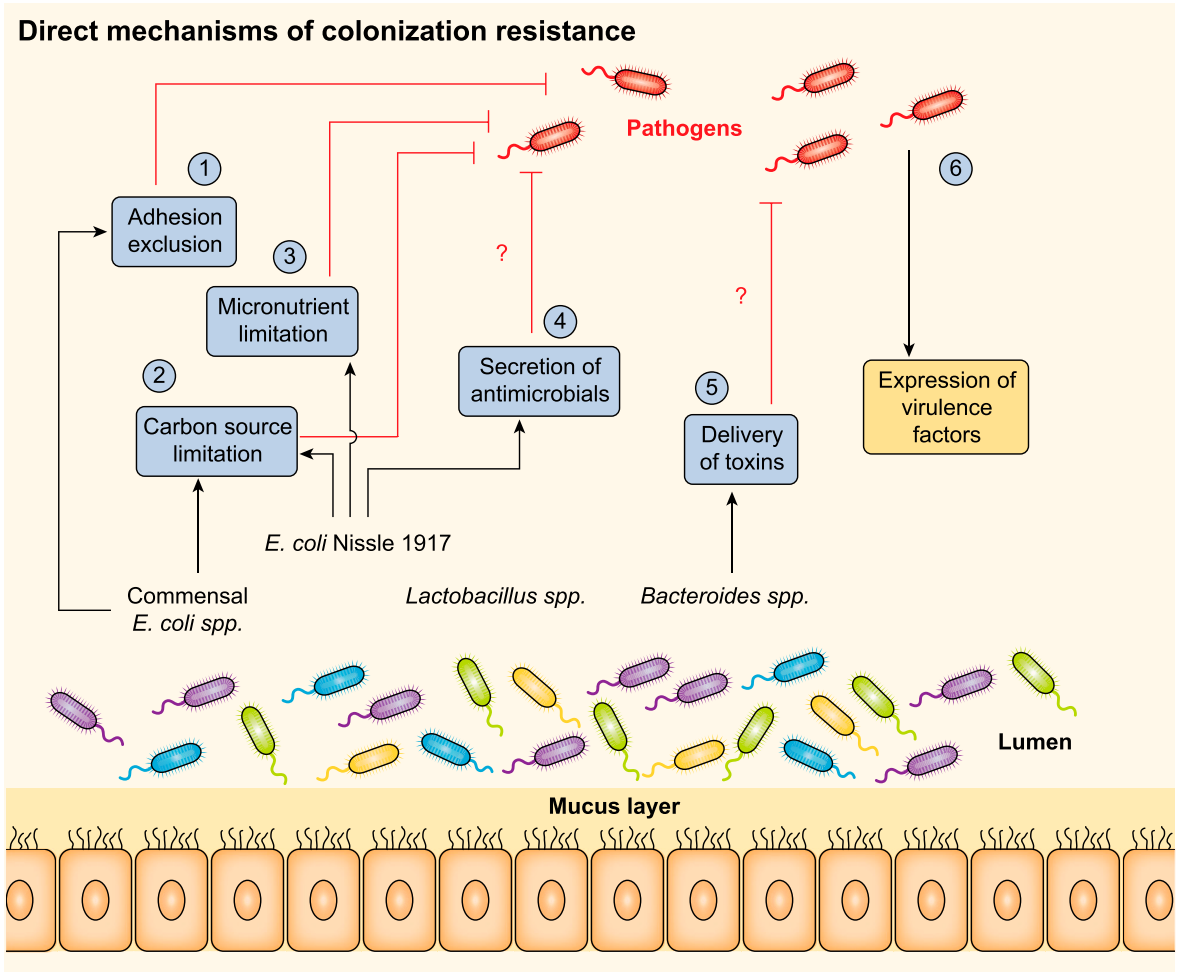
internalized by hijacking these transporters via a so-called “Trojan horse” mechanism (20, 21).

FIGURE 1.1

(Originally published in *The Journal of immunology* Sassone-Corsi M. and Raffatellu M. 2015. No Vacancy: How Beneficial Microbes Cooperate with Immunity to Provide Colonization Resistance to Pathogens. J. Immunol. 2015;194:4081-4087 http://jimmunol.org/content/194/9/4081.full?sid=129dc7e5-c28d-447b-98b1-04914da8886b)

Figure 1.1 Direct mechanisms of colonization resistance against enteropathogens
The microbiota provide a barrier against incoming enteric pathogens via multiple mechanisms. (1) Adhesion exclusion: Certain commensals reduce pathogen adherence to the intestinal mucosa. (2) Carbon source limitation: Human commensal *Escherichia coli* strain HS and probiotic strain *Escherichia coli* Nissle 1917 both metabolize multiple sugar molecules, which limits the availability of nutrients in the gut to certain pathogens. (3) Micronutrient limitation: The probiotic strain *E. coli* Nissle 1917 can uptake iron via several mechanisms, limiting its availability to pathogens such as *Salmonella* Typhimurium. (4) Secretion of antimicrobials: Commensals act against pathogens not only by limiting nutrients, but also by the production antimicrobial compounds, such as bacteriocins and microcins. (5) Direct delivery of toxins: Although not yet demonstrated *in vivo*, commensals can express type 6-secretion systems (T6SSs) and contact-dependent inhibition (CDI) systems, means by which to deliver growth-inhibiting toxins to close competitors. (6) Circumventing colonization resistance: Pathogens employ a variety of virulence factors to colonize the host and cause disease.

FIGURE 1.1


Direct mechanisms of colonization resistance
Pathogens
1
Adhesion exclusion
2
Carbon source limitation
3
Micronutrient limitation
4
Secretion of antimicrobials
5
Delivery of toxins
6
Expression of virulence factors
?
?
E. coli Nissle 1917
Commensal E. coli spp.
Lactobacillus spp.
Bacteroides spp.
Lumen
Mucus layer

1. 2 The Enterobacteriaceae bacterial family in the gut during health and disease

Enterobacteriaceae are a large family of bacteria that commonly cause infections in health care settings. The most frequently reported Enterobacteriaceae are *Escherichia coli*, *Salmonella* species and *Klebsiella* species (22). In healthy individuals, bacteria belonging to the Enterobacteriaceae family (Proteobacteria phylum) are commonly present in low abundance, which is a key for the maintenance of immune homeostasis (23-25). In particular, in a healthy gut environment microbe-host interaction maintain the intestinal immune homeostasis and so providing "host-directed nutritional exclusion" of bacterial belonging to the Proteobacteria phylum (26). However, perturbation in the diet, antibiotic treatment and infection lead to a substantial microbial alteration known as "dysbiosis", characterized by phylum level changes in the community structure. In particular, facultative anaerobe members of the Enterobacteriaceae family prevail, while obligate anaerobes such as Clostridia decrease in this condition (26, 27). In particular, several studies brought into light that inflammatory host responses mediated by these perturbations impose selective forces, which drive phylum changes in the gut microbial communities. Within Proteobacteria, pathogens and pathobionts (i.e. commensal microbes with the potential of causing diseases) of the Enterobacteriaceae family have been shown to benefit from the host nutritional environment that arises during inflammation (28). The emerging picture is that, instead of being controlled by the host mucosal immunity, Enterobacteriaceae exploit host inflammation to thrive (28). Only few bacterial species are fit to growth in the presence of inflammation, and few beneficial bacterial strains can effectively compete with enteric pathogens such as *Salmonella*

Typhimurium, which profoundly change the gut environment. In particular, the probiotic strain *Escherichia coli* Nissle 1917 is a prime example of how a commensal strain can provide colonization resistance against pathogens by better competing for the limited nutritional resources available in the inflamed intestine (29, 30) Some of these aspects including bacterial nutrients acquisitions together with descriptions of *E. coli* Nissle and the pathogens *Salmonella* will be described in detail below.

1.1.2 The probiotic strain *Escherichia coli* Nissle 1917

The first observation that certain commensal bacteria have beneficial properties dates back to 1907, when Elie Mechnikoff proposed that lactic acid-producing strains are beneficial to the host by inhibiting the growth of other species within the colon (31). Today, probiotics are defined by the World Health Organization as “live bacterial species that confer a health benefit when administered in adequate amounts” (32). *E. coli* Nissle 1917 (hereafter referred to as EcN) was isolated in 1917 by Dr. Alfred Nissle from the stool sample of a soldier who did not develop diarrhea during an outbreak of shigellosis (33). Today, EcN is the active component of a probiotic preparation used for the treatment of both infectious diarrheal diseases and inflammatory bowel disease (IBD) (34). Although EcN serotype O6:K5:H1 is typical of *E. coli* strains associated with urinary tract infections, EcN is completely nonpathogenic (35). Several putative fitness determinants of EcN are localized on four genomic islands that have been sequenced and analyzed. Comparative genomic hybridization studies with the available genomes of E. coli K-12 strain MG1655 and uropathogenic E. coli O6 strains CFT073 and 536

showed structural similarities on the genomic level and established that EcN is strongly related to the highly virulent uropathogenic strain CFT073 (36, 37). Some fitness factors encoded by both CFT073 and EcN are curli and both type 1 and F1C fimbriae. In particular, F1C fimbrie of EcN are required for biofilm formation, adherence to epithelial cells, intestinal colonization, and persistence in the gut of infant mice (38, 39). An important difference between EcN and CFT073 is in the structure of LPS. A point mutation introducing a stop codon in the gene for the O6 antigen polymerase makes the O6 polysaccharide side chain very short, consisting of only a single “repeating unit” of the oligosaccharide building block typical of the O6 antigen. This peculiar characteristic is believed to contribute to EcN serum-complement sensitivity and be responsible for the semirough phenotypic aspect of the colonies grown on solid nutrient media. This change could also play a role in the special immunomodulating properties exhibited by EcN, which is “free” of immunotoxic side effects in patients (40). Another characteristic of EcN is the presence of an extracellular capsule of the K5 serotype, which is found in only 1% of *E. coli* isolates and is important for adhesion and colonization (30, 41). Although the K5 capsule seems to play an important role in vitro, to date it is not known whether it contributes to the probiotic effect of EcN in vivo.

1.1.2.1 Beneficial Effects of *Escherichia coli* Nissle 1917

Since 1917, *E. coli* Nissle 1917 (EcN) has been used particularly in Germany for the treatment of inflammatory bowel disease (IBD) and others gastrointestinal-associated disorders. Modulation of the immunity (42) in the gut by the activation or repression of different important pathways is an example of beneficial properties associated with EcN. The EcN H1 flagellin is recognized by Toll-like receptor 5 (TLR5), which induces production and secretion of one of the main antimicrobial chemokines, CXCL-8 or IL-8. This cytokine is necessary for the neutrophil recruitment, and for the phagocytosis of pathogens *in situ*. Moreover, flagellin H1 induces the activation of defensins and the up-regulation antimicrobial protein calprotectin (43). Additionally, recent studies showed the importance of the EcN K5 capsule in stimulating the expression of Toll-like Receptor 5 (TLR5), MyD88 and IL-8 with the induction of Mitogen Activated Protein Kinases (MAPKs) in epithelial cells (44). Another beneficial effect of EcN is the modulation of the gut barrier by up-regulation of the tight junction proteins ZO-1 and ZO-2 (45). EcN also possesses several redundant fitness properties, including several (probably 14) iron uptake systems. Enterobactin and salmochelin are the main siderophores produced by EcN (46). These two systems synergize with other iron uptake systems (including the siderophores yersiniabactin and aerobactin, the hemin transporters ChuA and HemA and the ferrous iron transporter EfeU), making EcN well suited to grow in iron-limiting condition such as in the gut during inflammation, and so to out-compete the pathogen *Salmonella* Typhimurium (29). Also, recent studies have shown that this strain has

important anti-inflammatory effects in chronic colitis models (47). Furthermore, EcN produces two antimicrobial peptides called the microcins H47 and M (48), which have been shown with *in vitro* studies to target closely related competitors.

FIGURE 1.2

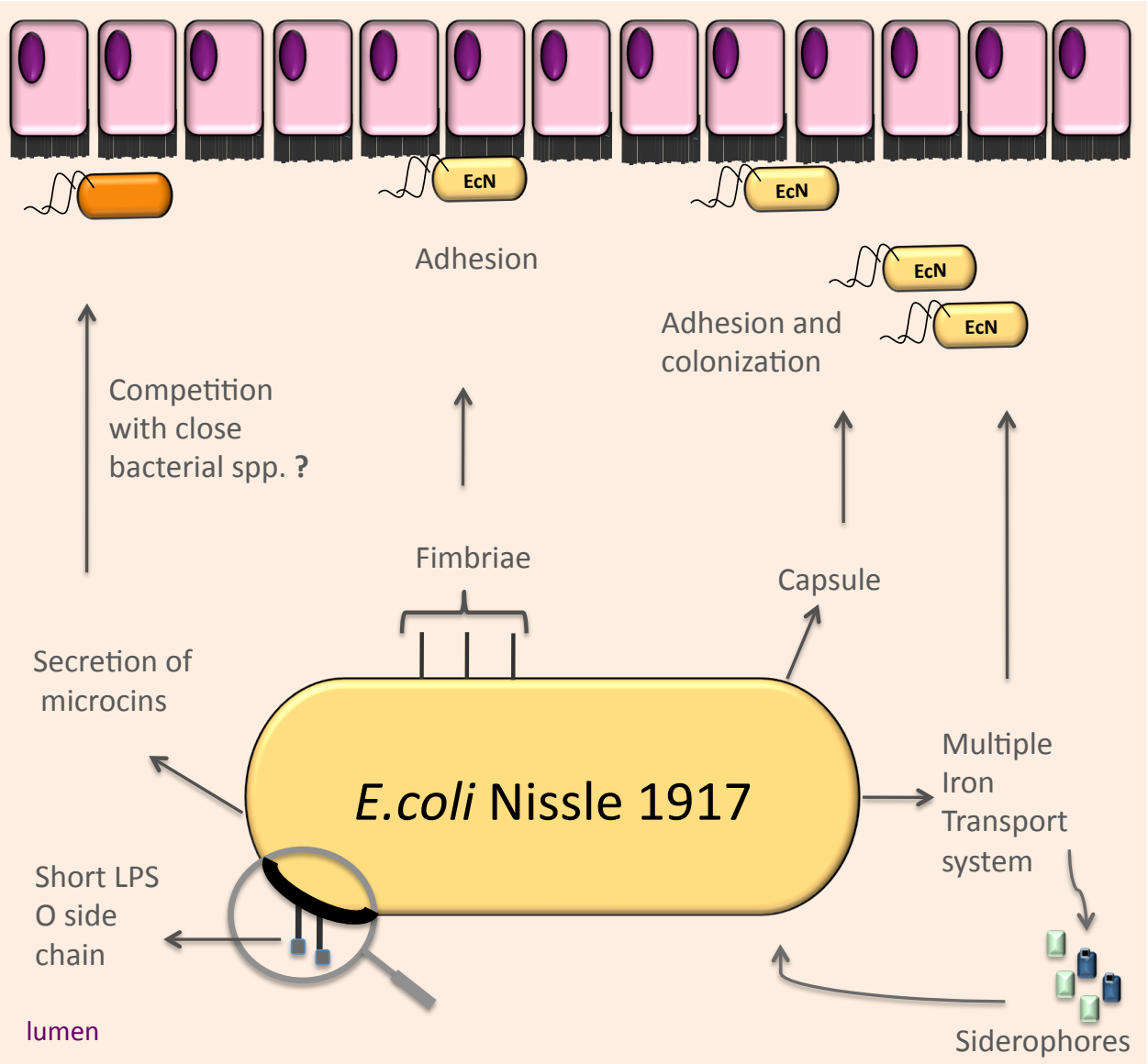


Figure 1.2 Fitness factors of *E. coli* Nissle 1917. Adapted from (49)

The probiotic *E. coli* Nissle 1917 possess multiple fitness factors that might facilitate the colonization of the gut when is inflamed.

1.2.2 *Salmonella enterica* and non-typhoidal salmonellosis (NTS)

Salmonellae are Gram-negative, facultative anaerobic bacteria of the family Enterebacteriaceae, composed of non-spore forming rods, usually motile with peritrichous flagella. Most *Salmonella* serovars have broad host range and cause zoonotic infections, meaning that these pathogens can be transferred between human and non- human species. The genus *Salmonella* contains over 2,000 serovars and is one of the most important pathogens of the Enterobacteriaceae family. Taxonomically, all strains of *Salmonella* fall within one species, *S. enterica*. The species *Salmonella enterica* subspecies *enterica* can be divided into over 2,400 antigenically distinct serovars, most of which with undefined pathogenicity. The majority of *Salmonella* infections in humans are caused by relatively few serovars. The serovars known to cause diseases in vertebrates can be subdivided into three groups on the basis of host prevalence. The first group consists of host-specific serovars. These typically cause systemic disease in a limited number of phylogenetically related species. For example, *S. enterica* serovar Typhi, serovar Gallinarum and serovar Abortusovis are most exclusively associated with systemic diseases in humans, poultry and sheep, respectively. *Salmonella* Typhi and Paratyphi cause typhoid fever, major sources of morbidity and mortality in developing countries. The World Health Organization (WHO) estimates that the annual global incidence of typhoid fever is about 22 million cases with a mortality of 1% (50). The second group consists of host-restricted strain. These are primarily associated with one or two closely related host species but may also

infrequently cause disease in other hosts. For example, *S. enterica* serovar Dublin and serovar Cholaraesuis are generally associated with severe systemic disease in ruminants and pigs, respectively (51) , but can also cause bacteremia in humans. The third group consists of the ubiquitous *S. enterica* serovars, which includes serovars Typhimurium and Enteridis, which are the most common serovars causing infection in the U.S. Non-typhoidal *Salmonellae* (NTS) are the single most common cause of death from diarrheal disease associated with viruses, parasites or bacteria. NTS are leading causes of acute food borne disease outbreaks in the U.S., costing $ 3.3 billion annually in medical care and lost productivity (52). The global burden for NTS was estimated at 93 million cases and 155,000 deaths in 2010 (53). In immuno-competent individuals, NTS are associated with gastroenteritis, a localized infection in the small and large intestines that manifests with fever, diarrhea and intestinal cramping. Usually, inflammatory diarrhea caused by NTS is a self-limited disease, which resolves in a few days, although prolonged fecal shedding is often observed. On the other hand, in immuno-compromised individuals, in children and the elderly, NTS can result in the development of bacteremia and sepsis. NTS infections have a significant prevalence in developing countries where there are approximately 2-3 million annual deaths caused by diarrheal diseases (54, 55). In particular in sub-Saharan Africa, NTS infections are leading causes of bacteremia in immuno-compromised individual. The essential risk factor in African children for developing NTS bacteremia are malnutrition, severe malaria, anemia and AIDS (56, 57). In contrast, NTS bacteremia in African adults is associated with AIDS as the sole major risk factor (58). In a year, about 10% of HIV

positive African adults develop invasive NTS infections, resulting in mortality rates of greater than 20% despite antibiotics therapy (59).

1.2.2.1 Molecular pathogenesis of NTS-induced gastroenteritis

The essential virulence traits that enable *S.* Typhimurium to elicit inflammation are its ability to penetrate the intestinal epithelium and to survive within macrophages. This ability is mediated by two different *S.* Typhimurium Pathogenicity Islands (PAI), which are expressed after activation of signals generated by the host defense (60). For example, the sensor kinase PhoQ controls the virulence gene expression after the interaction with small antimicrobial peptides produced by the host. *Salmonella* Pathogenicity Island 1 (SPI1), which has been first identified during the characterization of invasion-deficient strains of *S. enterica* (61), is required for the invasion on non-phagocytic cells (62). SPI1 encodes for a type three-secretion system (T3SS-1) that, by the delivery of effector proteins into the host, induces actin rearrangements in epithelial cells, resulting in membrane ruffling and bacteria internalization. Moreover, *Salmonella* Pathogenicity Island 2 (SPI2) is required to protect this pathogen within the Salmonella–containing vacuole (SCV) against the effects of innate immunity (63, 64). This mechanism enables *S.* Typhimurium to establish a replicative niche in macrophage. Also, it has been shown that the SPI2 type-three secretion system (T3SS-2), prevents co-localization of phagocyte oxidase (65) and inducible nitric oxidase (iNOS) to the SCV (66), resulting in *Salmonella* survival in macrophages. Both secretion systems

contribute to *S.* Typhimurium intestinal survival, where the pathogen is located intracellularly within epithelial cell, macrophages or dendritic cells (DC). Direct contact between host cells, including epithelial cells, macrophages, and DCs, with bacteria is required for the initiation of inflammatory responses in tissue. DCs and macrophages infected with *S.* Typhimurium are sources of cytokines, such as interleukin (IL)-23 and IL-18, both of which help to amplify responses in tissue through paracrine signaling mechanism (67). Antigen-experienced T cells rapidly secrete IFN-γ during bacterial infection by an antigen-independent manner in response to stimulation by IL-18 (68). On the other hand, IL-23 stimulates T cells in the intestinal mucosa to produce IL-17 and IL-22 (67). It has been shown that expression of these two T cell cytokines is highly induced in response to *S.* Typhimurium infection (69, 70). These cytokines orchestrate the mucosal response to *S.* Typhimurium and the gut barrier function by promoting the secretion of antimicrobial peptides and the recruitment of neutrophils (69, 71). In particular, IL-17 mainly orchestrates the neutrophil arm of the host response, in part by stimulating epithelial cells to secrete chemokines (CXC), and also by stimulating granulopoiesis in the bone marrow through the induction of granulocyte colony-stimulation factor (G-CSF). Neutrophil recruitment is coordinated by the IL-23/IL-17 axis, and it is a hallmark of *Salmonella* diarrhea, during which the intestine has a limited availability of nutrients that normally support bacterial growth. A second component of the antimicrobial response to *S.* Typhimurium infection is the production of antimicrobial proteins and peptides in the intestinal mucosa (69, 71, 72). An important cytokine that controls this host defense is IL-22 (70), which induces the expression of effectors molecules by epithelial cells. The release of antimicrobial products activated through the

IL-23/IL-22 axis converts the intestinal lumen into an increasingly hostile environment for microbes. Together, the IL-23/IL17 and IL-23/IL22 axes bring a dramatic change in the luminal environment that may be responsible for the alteration of the microbiota observed during inflammation (73). In fact the numbers of commensal microbes, mostly belonging to the Firmicutes and Bacteroides phyla, are reduced during *S.* Typhimurium infection (64).

1.2.2.2 *Salmonella* inflammation-adapted gut life style

Though intestinal inflammation is protective as it prevents NTS dissemination and bacteremia in healthy individuals, inflammation also enhances *Salmonella* replication in the gut via several mechanisms (74). *S.* Typhimurium is unable to colonize the mouse intestine in the absence of inflammation, as the microbiota in the non-inflamed gut is able to outcompete an avirulent strain *S.* Typhimurium that does not cause inflammation (REF). Several studies have shown that Enterobacteriaceae such as *S.* Typhimurium thrive in diarrheal environment, taking an advantage of host inflammatory response in order to promote their own growth. Acute *S.* Typhimurium and *Citrobacter rodentium* infection models have revealed that enteropathogenic bacteria can subvert inflammation in order to compete the microbiota (64, 73, 75). This growth advantage might be attributable in part to high levels of antimicrobial peptides and defensins secreted by the inflamed mucosa (76). Furthermore it has been shown that secretion of high-energy glycosylated proteins by the inflamed mucosa might help *S.* Typhimurium colonization

of the gut (77). At last, the Bäumler group discovered a new mechanism explaining how pathogens can exploit the host inflammatory responses in the gut to outcompete the commensal microbes. These authors have shown that the metabolic product thiosulfate, released by commensal bacteria in an inflamed environment, is converted by the inflamed mucosa into tetrathionate, a molecule that can serve as primary electron acceptor for *S.* Typhimurium (78). This mechanism of respiration allows *S.* Typhimurium to grow faster than the microbiota, which is not able to utilize tetrathionate. Therefore, the inflammatory response orchestrated by *Salmonella* during infection creates a nutritional environment that supports the pathogen's replication in the gut lumen. Moreover, bacteria belonging to the Enterobacteriaceae family have evolved mechanism to acquire essential nutrients like transition metals, which are scarce in the presence of inflammation. In particular, the role of iron and how the host and bacteria have evolved mechanisms to compete for this essential nutrient are discussed extensively in the next paragraphs.

1.3 Nutritional Immunity and the Battle for Iron Acquisition

Transition metal ions are involved in many biological processes and so crucial for sustaining life (79, 80). Among transition metal ions, iron is the most abundant in the human body and is an essential nutrient for both humans and microbes (81).

Under physiological conditions, iron is found mostly in the ferrous (Fe^{2+}) or ferric (Fe^{3+}) form and because of its ability to exist in one or two oxidation states is an essential redox catalyst for many cellular processes. In particular, in mammals iron is essential for nucleic acid and protein synthesis, electron transport and respiration (82). Most of the iron in the human body is found intracellular, in particular in erythrocytes complexed to heme. When extracellular is found bound to high-affinity iron binding proteins such as lactoferrin at mucosal surfaces and transferrin in the plasma. Because of its redox potential, iron can also be generating toxicity in condition of iron overload. Indeed, regulation of iron levels in the human body is essential for maintaining homeostasis. In particular, iron metabolism is tightly regulated to avoid cellular damage due to overload or anemia associated with deficiency. For example, hepcidin, an hormone produced by the liver, controls entry of iron into the plasma after absorption by enterocytes (83). Similarly to eukaryotic cells, bacteria need iron for several biological processes including DNA synthesis, electron transport and superoxide metabolism (84). Subsequently, another reason for the host to tightly regulate iron levels is to limit availability of this essential nutrient to pathogens trough a process named “nutritional immunity” (85). A review of the processes utilized by bacteria belonging to the

Enterobacteriaceae family to acquire iron and how the host has evolved mechanisms to impede this, will serve to help elucidate the objective of this work.

1.3.1 Microbial Mechanism for Iron Acquisition

As many others bacterial species, members of the Enterobacteriaceae family require micromolar concentration of iron to successfully replicate in the host. For this reason, the host strongly regulates free iron concentration by a number of iron chelating proteins. To overcome this metabolic deprivation members of the Enterobacteriaceae family have evolved specialized mechanisms to fulfill their average need of 10^{-7}-10^{-5} M of iron for optimal growth (85). Most of the mechanisms of iron uptake were described extensively in *E.coli*. Some of these mechanisms include, uptake of iron in is ferrous and its ferric form. In particular, the Feo-uptake system is involved in the uptake of the ferrous form, which seems to be essential only in low oxygen environments (86). In fact, studies have shown that both feoB isogenic mutants of *S*. Typhimurium and *E.coli* are outcompeted by their wild-type during colonization of the mouse intestine in the absence of inflammation (87, 88). On the other hand, in environment where iron is scarce, such as the inflamed intestine, certain bacterial species and also fungi express and secrete small chelating proteins called siderophores for the uptake of iron in the ferric form (89). Subsequently, bacteria internalize the sideropore-ferric complex via binding to specialized receptors and transporters where then iron will be released for metabolic use. One of the most studied siderophore is enterobactin, or also called enterochelin (Fig. 1.3). Enterobactin is produced by most Enteterobacteriaceae,

including *E.coli* and the pathogen *Salmonella* and can chelate ferric iron, Fe(III), with high affinity (Kd 10^{-25} M) (89) and then internalized by the specialized receptor FepA. This latter process is dependent on the TonB system that provides energy for this transport. However, in the next paragraph will be discussed extensively how the host has evolved ways to in part counteract this efficient way of bacterial iron acquisition.

1.3.2 Host Mechanisms for Iron Sequestration

As discussed above, siderophores molecules secreted by bacteria and fungi in order to sequester the metal iron. The production of siderophores in the gut improves pathogens survival and colonization (90). In particular, several findings suggest that siderophores are commonly produced by enteric pathogens in the intestinal lumen if the gut is inflamed (45, 66, 74). One feature of the inflammatory response to intestinal pathogens is the release of antimicrobial proteins that sequester metal ions to further limit their availability to pathogens, a process known as nutritional immunity. In particular, in response to infection, both neutrophils and epithelial cells secrete the antimicrobial peptide lipocalin-2. Lipocalin-2 binds to a subset of catecholate siderophores including enterobactin, the siderophore secreted by all Enterobacteriaceae to acquire iron, thereby limiting the growth of strains that rely on enterobactin as the sole scavenger of iron (91, 92). In particular, lipocalin-2 recognizes and forms a complex with ferric enterobactin, inhibiting its uptake by enterobactin-utilizing microbes (93). Although this antimicrobial defense mechanism controls the growth of commensal bacteria,

pathogens, including *Salmonella*, pathogenic *Escherichia coli* and *Klebsiella pneumoniae,* produce additional siderophores, which are not recognized by lipocalin-2 (94-97). For instance, *Salmonella* and pathogenic *E. coli* have acquired the *iroBCDE iroN* locus to synthesize a C-glucosylated form of enterobactin called salmochelin (98), which is too large to fit in the lipocalin-2 binding pocket (99) (Fig. 1.3). Thus salmochelin-dependent iron acquisition provides *Salmonella* and other bacteria a competitive advantage in the inflamed gut (90, 96) and its required for this pathogen's full virulence. Simultaneously, not only pathogens have the ability to express stealth siderophores, and the probiotic strain of *E. coli* Nissle is an example.

FIGURE 1.3

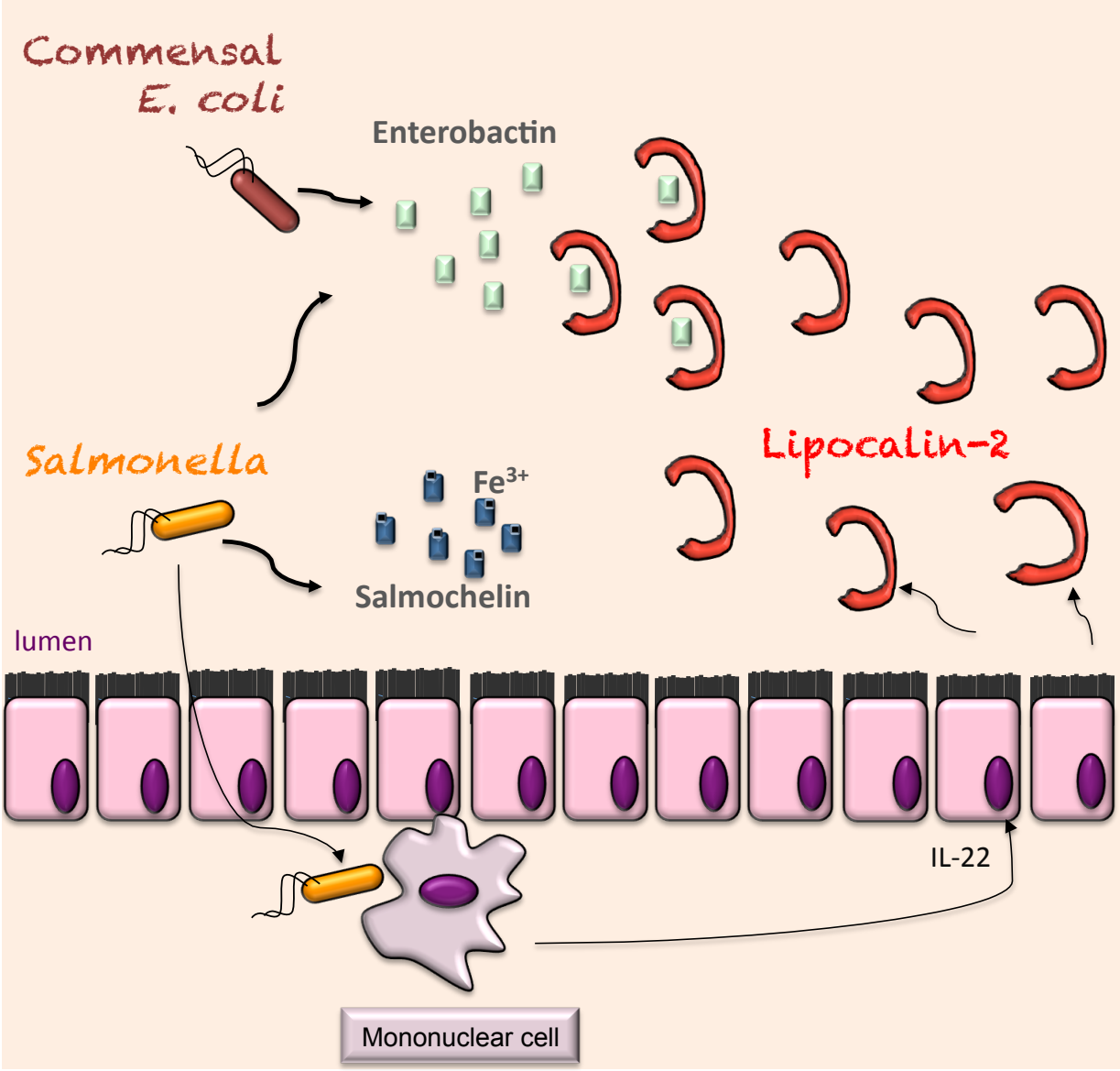


Figure 1.3 Mechanism of iron acquisition by *Salmonella* in the inflamed intestine. *Salmonella* enterica serotype Typhimurium trigger intestinal inflammation by invading epithelial cells and surviving inside macrophages. This results in the releases of pro-inflammatory cytokines such as IL-22, which triggers the production of the antimicrobial protein lipocalin-2. Lipocalin-2 can bind and sequester the siderophore enterobactin preventing bacteria such as commensal *Escherichia coli* to acquire iron. On the other hand, *Salmonella* has evolved mechanism to counteract lipocalin-2, by secreting a modified form of enterobactin called salmochelin. Salmochelin is modified by two glucosylations that make this structure too big to fit in the lipocalin-2 binding pocked and consequently allowing *Salmonella* to grow also in the presence of inflammation.

1.3.3 The Battle for Iron Acquisition in the Enterobacteriaceae Family

Pathogens and commensals have acquired mechanisms to compete with each other in nutrient-limited environments such as the inflamed gut, however the mechanistic bases for this competition are not completely understood. A very recent example of direct competition for iron acquisition comes from studies in which the probiotic strain of *E. coli* Nissle (EcN) was competed against the pathogens *Salmonella* Typhimurium. In fact, EcN produces several siderophores, including enterobactin, salmochelin, aerobactin, and yersiniabactin (98, 100, 101). All of these siderophores were found to be essential for EcN to compete with *Salmonella*, to effectively grow in the inflamed gut, and to promote EcN's competition for a niche with the resident microbiota (29). In addition to this, an interesting phenomenon is the cross feeding of heterologous siderophores, which makes certain bacteria capable of competing for and using each other's siderophores. To prevent cross feeding of siderophores, certain bacteria can directly target their close competitors. For instance, some pathogens as well as some commensal bacteria secrete their own antimicrobial peptides. Particularly, Enterobacteriaceae secrete a class of low-molecular mass antimicrobial peptides, termed microcins (**Fig. 1.4**). Similar to bacteriocins, which are secreted by Gram-positive bacteria, microcins exert potent antimicrobial activity against phylogenetically related bacterial strains (20). Microcins are usually produced under stress conditions such as iron limitation (19, 20). Previous studies demonstrated that these small peptides inhibit the growth *in vitro* of a variety of Gram-negative bacteria such as *Escherichia*, *Salmonella*, *Klebsiella*, *Citrobacter*, and *Shigella* (19, 75). The strategies by which these peptides enter and exercise their function involve the use of important nutrient

receptors. Like other Enterobacteriaceae, the probiotic *E. coli* Nissle 1917 encodes two distinct antimicrobial peptides: microcins MccH47 and MccM. Because bacteria secrete these antimicrobial peptides to compete for nutrients with each other, microcins are believed to be an efficient weapon of the intestinal microbiota. Therefore, a better understanding of the mechanism of action by *E. coli* Nissle microcins can ultimately lead to the development of new therapeutic strategies to target specific siderophore-utilizing bacteria. A detailed description of the microcins produces by EcN follows in the next paragraph.

1.3.3.1 Antimicrobial Peptides of *Escherichia coli* Nissle 1917: Microcins of Class IIb

Microcins are produced by different types of bacteria, mostly by the Enterobacteriaceae family, and are believe to be used as efficient weapons by the intestinal microbiota. These antimicrobial peptides possess important characteristics, including high stability to heat and resistance to degradation by proteases and pH changes (78). Microcins are encoded by gene clusters carried either by plasmids or by the chromosome. Organization of the microcin cluster is partially conserved, involving four clustered genes grouped in a single operon or in several operons. The cluster includes: (i) structural gene precursors, (ii) self-immunity genes important for protection of the producing strains, (iii) modification enzymes and genes encoding for the export system machinery (102). Microcins are usually produced under stress conditions such as nutrient depletion, and in particular during iron limitation (19). While large multi-domain

enzymes produce most antimicrobial peptides from microbial origin, microcins are typically produced as ribosomally synthesized precursors. Usually, they present common characteristics, such as a molecular mass below 10kDa, and a secretion system involving ABC transporters with an ATP-binding cassette (79). To date, several different microcins have been identified, but only seven have been structurally characterized: microcin B12 (MccB17), MccE492, MccC7/C51, MccJ25, MccL, MccM, and MccV (80). The structures of other microcins, including McccH47, Mccl47, and Mcc24, have been predicted by genetic studies alone. Class II microcins have a higher molecular mass and are divided into two subclasses: Class IIa, which includes microcins that do not undergo post-translational modifications and are plasmid encoded, and Class IIb, which includes microcins that carry a C-terminal modification and are chromosomally encoded (76, 77). The production of microcins involves three steps: (i) synthesis of the precursor gene, (ii) maturation of the pro-peptide, and (iii) secretion by their export system in a TolC-dependent fashion (78). To this date, mechanisms of action have been described for only a few microcins.

FIGURE 1.4

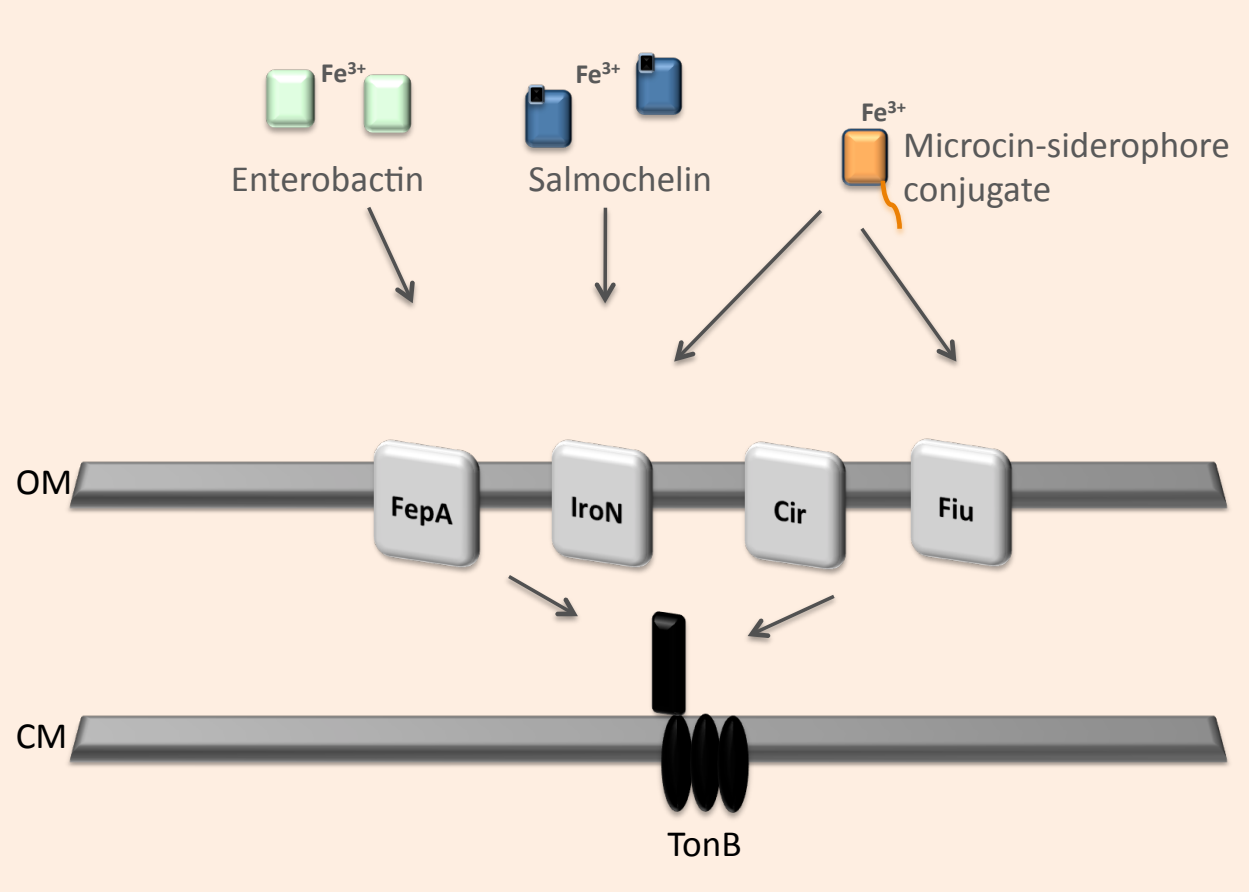


Figure 1.4 Mechanism of siderophores and microcin-siderophore conjugates uptake.
The siderophores enterobactin and salmochelin once bound to ferric iron (Fe3+) are uptake it by specialized receptors. FepA binds to enterobactin while IroN to salmochelin. Microcin-siderophore conjugates are recognized by common siderophore receptors including FepA, IroN, Cir and Fiu. All siderophore once in the periplasm will be transported by a TonB-dependent active transport inside the bacterial cell. (OM: outer membrane: CM: cytoplasmic membrane).

The strategies by which these peptides enter and exercise their function involve the use of important receptors for nutrients, including the iron uptake receptors for enterochelin and salmochelin. Once inside the cells, microcins can actively kill the target bacteria by inducing alterations of their membrane permeability, degradation of nucleic acids, or destruction of the cell wall (79, 81). Class IIb microcins, including MccM, MccH47, and MccE492, present a conserved serine-rich C-terminal region that is reminiscent of the serine backbone of enterochelin. Although MccM and MccH47 have not been thoroughly characterized, microcin E492, which belongs to the same class, has been characterized in detail. MccE492 is secreted by *Klebsiella pneumoniae* and is active against strains of *Escherichia*, *Klebsiella*, *Salmonella*, *Citrobacter* and *Enterobacter* (103). As described by Nolan et al, this microcin is found in two different forms: one form is post-translationally modified by covalent linkage of salmochelin-like molecules to serine-84, and one form is unmodified. The attachment of microcins to salmochelin promotes the uptake of these molecules by iron receptors of the target bacteria (104). This mechanism has been described as a “Trojan horse” mechanism, as MccE492 is able to target virulent bacteria expressing the siderophore uptake pumps FepA, Cir and Fiu on the cell surface (**Fig. 1.4**) (19). The probiotic *E. coli* Nissle 1917 (EcN) encodes the two microcins MccH47 and MccM. Both of these microcins are also produced by two commensals *E. coli* strains, CA46 and CA58 and encountered with 100% identity in the *serX* pathogenicity island of the uropathogenic strain *E. coli* CFT073 (105). The microcin gene cluster encoded by EcN is found in the Genomic Island I, suggesting that these genes have been acquired during Horizontal Gene Transfer. Recently, microcins MccM and MccH47 have been isolated and their structures have been solved. MccM

and MccH47 precursor peptide are derived respectively from the microcin gene *mcmA* and *mchB* (106). The genes *mcmI* and *mchI* encode for MccM and MccH47 self-immunity proteins, necessary for the producing bacteria to be protected from their own antimicrobial peptides. How the gene products of *mcmI* and *mchI* provide protection to the microcin producing strains is still not well understood. The gene cluster also contains the export genes *mchE* and *mchF* which are important, presumably, for the secretion of both microcins, as no export gene has been associated with microcin MccM. *mcmM* gene is found downstream of *mcmI* and *mcmA* with an opposite transcription polarity. The *mcmM* gene encodes for a protein with 62% similarity to MceF, which is involved in the maturation of the microcin MccE492 (107). The genes *mchC* and *mchD* are homologous to the MccE492 cluster genes *mceD* and are probably involved in microcin maturation. Notably, the *mchS4* gene was found to be responsible for the overproduction of the catechol enterobactin (108), suggesting a real cross-linkage between iron starvation and microcin production. Unlike in *E. coli* CA46 and CA58 strains, the EcN microcin cluster does not present the genes necessary for microcin maturation, namely *mchA* and *mchS1*. Moreover, the *iroA* locus, which encodes for salmochelin, is found in the Genomic Island I of EcN and only 14 kb downstream of the microcin cluster. The high similarity between the *iroB* and *iroD* genes with the MccE492 post-translational genes *mchA* and *mchS1* suggests the involvement of the EcN *iroA* locus in microcin maturation, further supporting a link between iron starvation and microcin secretion. In addition, the presence of elements known to be involved in genetic recombination, such as the insertion sequence *insE* and the gene

encoding for the transposase Tra5, strongly supports the hypothesis that the MccM/MccH47 gene cluster is horizontally transferred between bacteria.

Recent studies also revealed that MccM and MccH47 carry the same post-translational modification as the microcin E492, suggesting a similar mechanism of action and entry into the target bacteria (106). Through this strategy, microcins mimic the essential iron uptake molecules of the target bacteria. Furthermore, it has been demonstrated that both of EcN microcins are recognized by the cathecolate siderophore receptors. The genes encoding for the cathecolate receptors are present in different Gram-negative bacteria including *S.* Typhimurium, *E. coli*, and *K. pneumoniae*. It has also been demonstrated that microcins MccE492, MccM and MccH47 require the associated siderophore transporter, TonB, for their antimicrobial activity. In fact, strains lacking TonB are resistant to the activity of MccM, MccH47 and MccE492. The outer membrane receptors FepA, Cir and Fiu recognize MccM, which is then further translocated to the periplasmatic space by a TonB-dependent process. However, the precise mechanism of action by which this peptide kills the target bacteria cells remains unclear. In contrast, inhibition of the F0 subunit of the ATP synthase in the inner membrane is the proposed mechanism of action for MccH47-mediated killing.

1.4 Objectives

Enterobacteriaceae are a large family of bacteria that commonly cause infections in health care settings. The most frequently reported Enterobacteriaceae are *Escherichia coli*, *Salmonella* species and *Klebsiella* species (22). Furthermore, the past years have seen the rise of Enterobacteriaceae with resistance to a broad spectrum of antimicrobials. Resistance to antibiotics makes infections with Enterobacteriaceae difficult to treat and is associated with a high mortality rate. Therefore, the development of new preventive and therapeutic measures against infection with Enterobacteriaceae is necessary to overcome these public health problems. The ***long-term objective*** of this work is to develop innovative approaches to treat a narrow-spectrum of bacterial infections. As discussed in previous paragraphs, pathogens require micromolar concentrations of iron to better colonize the host. In order to do so, many pathogens have evolved multiple genetic mechanisms that confer resistance to iron starvation. To scavenge iron from the host, bacteria secrete small-molecule metal-ion chelators called “siderophores”. Specifically, most Enterobacteriaceae produce the siderophore enterobactin, which is essential for bacterial iron acquisition. However during inflammation, enterobactin is sequestered by the host antimicrobial peptide lipocalin-2. To overcome this host immune defense, some pathogens produce an additional siderophore called salmochelin, which cannot be sequestered by lipocalin-2. Because lipocalin-2 is effective in protecting the host from commensal bacteria and certain pathogens, we hypothesized that manipulating host iron sequestration to make it more

efficient could lead to innovative approaches for treating infection with Enterobacteriaceae. Additionally, pathogens and commensal bacteria have acquired several mechanisms to compete with each other in the gut. In particular, they can target specific competitors by delivering antimicrobial peptides, identified as microcins, which enter target bacteria through specific iron uptake systems. We also hypothesized that secretion of microcins could contribute to the beneficial activity of the probiotic *E. coli* Nissle by targeting competing Enterobacteriaceae in the inflamed gut, and therefore could lead to the development of new therapies against Enterobacteriaceae.

The primary objective of this research is to address the immediate need for novel therapeutic strategies against Enterobacteriaceae. Our **central hypothesis** is that targeting iron acquisition of pathogenic bacteria would result in the growth inhibition of selected bacterial sub-populations (Enterobacteriaceae), while having limited effects on the gut microbiota. This hypothesis is based on previous data revealing that iron acquisition promotes *S*. Typhimurium growth and competition with other microbes. Our work aimed to determine whether blocking iron acquisition, or targeting bacteria that express specific siderophore receptors, would result in bacterial growth inhibition. Specifically, we used the following two approaches:

1) The use of the probiotic *E. coli* Nissle strain to determine whether secreted antimicrobial peptides, called microcins (siderophore-conjugates) specifically target bacteria that express siderophore receptors in the inflamed gut.

2) The development of a novel immunization strategy against two siderophores produced by pathogenic Enterobacteriaceae.

Both approaches aim to selectively target members of the Enterobacteriaceae family that express both the targeted siderophores and their receptors. In particular, a major difference with broad-spectrum antibiotic treatments is that with our two approaches beneficial members of the microbiota will not be targeted. Moreover, a major advantage of our strategies is that siderophore synthesis and uptake machineries are conserved among species. Therefore, we hypothesized that our two strategies will be effective against several pathogenic Enterobacteriaceae, independently of differences in serotypes.

1.5 References

1. Hooper LV & Macpherson AJ Immune adaptations that maintain homeostasis with the intestinal microbiota. *Nat Rev Immunol* 10(3):159-169.
2. Spor A, Koren O, & Ley R (2011) Unravelling the effects of the environment and host genotype on the gut microbiome. *Nature reviews. Microbiology* 9(4):279-290.
3. Gill SR*, et al.* (2006) Metagenomic analysis of the human distal gut microbiome. *Science* 312(5778):1355-1359.
4. Ley RE*, et al.* (2008) Evolution of mammals and their gut microbes. *Science* 320(5883):1647-1651.
5. Sekirov I, Russell SL, Antunes LC, & Finlay BB (2010) Gut microbiota in health and disease. *Physiol Rev* 90(3):859-904.
6. Lawley TD & Walker AW (2013) Intestinal colonization resistance. *Immunology* 138(1):1-11.
7. Buffie CG & Pamer EG (2013) Microbiota-mediated colonization resistance against intestinal pathogens. *Nat Rev Immunol* 13(11):790-801.
8. Momose Y, Hirayama K, & Itoh K (2008) Competition for proline between indigenous *Escherichia coli* and *E. coli* O157:H7 in gnotobiotic mice associated with infant intestinal microbiota and its contribution to the colonization resistance against E. coli O157:H7. *Antonie Van Leeuwenhoek* 94(2):165-171.
9. Leatham MP*, et al.* (2009) Precolonized human commensal Escherichia coli strains serve as a barrier to *E. coli* O157:H7 growth in the streptomycin-treated mouse intestine. *Infection and immunity* 77(7):2876-2886.
10. Maltby R, Leatham-Jensen MP, Gibson T, Cohen PS, & Conway T (2013) Nutritional basis for colonization resistance by human commensal *Escherichia coli* strains HS and Nissle 1917 against *E. coli* O157:H7 in the mouse intestine. *PloS one* 8(1):e53957.
11. Hudault S, Guignot J, & Servin AL (2001) Escherichia coli strains colonising the gastrointestinal tract protect germfree mice against *Salmonella* typhimurium infection. *Gut* 49(1):47-55.
12. Fabich AJ*, et al.* (2008) Comparison of carbon nutrition for pathogenic and commensal *Escherichia coli* strains in the mouse intestine. *Infection and immunity* 76(3):1143-1152.
13. Schumann S, Alpert C, Engst W, Loh G, & Blaut M (2012) Dextran sodium sulfate-induced inflammation alters the expression of proteins by intestinal *Escherichia coli* strains in a gnotobiotic mouse model. *Appl Environ Microbiol* 78(5):1513-1522.
14. Theriot CM*, et al.* (2014) Antibiotic-induced shifts in the mouse gut microbiome and metabolome increase susceptibility to Clostridium difficile infection. *Nature communications* 5:3114.
15. Thiennimitr P*, et al.* (2011) Intestinal inflammation allows *Salmonella* to use ethanolamine to compete with the microbiota. *Proceedings of the National Academy of Sciences of the United States of America* 108(42):17480-17485.
16. Unterweger D*, et al.* (2014) The Vibrio cholerae type VI secretion system employs diverse effector modules for intraspecific competition. *Nat Commun* 5:3549.

17. Jani AJ & Cotter PA (2010) Type VI secretion: not just for pathogenesis anymore. *Cell host & microbe* 8(1):2-6.
18. Ruhe ZC, Low DA, & Hayes CS (2013) Bacterial contact-dependent growth inhibition. *Trends Microbiol* 21(5):230-237.
19. Patzer SI, Baquero MR, Bravo D, Moreno F, & Hantke K (2003) The colicin G, H and X determinants encode microcins M and H47, which might utilize the catecholate siderophore receptors FepA, Cir, Fiu and IroN. *Microbiology* 149(Pt 9):2557-2570.
20. Rebuffat S (Microcins in action: amazing defence strategies of Enterobacteria. *Biochem Soc Trans* 40(6):1456-1462.
21. Nolan EM & Walsh CT (2008) Investigations of the MceIJ-catalyzed posttranslational modification of the microcin E492 C-terminus: linkage of ribosomal and nonribosomal peptides to form "trojan horse" antibiotics. *Biochemistry* 47(35):9289-9299.
22. Nedialkova LP*, et al.* (2014) Inflammation Fuels Colicin Ib-Dependent Competition of *Salmonella* Serovar Typhimurium and *E. coli* in Enterobacterial Blooms. *PLoS pathogens* 10(1):e1003844.
23. Kamada N, Seo SU, Chen GY, & Nunez G. (2013) Role of the gut microbiota in immunity and inflammatory disease. *Nat Rev Immunol* 13(5):321-335.
24. Brestoff JR & Artis D (2013) Commensal bacteria at the interface of host metabolism and the immune system. *Nature immunology* 14(7):676-684.
25. Chu H & Mazmanian SK (2013) Innate immune recognition of the microbiota promotes host-microbial symbiosis. *Nature immunology* 14(7):668-675.
26. Spees AM, Lopez CA, Kingsbury DD, Winter SE, & Bäumler AJ (2013) Colonization resistance: battle of the bugs or Menage a Trois with the host? *PLoS pathogens* 9(11):e1003730.
27. Lupp C*, et al.* (2007) Host-mediated inflammation disrupts the intestinal microbiota and promotes the overgrowth of Enterobacteriaceae. *Cell host & microbe* 2(3):204.
28. Winter SE*, et al.* (2013) Host-derived nitrate boosts growth of *E. coli* in the inflamed gut. *Science* 339(6120):708-711.
29. Deriu E*, et al.* (2013) Probiotic bacteria reduce *salmonella* typhimurium intestinal colonization by competing for iron. *Cell host & microbe* 14(1):26-37.
30. Herias MV, Midtvedt T, Hanson LA, & Wold AE (1997) *Escherichia coli* K5 capsule expression enhances colonization of the large intestine in the gnotobiotic rat. *Infection and immunity* 65(2):531-536.
31. Podolsky S (1998) Cultural divergence: Elie Metchnikoff's Bacillus bulgaricus therapy and his underlying concept of health. *Bull Hist Med* 72(1):1-27.
32. FAO/WHO (2001) Expert consultation on evaluation of health and nutritional properties of probiotics in food including milk powder with live lactic acid bacteria. *(Food and Agriculture Organization/World Health Organization)*.
33. Nissle A (1961) Old and new experiences on therapeutic successes by restoration of the colonic flora with mutaflor in gastrointestinal diseases] *Med Welt* 29-30:1519-1523.
34. Jacobi CA & Malfertheiner P (2011) *Escherichia coli* Nissle 1917 (Mutaflor): new insights into an old probiotic bacterium. *Dig Dis* 29(6):600-607.

35. Westendorf AM*, et al.* (2005) Intestinal immunity of *Escherichia coli* NISSLE 1917: a safe carrier for therapeutic molecules. *FEMS immunology and medical microbiology* 43(3):373-384.
36. Grozdanov L*, et al.* (2004) Analysis of the genome structure of the nonpathogenic probiotic *Escherichia coli* strain Nissle 1917. *Journal of bacteriology* 186(16):5432-5441.
37. Vejborg RM, Friis C, Hancock V, Schembri MA, & Klemm P (2010) A virulent parent with probiotic progeny: comparative genomics of *Escherichia coli* strains CFT073, Nissle 1917 and ABU 83972. *Molecular genetics and genomics : MGG* 283(5):469-484.
38. Rabsch W, Tschape H, & Bäumler AJ (2001) Non-typhoidal salmonellosis: emerging problems. *Microbes Infect* 3(3):237-247.
39. Lasaro MA*, et al.* (2009) F1C fimbriae play an important role in biofilm formation and intestinal colonization by the *Escherichia coli* commensal strain Nissle 1917. *Appl Environ Microbiol* 75(1):246-251.
40. Grozdanov L*, et al.* (2002) A single nucleotide exchange in the wzy gene is responsible for the semirough O6 lipopolysaccharide phenotype and serum sensitivity of *Escherichia coli* strain Nissle 1917. *Journal of bacteriology* 184(21):5912-5925.
41. Burns SM & Hull SI (1998) Comparison of loss of serum resistance by defined lipopolysaccharide mutants and an acapsular mutant of uropathogenic Escherichia coli O75:K5. *Infection and immunity* 66(9):4244-4253.
42. Kruis W*, et al.* (1997) Double-blind comparison of an oral *Escherichia coli* preparation and mesalazine in maintaining remission of ulcerative colitis. *Aliment Pharmacol Ther* 11(5):853-858.
43. Splichalova A*, et al.* (2011) Interference of Bifidobacterium choerinum or *Escherichia coli* Nissle 1917 with *Salmonella* Typhimurium in gnotobiotic piglets correlates with cytokine patterns in blood and intestine. *Clin Exp Immunol* 163(2):242-249.
44. Hafez M, Hayes K, Goldrick M, Grencis RK, & Roberts IS (2010) The K5 capsule of *Escherichia coli* strain Nissle 1917 is important in stimulating expression of Toll-like receptor 5, CD14, MyD88, and TRIF together with the induction of interleukin-8 expression via the mitogen-activated protein kinase pathway in epithelial cells. *Infection and immunity* 78(5):2153-2162.
45. Ukena SN*, et al.* (2007) Probiotic *Escherichia coli* Nissle 1917 inhibits leaky gut by enhancing mucosal integrity. *PloS one* 2(12):e1308.
46. Valdebenito M, Crumbliss AL, Winkelmann G, & Hantke K (2006) Environmental factors influence the production of enterobactin, salmochelin, aerobactin, and yersiniabactin in *Escherichia coli* strain Nissle 1917. *Int J Med Microbiol* 296(8):513-520.
47. Kamada N*, et al.* (2008) Nonpathogenic E*scherichia coli* strain Nissle 1917 inhibits signal transduction in intestinal epithelial cells. *Infection and immunity* 76(1):214-220.
48. Grozdanov L*, et al.* (2004) Analysis of the genome structure of the nonpathogenic probiotic *Escherichia coli* strain Nissle 1917. *J Bacteriol* 186(16):5432-5441.

49. Behnsen J, Deriu E, Sassone-Corsi M, & Raffatellu M (2013) Probiotics: properties, examples, and specific applications. *Cold Spring Harb Perspect Med* 3(3):a010074.
50. Crump JA, Luby SP, & Mintz ED (2004) The global burden of typhoid fever. *Bull World Health Organ* 82(5):346-353.
51. Sojka WJ, Wray C, Shreeve J, & Benson AJ (1977) Incidence of *salmonella* infection in animals in England and Wales 1968--1974. *J Hyg (Lond)* 78(1):43-56.
52. Hoffmann S, Batz MB, & Morris JG, Jr. (2012) Annual cost of illness and quality-adjusted life year losses in the United States due to 14 foodborne pathogens. *Journal of food protection* 75(7):1292-1302.
53. Majowicz SE, *et al.* (2010) The global burden of nontyphoidal *Salmonella* gastroenteritis. *Clinical infectious diseases : an official publication of the Infectious Diseases Society of America* 50(6):882-889.
54. Okoro CK, *et al.* (2012) Intracontinental spread of human invasive *Salmonella* Typhimurium pathovariants in sub-Saharan Africa. *Nature genetics* 44(11):1215-1221.
55. Ao TT, *et al.* (2015) Global burden of invasive nontyphoidal *Salmonella* disease, 2010(1). *Emerging infectious diseases* 21(6).
56. Feasey NA, *et al.* (2015) Modelling the Contributions of Malaria, HIV, Malnutrition and Rainfall to the Decline in Paediatric Invasive Non-typhoidal *Salmonella* Disease in Malawi. *PLoS neglected tropical diseases* 9(7):e0003979.
57. Park SE, *et al.* (2016) The Relationship Between Invasive Nontyphoidal *Salmonella* Disease, Other Bacterial Bloodstream Infections, and Malaria in Sub-Saharan Africa. *Clinical infectious diseases : an official publication of the Infectious Diseases Society of America* 62 Suppl 1:S23-31.
58. Cheng MW, *et al.* (2015) Clinical characteristics in adult patients with *Salmonella* bacteremia and analysis of ciprofloxacin-nonsusceptible isolates. *Journal of microbiology, immunology, and infection = Wei mian yu gan ran za zhi* 48(6):692-698.
59. Havelaar AH, *et al.* (2015) World Health Organization Global Estimates and Regional Comparisons of the Burden of Foodborne Disease in 2010. *PLoS medicine* 12(12):e1001923.
60. Valdez Y, Ferreira RB, & Finlay BB (2009) Molecular mechanisms of *Salmonella* virulence and host resistance. *Current topics in microbiology and immunology* 337:93-127.
61. Galan JE & Curtiss R, 3rd (1991) Distribution of the invA, -B, -C, and -D genes of *Salmonella* typhimurium among other *Salmonella* serovars: *invA* mutants of *Salmonella* typhi are deficient for entry into mammalian cells. *Infection and immunity* 59(9):2901-2908.
62. Galan JE (2001) *Salmonella* interactions with host cells: type III secretion at work. *Annu Rev Cell Dev Biol* 17:53-86.
63. Coburn B, Li Y, Owen D, Vallance BA, & Finlay BB (2005) *Salmonella* enterica serovar Typhimurium pathogenicity island 2 is necessary for complete virulence in a mouse model of infectious enterocolitis. *Infection and immunity* 73(6):3219-3227.
64. Stecher B, *et al.* (2007) *Salmonella* enterica serovar typhimurium exploits inflammation to compete with the intestinal microbiota. *PLoS Biol* 5(10):2177-2189.

65. Vazquez-Torres A, *et al.* (2000) *Salmonella* pathogenicity island 2-dependent evasion of the phagocyte NADPH oxidase. *Science* 287(5458):1655-1658.
66. Chakravortty D, Hansen-Wester I, & Hensel M (2002) *Salmonella* pathogenicity island 2 mediates protection of intracellular *Salmonella* from reactive nitrogen intermediates. *J Exp Med* 195(9):1155-1166.
67. Godinez I, *et al.* (2009) Interleukin-23 orchestrates mucosal responses to *Salmonella* enterica serotype Typhimurium in the intestine. *Infection and immunity* 77(1):387-398.
68. Srinivasan A, *et al.* (2007) Innate immune activation of CD4 T cells in *salmonella*-infected mice is dependent on IL-18. *J Immunol* 178(10):6342-6349.
69. Raffatellu M, *et al.* (2008) Simian immunodeficiency virus-induced mucosal interleukin-17 deficiency promotes *Salmonella* dissemination from the gut. *Nat Med* 14(4):421-428.
70. Behnsen J, *et al.* (2014) The cytokine IL-22 promotes pathogen colonization by suppressing related commensal bacteria. *Immunity* 40(2):262-273.
71. Godinez I, *et al.* (2008) T cells help to amplify inflammatory responses induced by *Salmonella* enterica serotype Typhimurium in the intestinal mucosa. *Infection and immunity* 76(5):2008-2017.
72. Zheng J, Cui S, & Meng J (2009) Effect of transcriptional activators RamA and SoxS on expression of multidrug efflux pumps AcrAB and AcrEF in fluoroquinolone-resistant *Salmonella* Typhimurium. *J Antimicrob Chemother* 63(1):95-102.
73. Lupp C, *et al.* (2007) Host-mediated inflammation disrupts the intestinal microbiota and promotes the overgrowth of Enterobacteriaceae. *Cell host & microbe* 2(2):119-129.
74. Thiennimitr P, Winter SE, & Bäumler AJ (2012) *Salmonella,* the host and its microbiota. *Curr Opin Microbiol* 15(1):108-114.
75. Barman M, *et al.* (2008) Enteric salmonellosis disrupts the microbial ecology of the murine gastrointestinal tract. *Infection and immunity* 76(3):907-915.
76. Rodenburg W, *et al.* (2007) *Salmonella* induces prominent gene expression in the rat colon. *BMC Microbiol* 7:84.
77. Stecher B, *et al.* (2008) Motility allows *S*. Typhimurium to benefit from the mucosal defence. *Cell Microbiol* 10(5):1166-1180.
78. Winter SE, *et al.* (2010) Gut inflammation provides a respiratory electron acceptor for *Salmonella. Nature* 467(7314):426-429.
79. Aisen P, Enns C, & Wessling-Resnick M (2001) Chemistry and biology of eukaryotic iron metabolism. *The international journal of biochemistry & cell biology* 33(10):940-959.
80. Andreini C, Bertini I, Cavallaro G, Holliday GL, & Thornton JM (2008) Metal ions in biological catalysis: from enzyme databases to general principles. *Journal of biological inorganic chemistry : JBIC : a publication of the Society of Biological Inorganic Chemistry* 13(8):1205-1218.
81. Lieu PT, Heiskala M, Peterson PA, & Yang Y (2001) The roles of iron in health and disease. *Molecular aspects of medicine* 22(1-2):1-87.
82. Cassat JE & Skaar EP (2013) Iron in infection and immunity. *Cell host & microbe* 13(5):509-519.

83. Rishi G, Wallace DF, & Subramaniam VN (2015) Hepcidin: regulation of the master iron regulator. *Bioscience reports* 35(3).
84. Becker KW & Skaar EP (2014) Metal limitation and toxicity at the interface between host and pathogen. *FEMS microbiology reviews* 38(6):1235-1249.
85. Skaar EP & Raffatellu M (2015) Metals in infectious diseases and nutritional immunity. *Metallomics : integrated biometal science* 7(6):926-928.
86. Andrews SC, Robinson AK, & Rodriguez-Quinones F (2003) Bacterial iron homeostasis. *FEMS microbiology reviews* 27(2-3):215-237.
87. Stojiljkovic I, Cobeljic M, & Hantke K (1993) *Escherichia coli* K-12 ferrous iron uptake mutants are impaired in their ability to colonize the mouse intestine. *FEMS microbiology letters* 108(1):111-115.
88. Tsolis RM, Bäumler AJ, Heffron F, & Stojiljkovic I (1996) Contribution of TonB- and Feo-mediated iron uptake to growth of *Salmonella* typhimurium in the mouse. *Infection and immunity* 64(11):4549-4556.
89. Miethke M & Marahiel MA (2007) Siderophore-based iron acquisition and pathogen control. *Microbiology and molecular biology reviews : MMBR* 71(3):413-451.
90. Raffatellu M & Bäumler AJ (2010) *Salmonella*'s iron armor for battling the host and its microbiota. *Gut microbes* 1(1):70-72.
91. Goetz DH*, et al.* (2002) The neutrophil lipocalin NGAL is a bacteriostatic agent that interferes with siderophore-mediated iron acquisition. *Mol Cell* 10(5):1033-1043.
92. Flo TH*, et al.* (2004) Lipocalin 2 mediates an innate immune response to bacterial infection by sequestrating iron. *Nature* 432(7019):917-921.
93. Bachman MA, Miller VL, & Weiser JN (2009) Mucosal lipocalin 2 has pro-inflammatory and iron-sequestering effects in response to bacterial enterobactin. *PLoS Pathog* 5(10):e1000622.
94. Fischbach MA*, et al.* (2006) The pathogen-associated iroA gene cluster mediates bacterial evasion of lipocalin 2. *Proc Natl Acad Sci U S A* 103(44):16502-16507.
95. Bachman MA*, et al.* (2011) *Klebsiella pneumoniae* yersiniabactin promotes respiratory tract infection through evasion of lipocalin 2. *Infect Immun* 79(8):3309-3316.
96. Raffatellu M*, et al.* (2009) Lipocalin-2 resistance confers an advantage to *Salmonella* enterica serotype Typhimurium for growth and survival in the inflamed intestine. *Cell Host Microbe* 5(5):476-486.
97. Fischbach MA, Lin H, Liu DR, & Walsh CT (2006) How pathogenic bacteria evade mammalian sabotage in the battle for iron. *Nat Chem Biol* 2(3):132-138.
98. Hantke K, Nicholson G, Rabsch W, & Winkelmann G (2003) Salmochelins, siderophores of *Salmonella* enterica and uropathogenic Escherichia coli strains, are recognized by the outer membrane receptor IroN. *Proc Natl Acad Sci U S A* 100(7):3677-3682.
99. Fischbach MA, Lin H, Liu DR, & Walsh CT (2005) In vitro characterization of IroB, a pathogen-associated C-glycosyltransferase. *Proc Natl Acad Sci U S A* 102(3):571-576.
100. Bäumler AJ*, et al.* (1998) IroN, a novel outer membrane siderophore receptor characteristic of *Salmonella* enterica. *Journal of bacteriology* 180(6):1446-1453.
101. Valdebenito M, Crumbliss AL, Winkelmann G, & Hantke K (2006) Environmental factors influence the production of enterobactin, salmochelin, aerobactin, and

yersiniabactin in *Escherichia coli* strain Nissle 1917. *Int J Med Microbiol* 296(8):513-520.
102. Gonzalez-Pastor JE, San Millan JL, & Moreno F (1994) The smallest known gene. *Nature* 369(6478):281.
103. de Lorenzo V (1984) Isolation and characterization of microcin E492 from Klebsiella pneumoniae. *Arch Microbiol* 139(1):72-75.
104. Nolan EM, Fischbach MA, Koglin A, & Walsh CT (2007) Biosynthetic tailoring of microcin E492m: post-translational modification affords an antibacterial siderophore-peptide conjugate. *J Am Chem Soc* 129(46):14336-14347.
105. Welch RA*, et al.* (2002) Extensive mosaic structure revealed by the complete genome sequence of uropathogenic *Escherichia coli. Proceedings of the National Academy of Sciences of the United States of America* 99(26):17020-17024.
106. Vassiliadis G, Destoumieux-Garzon D, Lombard C, Rebuffat S, & Peduzzi J (2010) Isolation and characterization of two members of the siderophore-microcin family, microcins M and H47. *Antimicrob Agents Chemother* 54(1):288-297.
107. Lagos R*, et al.* (2001) Structure, organization and characterization of the gene cluster involved in the production of microcin E492, a channel-forming bacteriocin. *Mol Microbiol* 42(1):229-243.
108. Azpiroz MF & Lavina M (2004) Involvement of enterobactin synthesis pathway in production of microcin H47. *Antimicrob Agents Chemother* 48(4):1235-1241.

CHAPTER 2

Microcins mediate interspecies and intraspecies competition among Enterobacteriaceae in the inflamed gut

2.1 Summary

The Enterobacteriaceae are Gram-negative bacteria and include commensal organisms as well as primary and opportunistic pathogens that are among the leading causes of morbidity and mortality worldwide. Although Enterobacteriaceae often comprise only a small fraction (less than 1%) of the gut microbiota in the healthy intestine, some of these organisms can bloom in the inflamed gut (1, 2); indeed, expansion of enterobacteria is a hallmark of microbial imbalance known as “dysbiosis” (3). Microcins are small enterobacterial secreted proteins that possess antimicrobial activity *in vitro* (4, 5), but whose role *in vivo* has been unclear. Here we demonstrate that microcins enable the probiotic bacterium *Escherichia coli* Nissle 1917 to limit the expansion of competing Enterobacteriaceae (including pathogens and pathobionts) during intestinal inflammation. Only microcin-producing *E. coli* Nissle 1917 strains were able to limit the growth of competitors in the inflamed intestine, including competing *E. coli* strains (commensal *E. coli*, adherent-invasive *E. coli*) as well as the related pathogen *Salmonella enterica*. Moreover, therapeutic administration of *E. coli* Nissle 1917 wild-type, but not of the microcin mutant strain, to mice previously infected with *S. enterica*

reduced intestinal colonization of the pathogen. Our work provides the first evidence that microcins are important for inter and intra-species competition among the Enterobacteriaceae in the inflamed gut and indicate that microcins may provide a narrow-spectrum tool to inhibit enteric pathogens and to reduce the enterobacterial blooms observed in patients with dysbiosis.

2.2 Introduction

The mammalian gastrointestinal tract is colonized by trillions of microbes that are essential for the development of the mucosal immune system and for controlling enteric pathogens growth, a mechanism known as colonization resistance (6, 7). Obligate anaerobes belonging to the Bacteroidetes and Firmicutes phyla predominate during homeostatic conditions, whereas Proteobacteria constitute only a small fraction of the microbiota in the healthy gut (8). In contrast, use of antibiotics or development of intestinal inflammation can profoundly alter the microbiota, with the reduction in obligate anaerobes and expansion of Proteobacteria leading to a state known as dysbiosis (9, 10). Among the Proteobacteria, pathogens and pathobionts (i.e., commensal microbes with the potential to cause disease) of the Enterobacteriaceae family have been shown to benefit from the nutritional environment created in the host during inflammation (11). Indeed, the emerging picture is that instead of being controlled by the host's mucosal immunity, some enterobacteria exploit host inflammation to thrive (11).

As use of broad-spectrum antibiotics is largely unsuccessful in limiting enterobacterial replication in the gut, and as many Enterobacteriaceae are global causes of morbidity and mortality, novel strategies are needed to limit the expansion of these pathogens and pathobionts. Such efforts can be guided by identifying mechanisms employed by beneficial microbes to provide colonization resistance to pathogens and pathobionts (7). Here we sought to identify an *in vivo* role for a class of microcins by studying the interplay between the probiotic, microcin-producing bacterium *Escherichia coli* Nissle 1917 (EcN) (12, 13) and some of its related, potentially harmful competitors in the

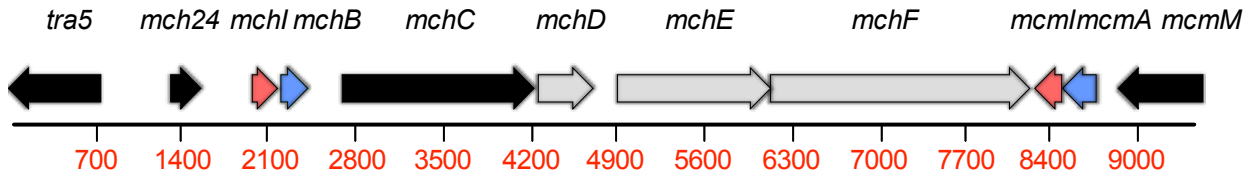
intestinal tract. Similar to bacteriocins secreted by Gram-positive bacteria, microcins can exert potent antimicrobial activity against related bacterial strains *in vitro* (14-16). In contrast to bacteriocins (15), an *in vivo* role for microcins has not been convincingly demonstrated since their discovery in 1976 (17). Early reports that microcin-producing Enterobacteriaceae are present in human stool samples led to the hypothesis that microcins may contribute to microbial ecology in the gut (18). However, this claim has never been thoroughly investigated and the biological role of microcins *in vivo* is still unclear (19).

2.3 Results

Microcins are dispensable in the absence of intestinal inflammation.

The microcin gene cluster of EcN is located on Genomic Island I (**Fig. 2.1)** and encodes for two microcins: microcin M (*mcmA*) and microcin H47 (*mchB*). To determine whether these microcins are involved in establishing a niche in the intestine, we intragastrically inoculated wild-type mice with an equal mixture of a commensal *E. coli* strain previously isolated from the mouse intestine(20) and either wild-type EcN or an isogenic mutant unable to secrete both microcins (EcN *mchDEF*) (**Fig. 2.2 A**).

FIGURE 2.1



Gene name	Gene size	Annotation	Source of reference
tra5	753 bp	transposase	(21)
mch24	246 bp	enterobactin production	(22)
mchI	210 bp	self-immunity for MccH47	(23)
mchB	228 bp	microcin H47 precursor	(24)
mchC	1551 bp	glycotransferase	(25, 26)
mchD	453 bp	enterobactin esterase	(25, 26)
mchE	1242 bp	microcin export	(14, 24, 27)
mchF	2097 bp	microcin export	(14, 24, 27)
mcmI	222 bp	self-immunity for MccM	(14)
mcmA	279 bp	microcin M precursor	(28)
mcmM	687 bp	microcin export	(14, 24, 27)

Figure 2.1 Representation of microcin gene cluster in *E. coli* Nissle. Organization of *E.coli* Nissle microcins genes cluster and annotation of genes functions.

Although all strains poorly colonized the intestine of healthy mice (as stated earlier, enterobacteria typically colonize the intestine at low levels in the absence of perturbation), similar numbers of the commensal *E. coli* or of the wild-type EcN and *mchDEF* mutant were recovered beginning at day 1 to 5 post oral administration (**Fig. 2.2 A-C**. Because, all strains poorly colonized SPF mice, we performed similar studies in streptomycin-treated SPF or germ-free mice, by administering the commensal *E. coli* alone or in competition with wild-type EcN, EcN *mchDEF* or the EcN *mcmA mchB* mutants (which lacks both microcins precursor genes). In these settings all strains highly colonized the mouse gut and similarly we found comparable numbers of the commensal *E. coli* (**Fig. 2.3 A, B**) and of the three EcN strains in the fecal content, up to day 5 post-inoculation in the absence of intestinal inflammation (**Fig. 2.3 C, D, G**). Moreover, the commensal *E. coli* outcompeted both wild-type EcN and the EcN *mchDEF* or the EcN *mcmA mchB* mutants to a similar extent in both SPF streptomycin-treated and germ-free mice, most likely because this mouse commensal *E.coli* strain is better adapt to colonize the mouse gut (**Fig. 2.3 E, F**). These results indicated that EcN's microcins are dispensable under homeostatic conditions, a result that may explain why a phenotype for microcins *in vivo* has not been convincingly demonstrated to date.

A prior study showed that the two EcN microcins exhibit antibacterial activity in iron-limited media (14). Moreover, a subset of microcins (including the two produced by EcN) are post-translationally modified at the C-terminus with a siderophore moiety (21, 29, 30). Siderophores are small molecules that chelate iron. Commensals and pathogens secrete these molecules to acquire the essential metal nutrient iron from

environments where this metal is limited (31). Bacterial uptake of iron-bound siderophores occurs via specific membrane receptors (14). Like siderophores, microcins linked to siderophore-like platforms can target bacteria *in vitro* through siderophore receptors (14, 16), a mechanism described as a 'Trojan horse' mode of action (4). This mechanism allows strains that produce these microcins to specifically target closely related strains under iron limitation *in vitro*, on the basis of the expression of common siderophore receptors (14). Incorporating these observations, we hypothesized that microcins can contribute to competition among enterobacteria in the inflamed gut, where iron is limited (32).

In agreement with the aforementioned study (14), we found that EcN's two microcin genes (*mcmA* and *mchB*) are expressed in iron-limited media, and that their expression is completely ablated following iron supplementation (**Fig. 2.3 H**).

FIGURE 2.2

Figure 2.2 *E. coli* Nissle wild-type and microcin mutant (*mchDEF*) gut colonization during competition with commensal *E. coli* in the absence of intestinal inflammation.

A-F Groups of mice conventional mice (SPF) were intragastrically inoculated with commensal *E. coli* alone or in competition at a 1:1 ratio with either wild-type EcN or EcN *mchDEF* mutant. **A**, Competitive index (CI) of wild-type EcN or EcN *mchDEF* over commensal *E. coli* in conventional mice (SPF) fecal content at day 1-5 post-inoculation (n = 5 per group). **B**, CFU/mg of commensal *E.coli* in conventional mice (SPF) fecal content from at day 1-5 post-inoculation, when in competition with wild-type EcN or EcN *mchDEF*. **C**, CFU/mg of wild-type EcN or EcN *mchDEF* when in competition with commensal *E. coli* in conventional mice (SPF) fecal content, at day 1-5 post-inoculation. **D**, Histopathology scores in the caecum at day 5 post-inoculation with commensal *E. coli* alone and in competition with either wild-type EcN or EcN *mchDEF* (n = 5 per group). **E**, Expression of *Lcn2*, *Il17a*, *Ly6g*, *Il22*, *Tnfa*, *Nos2,* and *Il10* genes at day 5 post-inoculation in the caecum of mice inoculated with commensal *E. coli* alone and in competition with either wild-type EcN or EcN *mchDEF* (n = 5 per group). Data are expressed as fold increase over mock treated mice. **F**, H&E stained sections from representative animals for each groups at day 5 post-inoculation. **A**,**E**, Bars represent the geometric mean ± standard error. **B-D**, Each circle represents an individual mouse and bars represent the geometric mean. n.s.=not significant.

FIGURE 2.2

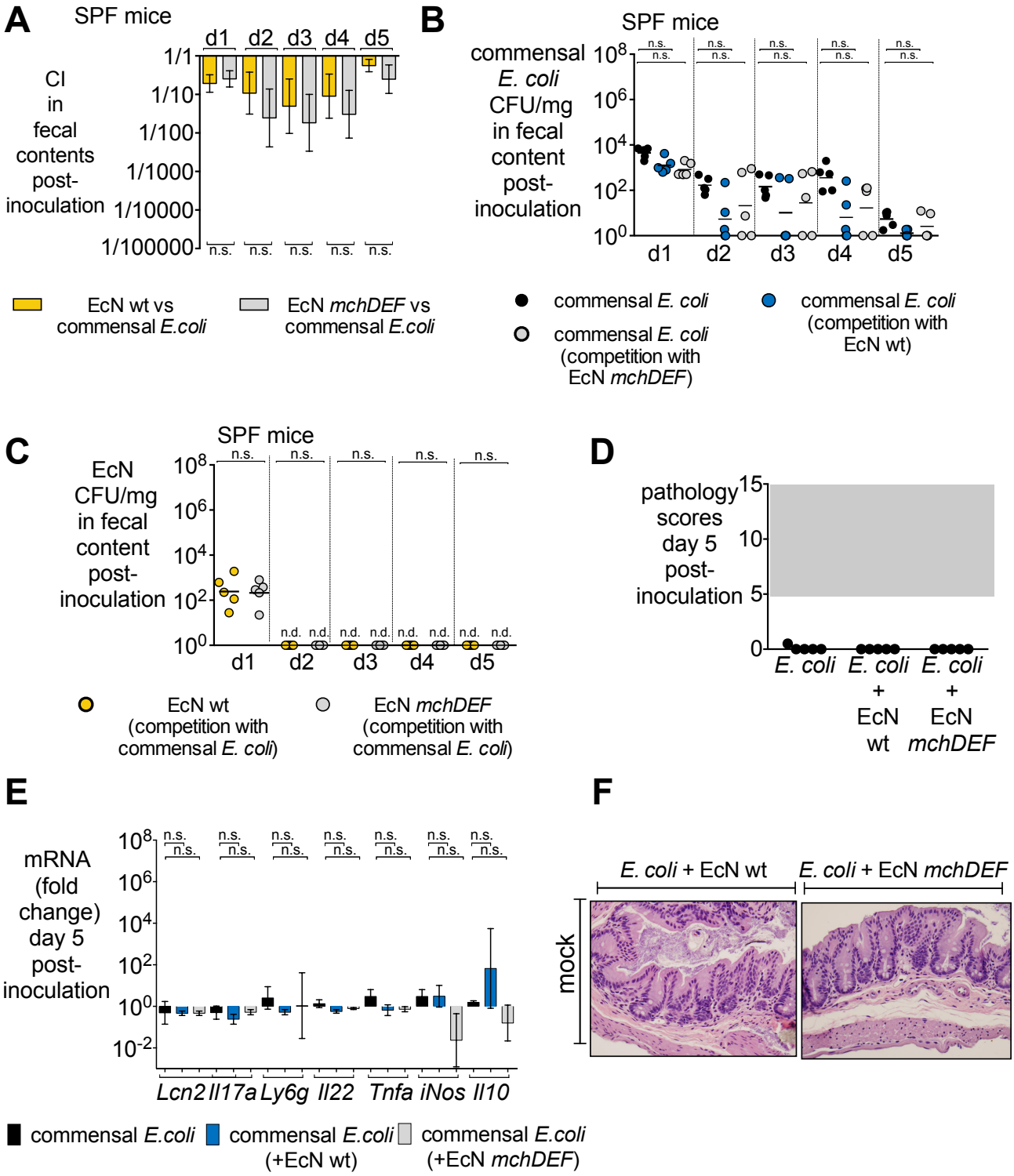
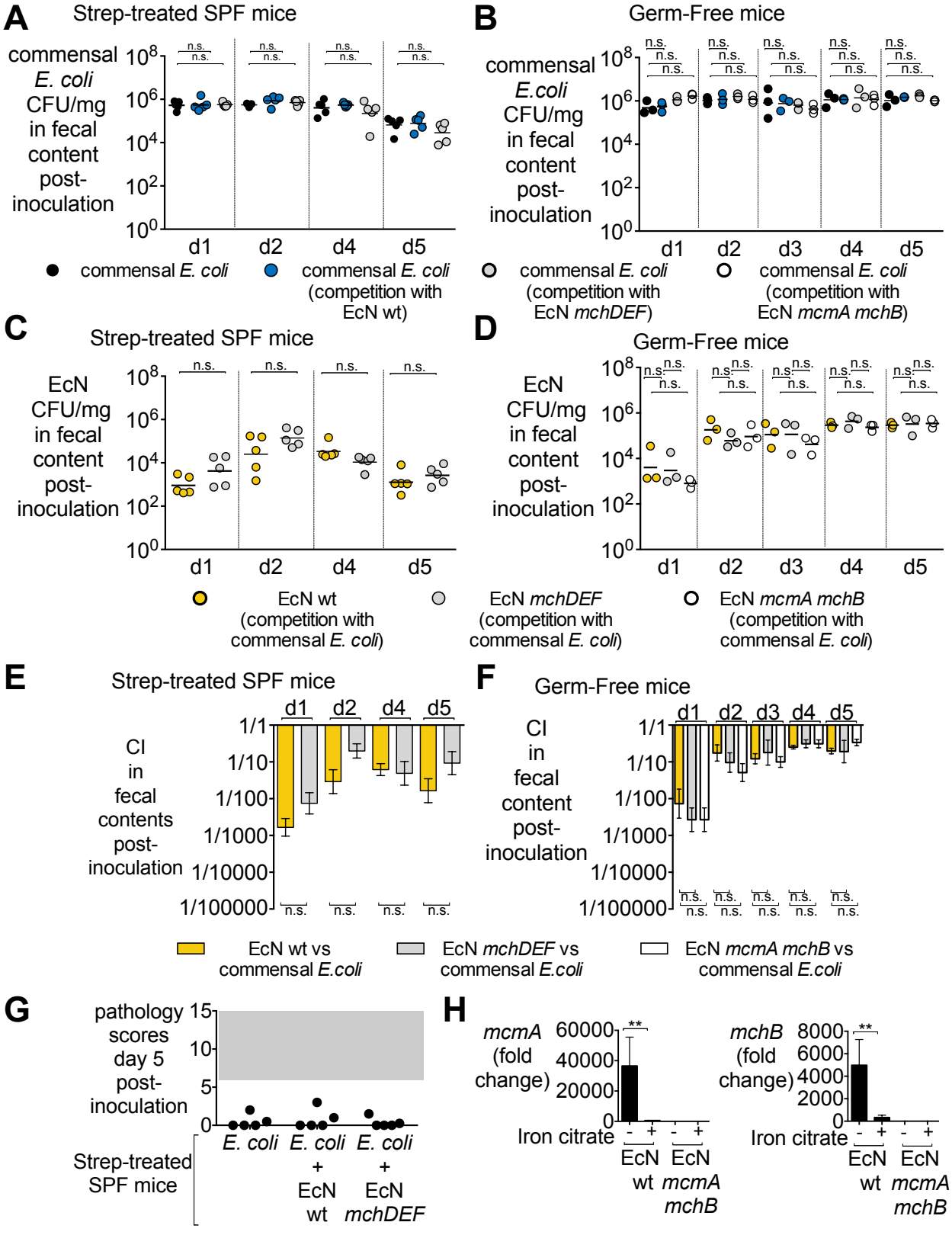

A
SPF mice
d1 d2 d3 d4 d5
CI in fecal contents post-inoculation
1/1
1/10
1/100
1/1000
1/10000
1/100000
n.s.
EcN wt vs commensal E.coli
EcN mchDEF vs commensal E.coli
B
SPF mice
commensal E. coli CFU/mg in fecal content post-inoculation
d1 d2 d3 d4 d5
commensal E. coli
commensal E. coli (competition with EcN mchDEF)
commensal E. coli (competition with EcN wt)
C
SPF mice
EcN CFU/mg in fecal content post-inoculation
n.d.
d1 d2 d3 d4 d5
EcN wt (competition with commensal E. coli)
EcN mchDEF (competition with commensal E. coli)
D
pathology scores day 5 post-inoculation
E. coli
E. coli + EcN wt
E. coli + EcN mchDEF
E
mRNA (fold change) day 5 post-inoculation
Lcn2 Il17a Ly6g Il22 Tnfa iNos Il10
commensal E.coli
commensal E.coli (+EcN wt)
commensal E.coli (+EcN mchDEF)
F
E. coli + EcN wt
E. coli + EcN mchDEF
mock

FIGURE 2.3

Figure 2.3. Microcins are dispensable in the absence of intestinal inflammation. **A**,**C**,**E**,**G** Groups of conventional mice specific pathogen-free (SPF) were treated with streptomycin a day prior being intragastrically inoculated with commensal *E. coli* alone or in competition with either wild-type EcN or EcN *mchDEF.* **B**,**D**,**F** Groups of germ-free (GF) mice were intragastrically inoculated with commensal *E. coli* alone or in competition with either wild-type EcN, EcN *mchDEF* or EcN *mcmA mchB.* **A**,**B**, commensal *E. coli* CFU/mg of feces in mouse fecal content at day 1-5 post-inoculation, when in competition with wild-type EcN, EcN *mchDEF* or EcN *mcmA mchB* in SPF (**A**) or germ free animals (**B**). **C**,**D**, CFU/mg of wild-type EcN, EcN *mchDEF* and EcN *mcmA mchB* when in competition with commensal *E. coli* in mouse fecal content, at day 1-post-inoculation in SPF (**c**) or germ free animals (**D**). **A**-**D** Each circle represents an individual mouse; bars represent the geometric mean. **E**,**F**, Competitive index (CI) of wild-type EcN, EcN *mchDEF* or EcN *mcmA mchB* over commensal *E. coli* in mouse fecal content at day 1-5 post-inoculation in SPF (n = 5 per group) (**E**) or germ free animals (**F**) (n = 3 per group). Bars represent the mean ± standard error. **G**, Histopathology scores in the caecum of streptomycin-treated mice at day 5 after inoculation with commensal *E. coli* and either wild-type EcN or EcN *mchDEF* (n = 5 per group). **A**-**D** and **G,** Each circle represents an individual mouse; bars represent the geometric mean. **H**, *In vitro* expression of (**A**) *mcmA* (encoding for microcin M) and (**B**) *mchB* (encoding for microcin H47) in iron-rich and iron-limited media. Wild-type EcN and the *mcmA mchB* mutant were grown either in low iron conditions (DMEM+10%FBS) or in DMEM+10%FBS supplemented with 1 μM iron citrate. At 7 hours post-inoculation, relative levels of *mcmA* and *mchB* mRNA were measured by quantitative real time PCR. Transcription of *mchB* and *mcmA* was normalized to the respective levels of bacterial *gapA* mRNA. Bars represent the geometric mean of three independent experiments ± standard error. ***P*<0.01; n.s.=not significant.

FIGURE 2.3


A
Strep-treated SPF mice
commensal E. coli CFU/mg in fecal content post-inoculation
n.s.
d1
d2
d4
d5
commensal E. coli
commensal E. coli (competition with EcN wt)
B
Germ-Free mice
commensal E.coli CFU/mg in fecal content post-inoculation
d3
commensal E. coli (competition with EcN mchDEF)
commensal E. coli (competition with EcN mcmA mchB)
C
Strep-treated SPF mice
EcN CFU/mg in fecal content post-inoculation
EcN wt (competition with commensal E. coli)
D
Germ-Free mice
EcN mchDEF (competition with commensal E. coli)
EcN mcmA mchB (competition with commensal E. coli)
E
Strep-treated SPF mice
CI in fecal contents post-inoculation
1/1
1/10
1/100
1/1000
1/10000
1/100000
EcN wt vs commensal E.coli
EcN mchDEF vs commensal E.coli
EcN mcmA mchB vs commensal E.coli
F
Germ-Free mice
CI in fecal content post-inoculation
G
pathology scores day 5 post-inoculation
15
10
5
0
E. coli
E. coli + EcN wt
E. coli + EcN mchDEF
Strep-treated SPF mice
H
mcmA (fold change)
60000
40000
20000
0
**
Iron citrate
EcN wt
EcN mcmA mchB
mchB (fold change)
8000
6000
4000
2000

Microcins are dispensable in the absence of intestinal inflammation.

Microcins enhance *E. coli* Nissle growth and competition against commensal *E. coli* for a niche in the inflamed gut.

To test whether microcins play a role during intestinal inflammation, we utilized the dextran sulfate sodium (DSS)-treated mouse model of colitis (**Fig. 2.4 A**). First, we intragastrically inoculated SPF, DSS-treated mice with an equal mixture of commensal *E. coli* and either wild-type EcN. EcN *mchDEF* or EcN *mcmA mchB*. We found that commensal *E. coli* initially had a low competitive advantage (approximately 10-fold) over wild-type EcN in the fecal content, however both strains colonized equally well at day 5 post-inoculation. In contrast, commensal *E. coli* exhibited a much larger competitive advantage (up to 10,000-fold) over the EcN *mchDEF* or EcN *mcmA mchB* mutants both in the fecal and the cecal content (**Fig. 2.4 B and 2.5 A**), and this phenotype was reversed by complementing the EcN *mchDEF* mutant *in trans* (**Fig. 2.4 B**). Although intestinal colonization of commensal *E. coli* was similar when alone or in competition with either wild-type EcN or the EcN *mchDEF* mutant at day 1-3 post-inoculation, only wild-type EcN was able to significantly reduce commensal *E. coli* colonization in the following days (**Fig. 2.4 C and 2.5 B**). Similarly, the EcN *mcmA mchB* mutant did not reduced the commensal *E. coli* colonization compared to the wild-type EcN as this strain is the phenocopy of EcN *mchDEF* mutant. (**Fig. 2.6 A**).

FIGURE 2.4

Figure 2.4 Microcins enhance *E. coli* Nissle growth and competition against commensal *E. coli* for a niche in the inflamed gut.
A, Schematic representation of the experimental design for (**A**-**D**). Groups of mice were treated with 4% dextran sodium sulfate (DSS) *per os* for 4 days, then intragastrically inoculated with wild-type EcN, EcN *mchDEF,* EcN *mcmA mchB* or EcN *mchDEF* complemented *in trans* (pWSK29::*mchDEF*), in competition at a 1:1 ratio with commensal *E. coli*. DSS treatment was suspended for 24 hours at day 1 and restarted at 2% for the remainder of the experiment. **B**, Competitive index (CI) of wild-type EcN, EcN *mchDEF*, EcN *mcmA mchB* or EcN *mchDEF* (pWSK29::*mchDEF*) over commensal *E. coli* in mouse fecal content (day 1-4) and caecum (day 5) post-inoculation (n = 5-6 per group). **C**, commensal *E. coli* CFU per mg of feces in mouse fecal (day 1-4) and caecum content (day 5) post-inoculation, in competition with wild-type EcN, EcN *mchDEF* or EcN *mchDEF* (pWSK29::*mchDEF*) **D**, CFU/mg of wild-type EcN, EcN *mchDEF*, or EcN *mchDEF* (pWSK29::*mchDEF*), in competition with commensal *E. coli* in mouse fecal (day 1-4) and caecum content (day 5) post-inoculation. **E**, Schematic representation of the experimental design for (**F**,**G**). Groups of mice were treated with 4% dextran sodium sulfate (DSS) *per os* for 4 days, then intragastrically inoculated with wild-type EcN in competition at 1:1 ratio with either EcN *mchDEF or* EcN *mcmA mchB.* **F**, CFU/mg of wild-type EcN and EcN *mchDEF* when in competition or wild-type EcN and EcN *mcmA mchB* when in competition in mouse fecal content at day 1 to day 5 post-inoculation. **G**, Competitive index (CI) of wild-type EcN over EcN *mchDEF* or of wild-type EcN over EcN *mcmA mchB* at day 1 to day 5 post-inoculation (n = 5). **B**,**G** Bars represent the mean ± standard error. **C**,**D**,**F**, Each circle represents an individual mouse; bars represent the geometric mean. Data are representative of n = 2 experiments. **P*<0.05 ***P*<0.01; n.s.=not significant.

FIGURE 2.4

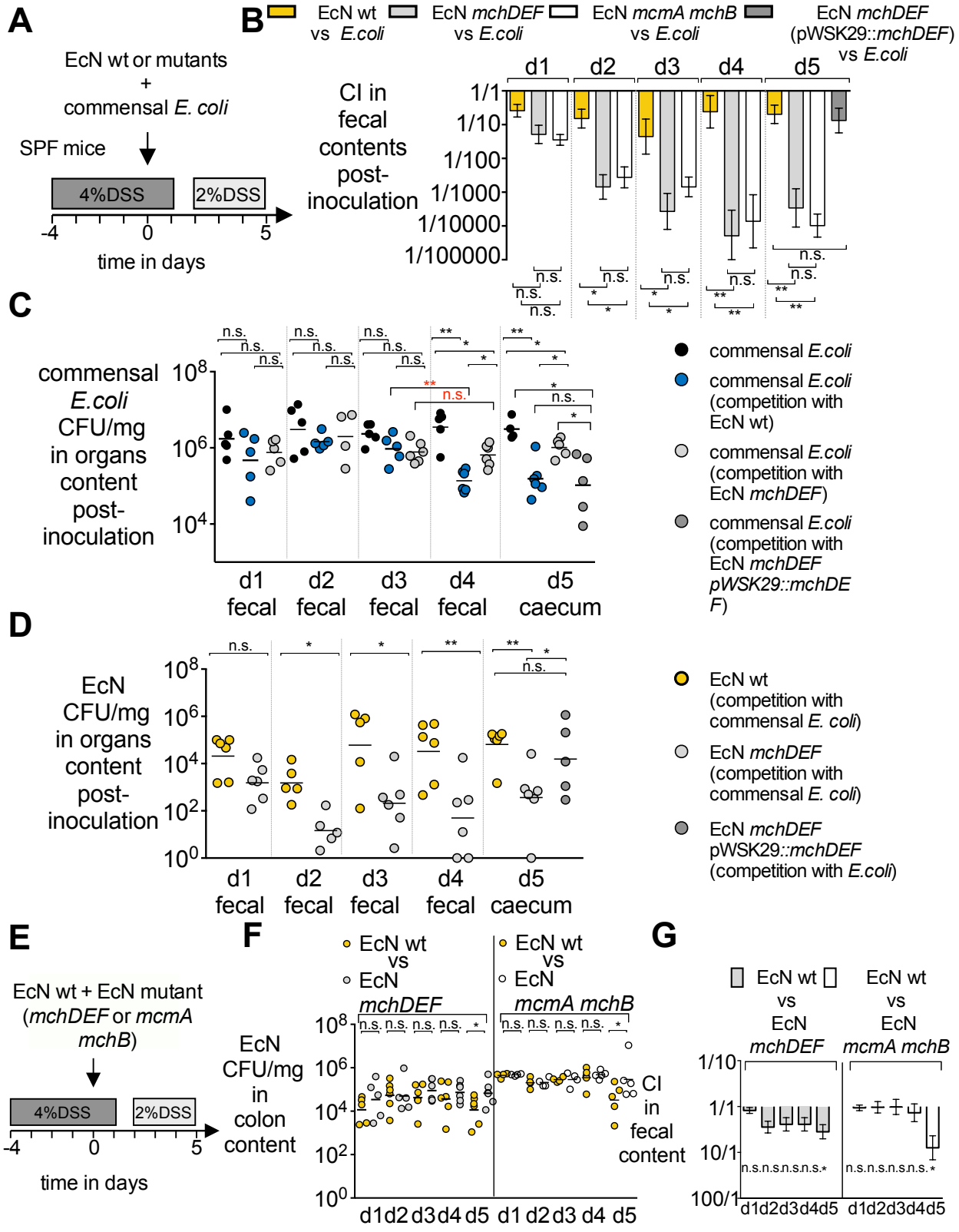

A
EcN wt or mutants
+
commensal E. coli
SPF mice
4%DSS
2%DSS
-4
0
5
time in days
B
EcN wt vs E.coli
EcN mchDEF vs E.coli
EcN mcmA mchB vs E.coli
EcN mchDEF (pWSK29::mchDEF) vs E.coli
CI in fecal contents post-inoculation
d1
d2
d3
d4
d5
1/1
1/10
1/100
1/1000
1/10000
1/100000
n.s.
C
commensal E.coli CFU/mg in organs content post-inoculation
d1 fecal
d2 fecal
d3 fecal
d4 fecal
d5 caecum
commensal E.coli
commensal E.coli (competition with EcN wt)
commensal E.coli (competition with EcN mchDEF)
commensal E.coli (competition with EcN mchDEF pWSK29::mchDEF)
D
EcN CFU/mg in organs content post-inoculation
EcN wt (competition with commensal E. coli)
EcN mchDEF (competition with commensal E. coli)
EcN mchDEF pWSK29::mchDEF (competition with E.coli)
E
EcN wt + EcN mutant (mchDEF or mcmA mchB)
4%DSS
2%DSS
time in days
F
EcN wt vs EcN mchDEF
EcN wt vs EcN mcmA mchB
EcN CFU/mg in colon content
CI in fecal content
G
EcN wt vs EcN mchDEF
EcN wt vs EcN mcmA mchB

FIGURE 2.5

Figure 2.5 Colonization and histopathology of EcN wild-type and microcin mutant (*mchDEF*) in competition with commensal *E. coli*, in mice with DSS-colitis.
A-G, Mice were treated with 4% dextran sodium sulfate (DSS) in the drinking water for 4 days, then intragastrically inoculated with commensal *E. coli* alone or in competition at a 1:1 ratio with either wild-type EcN or a mutant in microcin export (EcN *mchDEF*). **A**, Competitive index (CI) of wild-type EcN or EcN *mchDEF* over commensal *E. coli* at day 5 post-inoculation in cecal content (n = 6 per group). Bars represent the mean ± standard error. **B**, CFU/mg at day 5 post-inoculation in fecal content of commensal *E.coli* when in competition with either wild-type EcN or EcN *mchDEF*. **C**, CFU/mg at day 5 post-inoculation in fecal content of wild-type EcN or EcN *mchDEF* when in competition with the commensal *E.coli*. **D**, Expression of *Lcn2*, *Il17a*, *Ly6g*, *Il22*, *Tnfa*, *Nos2,* and *Il10* genes at day 5 post-inoculation in the caecum of mice inoculated with commensal *E. coli* alone and in competition with either wild-type EcN or EcN *mchDEF* (n = 5 per group). Data are expressed as fold increase over mock treated mice. **E**, Histopathology scores in the caecum at day 5 post-inoculation with commensal *E. coli* alone and in competition with either wild-type EcN or EcN *mchDEF* (n = 5 per group). **F**, Detailed histopathology scoring of the animals shown in (**E**). **G**, H&E stained sections from representative animals for each groups at day 5 post-inoculation. **A**,**D**, Bars represent the geometric mean ± standard error. **B**,**C**,**E**, Each circle represents an individual mouse and bars represent the geometric mean. **P*<0.05 ***P*<0.01; n.s.=not significant.

FIGURE 2.5

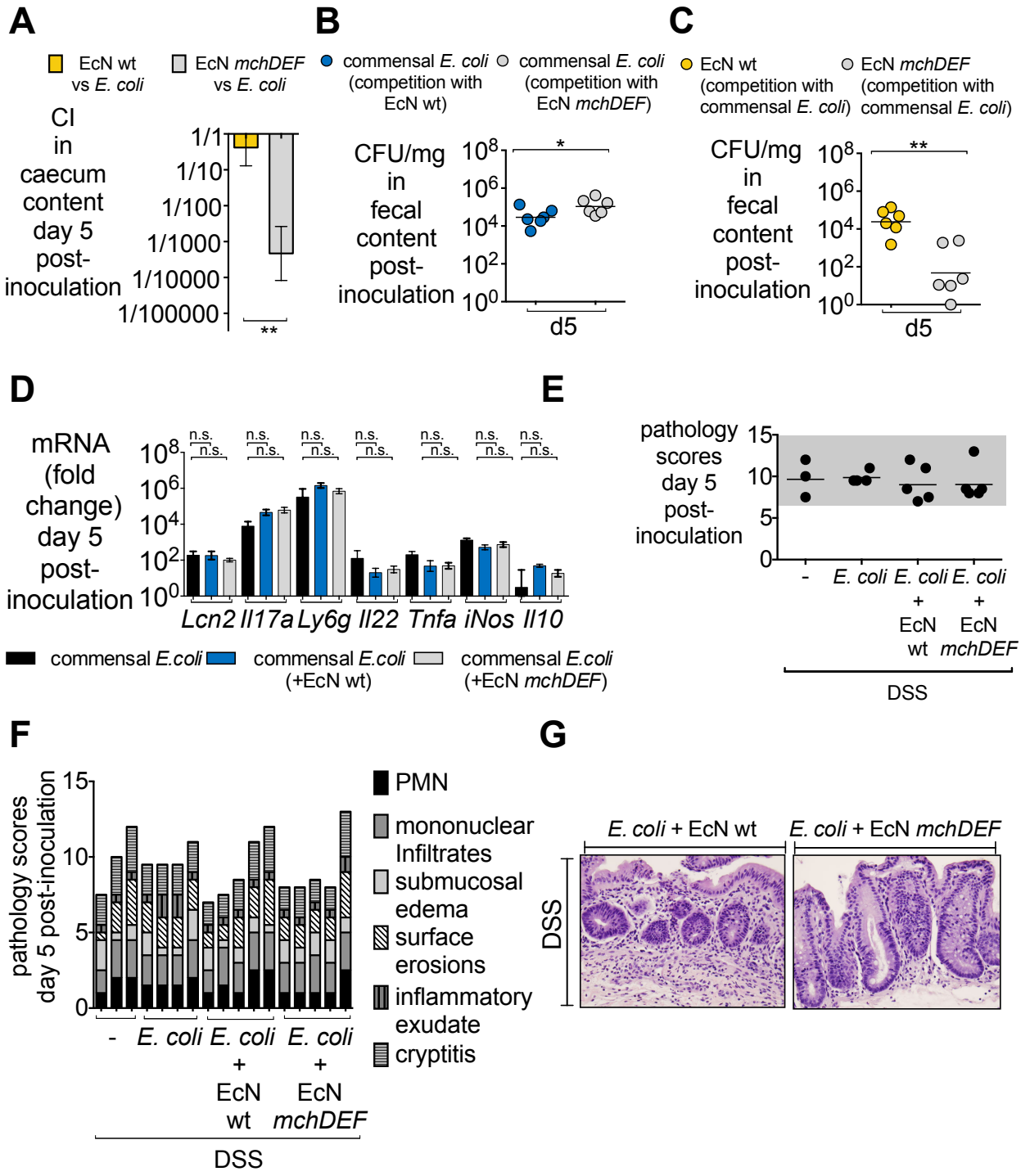

A
EcN wt vs E. coli
EcN mchDEF vs E. coli
CI in caecum content day 5 post-inoculation
1/1
1/10
1/100
1/1000
1/10000
1/100000
**
B
commensal E. coli (competition with EcN wt)
commensal E. coli (competition with EcN mchDEF)
CFU/mg in fecal content post-inoculation
*
d5
C
EcN wt (competition with commensal E. coli)
EcN mchDEF (competition with commensal E. coli)
CFU/mg in fecal content post-inoculation
**
d5
D
mRNA (fold change) day 5 post-inoculation
n.s.
Lcn2 Il17a Ly6g Il22 Tnfa iNos Il10
commensal E.coli
commensal E.coli (+EcN wt)
commensal E.coli (+EcN mchDEF)
E
pathology scores day 5 post-inoculation
- E. coli E. coli + EcN wt E. coli + EcN mchDEF
DSS
F
pathology scores day 5 post-inoculation
PMN
mononuclear Infiltrates
submucosal edema
surface erosions
inflammatory exudate
cryptitis
- E. coli E. coli + EcN wt E. coli + EcN mchDEF
DSS
G
E. coli + EcN wt
E. coli + EcN mchDEF
DSS

FIGURE 2.6

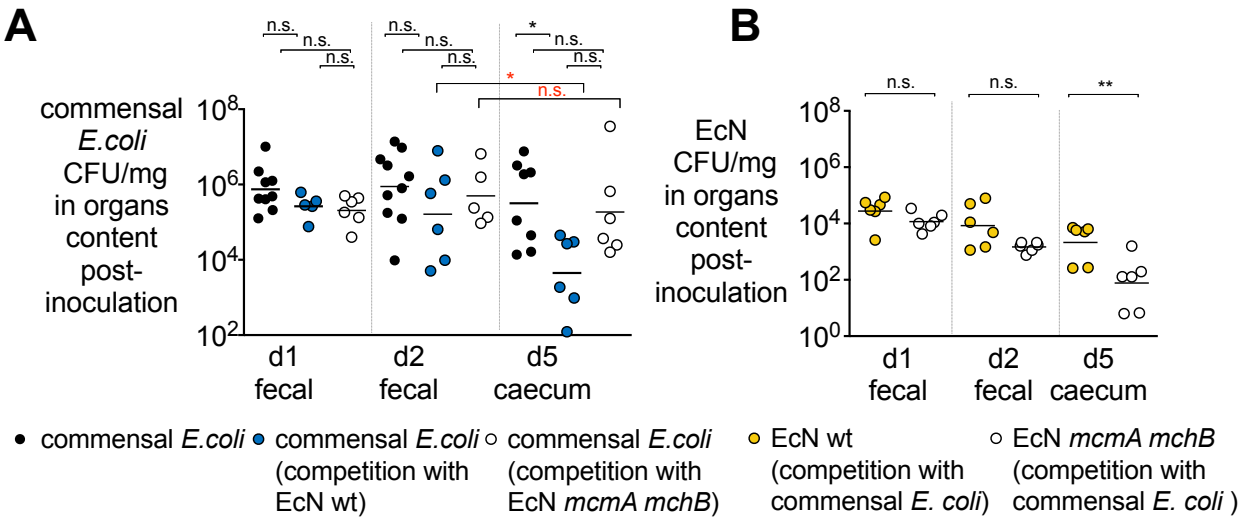


Figure 2.6 Colonization of wild-type EcN and microcin mutant (*mcmA mchB*) in competition with commensal *E. coli*, in mice with DSS-colitis.
A,**B**, Mice were treated with 4% DSS in the drinking water for 4 days, then intragastrically inoculated with a mixture of commensal *E. coli* and either wild-type EcN or a mutant lacking microcin genes precursors (EcN *mcmA mchB*). **A**, CFU/mg at day 1, 2 and 5 post-inoculation in fecal content of commensal *E.coli* when in competition with either wild-type EcN or EcN *mcmA mchB*. **B**, CFU/mg at day 1, 2 and 5 post-inoculation in colon content of wild-type EcN or EcN *mcmA mchB* when in competition with the commensal *E.coli*. Each circle represents an individual mouse and bars represent the geometric mean. **P*<0.05 ***P*<0.01; n.s.=not significant.

Consistent with our *in vivo* results, *in vitro* killing of commensal *E. coli* was only observed in competition with wild-type EcN in iron-limited media, and not when in competition with the EcN *mchDEF* or EcN *mchB mcmA* mutants (**Fig. 2.7 A and B**). Although, the growth of the EcN *mchDEF* or EcN *mchB mcmA* mutants was not impaired *in vitro* under conditions of iron starvation in non-competitive or competitive settings (**Fig. 2.7 A and B and Fig. 2.8 A-E**). both strains growth was impaired during *in vivo* gut colonization when in competition with the commensal *E.coli* (**Fig. 2.4 D and Fig. 2.5 6B)**, but rescued when the EcN *mchDEF* was complemented *in trans* (**Fig. 2.4 D)**. Collectively, these results indicate that microcin enable EcN to limit the expansion of a related commensal organism in the inflamed gut (**Fig. 2.5 D-G),** where both strains most likely compete for a similar niche.

Microcins provide a competitive advantage to *E. coli* Nissle in the inflamed gut only in the presence of a closely related competitor

In addition, wild-type EcN, EcN *mchDEF or* EcN *mcmA mchB* mutants colonized DSS-treated mice equally well when alone or when in competition with wild-type EcN but in the absence of the commensal *E. coli* (**Fig. 2.4 E-G**).. We even observed a competitive advantage of the mutant strains over the wild-type EcN at later time points (day 5 post-inoculation) (**Fig. 2.4 G)**. These latter data suggest that microcin expression may be metabolically unfavorable for wild-type EcN in the presence of a competitor whose growth cannot be inhibited due to the expression of immunity genes (*mcmI* and *mchI*). Additionally, wild-type EcN rescued the colonization defect of the EcN *mchDEF* or EcN

mcmA mchB mutants when both strains were administered together with commensal *E. coli* in DSS-treated mice (**Fig. 2.9 and Fig. 2.10**). Taken together, these findings indicate that microcin mutants are not attenuated *per se*, and that microcins are dispensable unless two simultaneous conditions occur: intestinal inflammation and the presence of a related competitor.

Interestingly, the wild-type EcN did not reduce the commensal *E.coli* growth when mice were fed an iron-rich diet for 3 weeks prior DSS treatment (**Fig. 2.11 A**). Moreover both wild-type EcN and EcN *mchDEF* colonized at similar levels although the presence of inflammation (**Fig. 2.11 B-C**), suggesting that in the absence of iron starvation but in the presence of inflammation wild-type EcN is unable to employ microcins in order to compete for a niche.

FIGURE 2.7

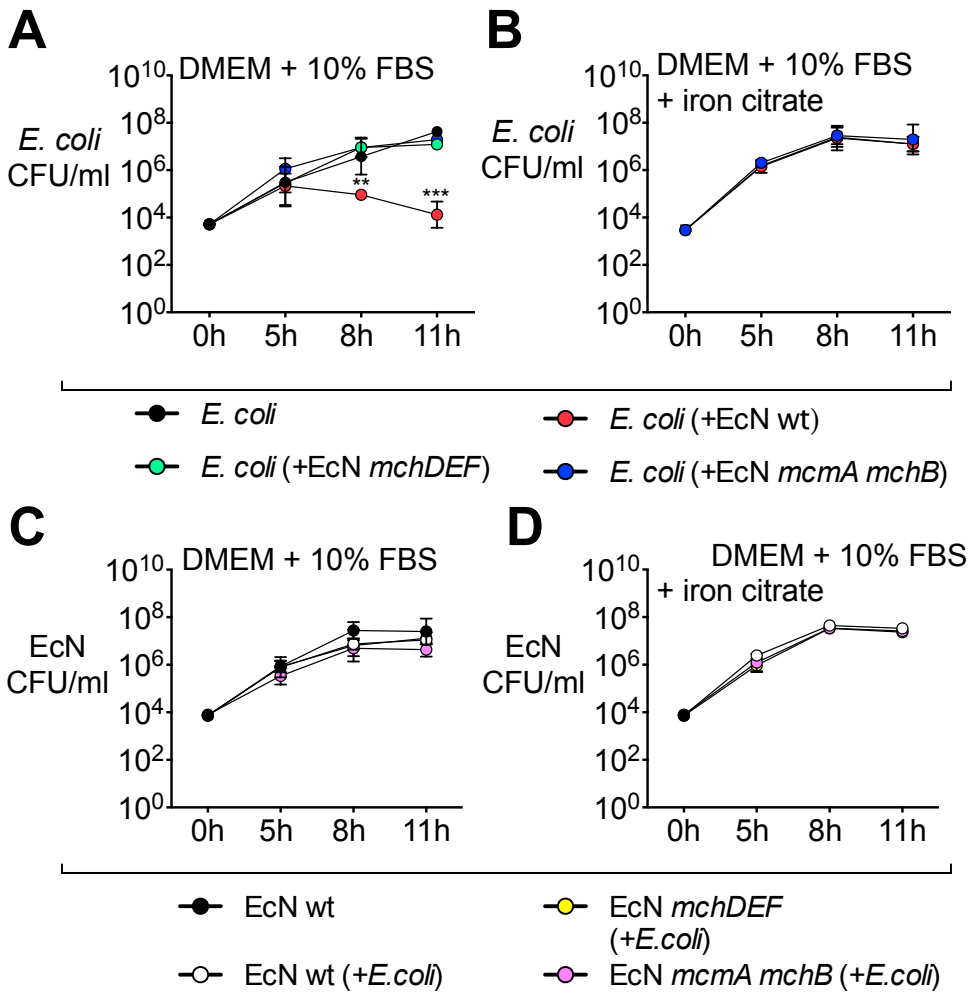


Figure 2.7 *In vitro* competition growth curves between wild-type EcN and microcin mutants against commensal *E. coli.*
A-D, Commensal *E. coli*, wild-type EcN, EcN *mchDEF* and EcN *mcmA mchB* mutants were grown overnight in Nutrient Broth + 0.2 mM 2,2'-dipyridyl. Competition growth assays were performed in iron-limiting conditions (DMEM/F12 + 10%FBS) or in media supplemented with 1 μM of iron citrate and time points at 0, 5, 8 and 11 hours post-inoculation were collected. **A**,**B**, show commensal *E. coli* CFU/ml at 5, 8, and 11 hours post-inoculation when alone or in competition with either wild-type EcN or the indicated EcN mutants in iron limiting conditions (**A**) or in media supplemented with 1 μM of iron citrate (**B**). **C**,**D**, show CFU/mL of wild-type EcN grown alone, and of wild-type EcN or the indicated EcN mutants in competition with commensal *E. coli* in iron limiting conditions (**c**) or in media supplemented with 1 μM of iron citrate (**D**). Each symbol represents the geometric mean of three independent experiments ± standard error. ***P*<0.01 ****P*<0.001.

FIGURE 2.8

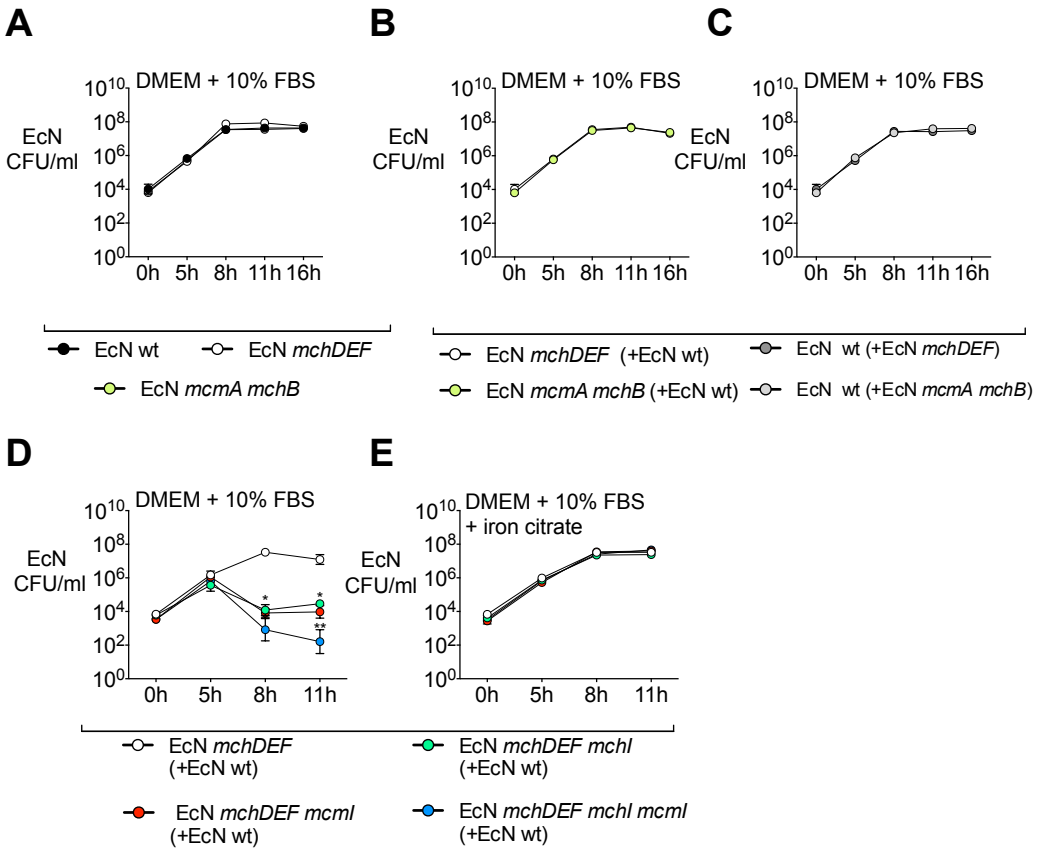


Figure 2.8 *In vitro* growth curves of wild-type EcN and microcin mutants alone or in competition.

A-C, EcN wild-type, EcN *mchDEF* and EcN *mcmA mchB* mutants were grown overnight in Nutrient Broth + 0.2 mM 2,2'-dipyridyl. Growth curves of strains alone or in competition were performed in iron-limiting conditions (DMEM/F12 + 10%FBS) and time points at 0, 5, 8, 11 and 16 hours post-inoculation were collected. **A**, CFU/mL of wild-type EcN or the indicated microcin mutants grown individually in iron-limiting media**. B,** CFU/mL of EcN *mchDEF* and EcN *mcmA mchB* mutants when grown in competition with EcN wild-type. **C.** CFU/mL of wild-type EcN when grown in competition with either EcN *mchDEF* or EcN *mcmA mchB* mutants.**D**,**E**, EcN wild-type, EcN *mchDEF* and EcN *mchDEF* mutant additionally lacking microcin immunity genes (*mchDEF mchI*, *mchDEF mcmI* and *mchDEF mchI mcmI*) were grown overnight in Nutrient Broth + 0.2 mM 2,2'-dipyridyl. Growth curves of strains in competition were performed in iron-limiting conditions (DMEM/F12 + 10%FBS) or in media supplemented with 1 µM of iron citrate and time points at 0, 5, 8 and 11 hours post-inoculation were collected. **D**,**E**, show CFU/mL of the indicated EcN microcin mutants when in competition with wild-type EcN, either in low iron conditions (**D**) or in media supplemented with 1 µM iron citrate (**E**). Each symbol represents the geometric mean of three independent experiments ± standard error. * P<0.05 ** P<0.01 *** P<0.001.

FIGURE 2.9

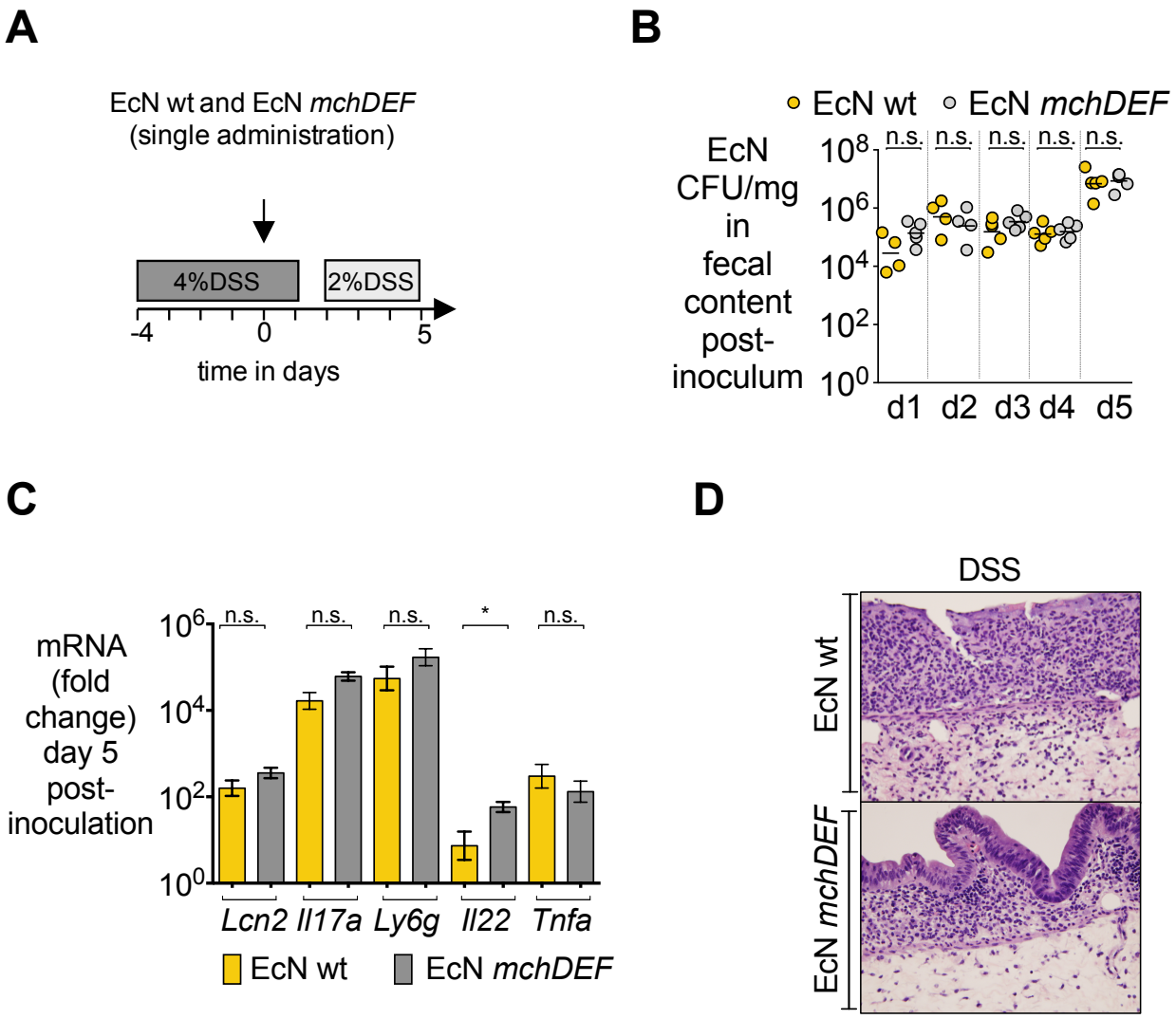


Figure 2.9 *E. coli* Nissle wild-type and microcins mutant gut colonization during inflammation. **A**, Schematic representation of the experimental design for (**b**-**d**). Groups of mice were treated with 4% DSS for 4 days, then intragastrically inoculated with wild-type EcN and EcN *mchDEF* (single inoculations). **B**, CFU/mg of wild-type EcN or EcN *mchDEF* in mouse fecal content at day 1 to day 5 post-inoculation (n = 5 per group). Each circle represents an individual mouse and bars represent the geometric mean. **C**, Expression of *Lcn2*, *Il17a*, *Ly6g*, *Il22* and *Tnfa*, at day 5 post inoculation in the caecum of mice inoculated with wild-type EcN alone EcN *mchDEF* alone. Bars represent the geometric mean ± standard error. Data are expressed as fold increase over mock treated mice. **D**, H&E stained sections from representative animals for each groups. n.s.=not significant.

FIGURE 2.10

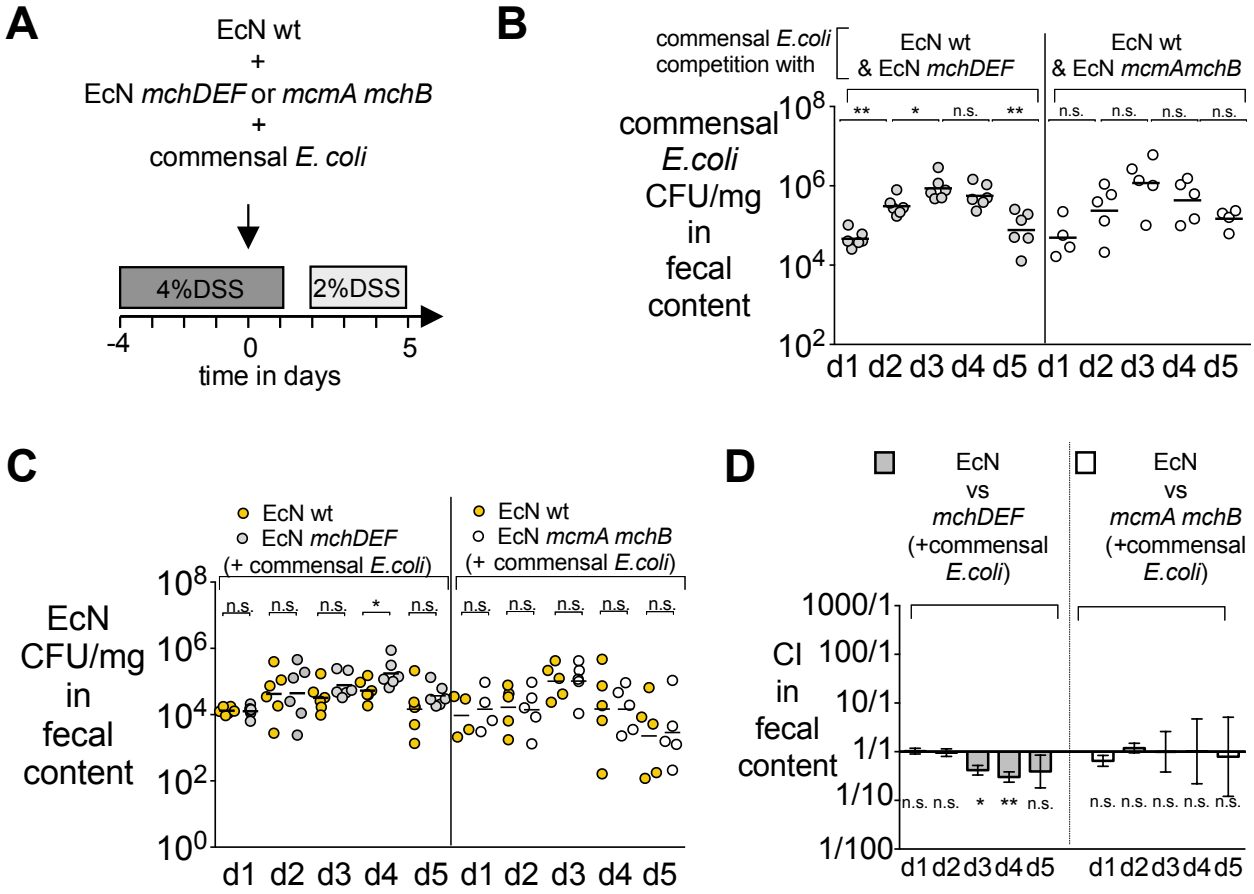


Figure 2.10 ***E. coli*** **Nissle wild-type and microcins mutant gut colonization when in competition and in the presence of the commensal** ***E.coli*** **during DSS-colitis**. **A**, Schematic representation of the experimental design for (**B-D**). Groups of mice were treated with 4% DSS for 4 days, then intragastrically inoculated with a 1:1:1 mixture of wild-type EcN + EcN *mchDEF* and commensal *E.coli* or wild-type EcN + EcN *mcmA mchB* and commensal *E. coli*. **B**, CFU/mg of commensal *E. coli* when in competition with EcN wild-type and EcN *mchDEF* or with EcN wild-type and EcN *mcmA mchB* at day 1 to day 5 post-inoculation. **c**, CFU/mg of wild-type EcN and EcN *mchDEF* or of wild-type EcN and EcN *mcmA mchB* when in competition with the commensal *E.coli* in mouse fecal content at day 1 to day 5 post-inoculation. **D**, Competitive index (CI) of wild-type EcN over EcN *mchDEF* or wild-type EcN over EcN *mcmA mchB* at day 1 to day 5 post-inoculation, when in competition with the commensal *E.coli* (n = 5). Bars represent the geometric mean ± standard error. **B**,**C**, Each circle represents an individual mouse and bars represent the geometric mean. **P*<0.05 ***P*<0.01; n.s.=not significant.

FIGURE 2.11

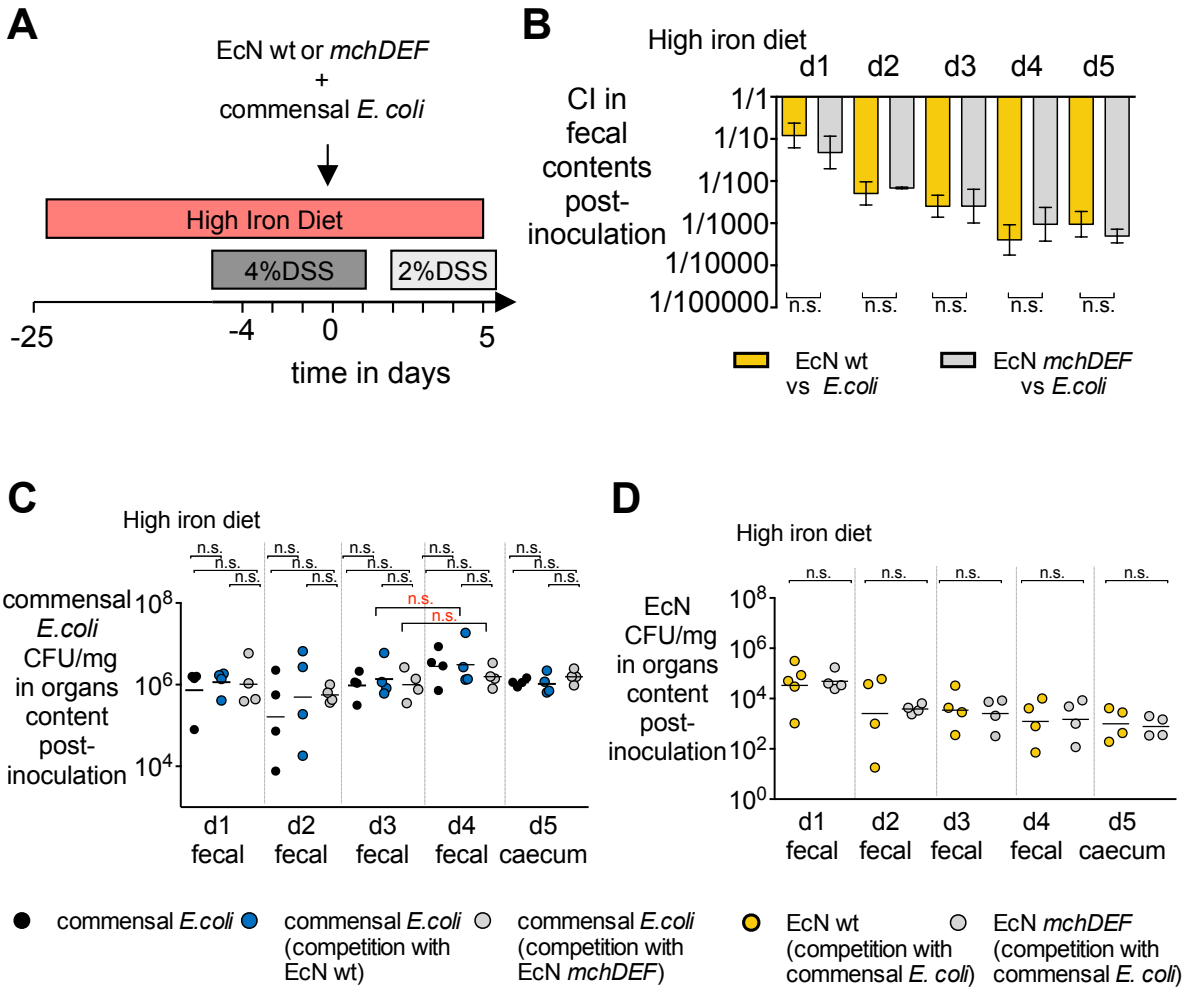


Figure 2.11 *E. coli* Nissle wild-type and microcins mutants gut colonization during competition with commensal *E. coli* post iron rich diet and in the presence of intestinal in inflammation. A, Schematic representation of the experimental design for (**A-D**), Mice were fed high iron diet (Envigo Rx 1980611 TD. 160234 1% FeSO4 2020) 3 weeks prior DSS treatment and through out the experiment. Mice were then treated with 4% DSS in the drinking water for 4 days, then intragastrically inoculated with a mixture of commensal *E. coli* and either wild-type EcN or a mutant in microcin export (EcN *mchDEF*). **B**, Competitive index (CI) of wild-type EcN or EcN *mchDEF* over commensal *E. coli* at day 1 to 5 post-inoculation in fecal content (n = 4-5 per group). **C**, CFU/mg at day 1 to 5 post-inoculation in colon and caecum content of commensal *E.coli* when in competition with either wild-type EcN or EcN *mchDEF*. **D**, CFU/mg at day 1 to 5 post-inoculation in colon and caecum content of wild-type EcN or EcN *mchDEF* when in competition with the commensal *E.coli*. **B**, Bars represent the mean ± standard error. **C**,**D**, Each circle represents an individual mouse and bars represent the geometric mean. n.s.=not significant.

Microcins reduce colonization of enteric pathogens and pathobionts in the inflamed gut.

In addition to commensal Enterobacteriaceae, pathogens of this family are known to bloom in the inflamed gut[2]. We therefore investigated whether microcins could limit the expansion of the diarrheal pathogen *Salmonella enterica* serovar Typhimurium (*S*. Typhimurium). We first established that wild-type EcN, but not the EcN *mchDEF* or EcN *mcmA mchB* mutants, could kill *S*. Typhimurium in iron-limited but not in iron-rich media and that in addition the killing of STm was rescued when the EcN *mchDEF* was complemented *in trans* (**Fig. 2.12**), Similarly, when streptomycin-treated mice (*Salmonella* colitis model) were infected with equal numbers of *S*. Typhimurium and either wild-type EcN or the EcN *mchDEF* mutant, only wild-type EcN outcompeted *S*. Typhimurium beginning at day 4 post-infection (**Fig. 2.13 A, B**). Although all strains employed initially colonized the gut to similar levels, we observed a significant reduction of *S.* Typhimurium colonization beginning at day 4 post-infection, and this phenotype was greater in the presence of microcin-producing EcN (**Fig. 2.13 C**). At later time points the microcins activity against STm was not observed, probably due to all the iron uptake systems EcN posses as previously reported (19). In accordance with our results with commensal *E. coli* **(Fig. 2.4)** gut colonization of the EcN *mchDEF* mutant was also drastically reduced in competition with *S*. Typhimurium by day 7 post-infection (**Fig. 2.13 D**). Moreover, the competitive advantage of wild-type EcN over *S.* Typhimurium was again only observed when the intestine was inflamed **(Fig. 2.14 A, B)**. Indeed, in competition experiments with a *S*. Typhimurium mutant (*invA spiB*) that is unable to invade the intestinal epithelial layer and so trigger gut inflammation, both wild-type EcN

and the EcN *mchDEF* mutant showed similar levels of intestinal colonization (**Fig. 2.14 C-D)**. Additionally, no competitive advantage for either wild-type EcN or the EcN *mchDEF* mutant over the *S*. Typhimurium *invA spiB* mutant was observed (**Fig. 2.14 E**). Consistent with what we observed for *in vivo* competition with the commensal *E. coli* and STm, we found similar microcin-dependent growth reduction of the pathobiont adherent invasive *E. coli* (AIEC, an organism frequently isolated from Crohn's disease patients), *in vitro* (**Fig. 2.12)** and *in vivo* when in competition with the wild-type EcN but not with EcN *mchDEF* during DSS-induced colitis (**Fig. 2.15)**.

FIGURE 2.12

Figure 2.12 *In vitro* activity of EcN microcins against enteric pathogens and pathobionts

A-I*, In vitro* competition assays between wild-type EcN or microcin mutants (EcN *mchDEF* or EcN *mcmA mchB*) against *Salmonella* Typhimurium (STm) and AIEC. STm, AIEC, wild-type EcN, EcN *mchDEF* and EcN *mcmA mchB* mutants were grown overnight in Nutrient Broth + 0.2 mM 2,2'-dipyridyl. Growth curves of strains in competition were performed in iron-limiting conditions (DMEM/F12 + 10%FBS) or in media supplemented with 1 μM of iron citrate and time points at 0, 5, 8 and 11 hours post-inoculation were collected. **A**,**B**, show STm CFU/mL at 5, 8, and 11 hours post-inoculation when alone or in competition with either wild-type EcN or the indicated EcN mutants in iron-limiting conditions (**A**) or in media supplemented with 1 μM of iron citrate (**B**). **C**, STm CFU/mL at 5, 8, and 11 hours post-inoculation in iron-limiting conditions when in competition with either wild-type EcN and the indicated EcN *mchDEF* mutant or EcN *mchDEF* complemented *in trans* (pWSK29::*mchDEF*). **D**, CFU/ml of EcN wt grown alone, and of wild-type EcN or the indicated EcN mutants grown in competition with STm in iron-limiting conditions or in media supplemented with 1 μM of iron citrate (**E**). **F**,**E,** show AIEC CFU/ml when alone or in competition with either wild-type EcN or the indicated EcN mutants in iron-limiting conditions (**F**) or in media supplemented with 1 μM iron citrate (**E**). **H**, CFU/mL of wild-type EcN grown alone, and of wild-type EcN or the indicated EcN mutants in competition with AIEC in iron-limiting conditions or in media supplemented with 1 μM iron citrate (**I**). Each symbol represents the geometric mean of three independent experiments ± standard error.* $P \leq 0.05$, *** $P \leq 0.001$, **** $P \leq 0.0001$.

FIGURE 2.12

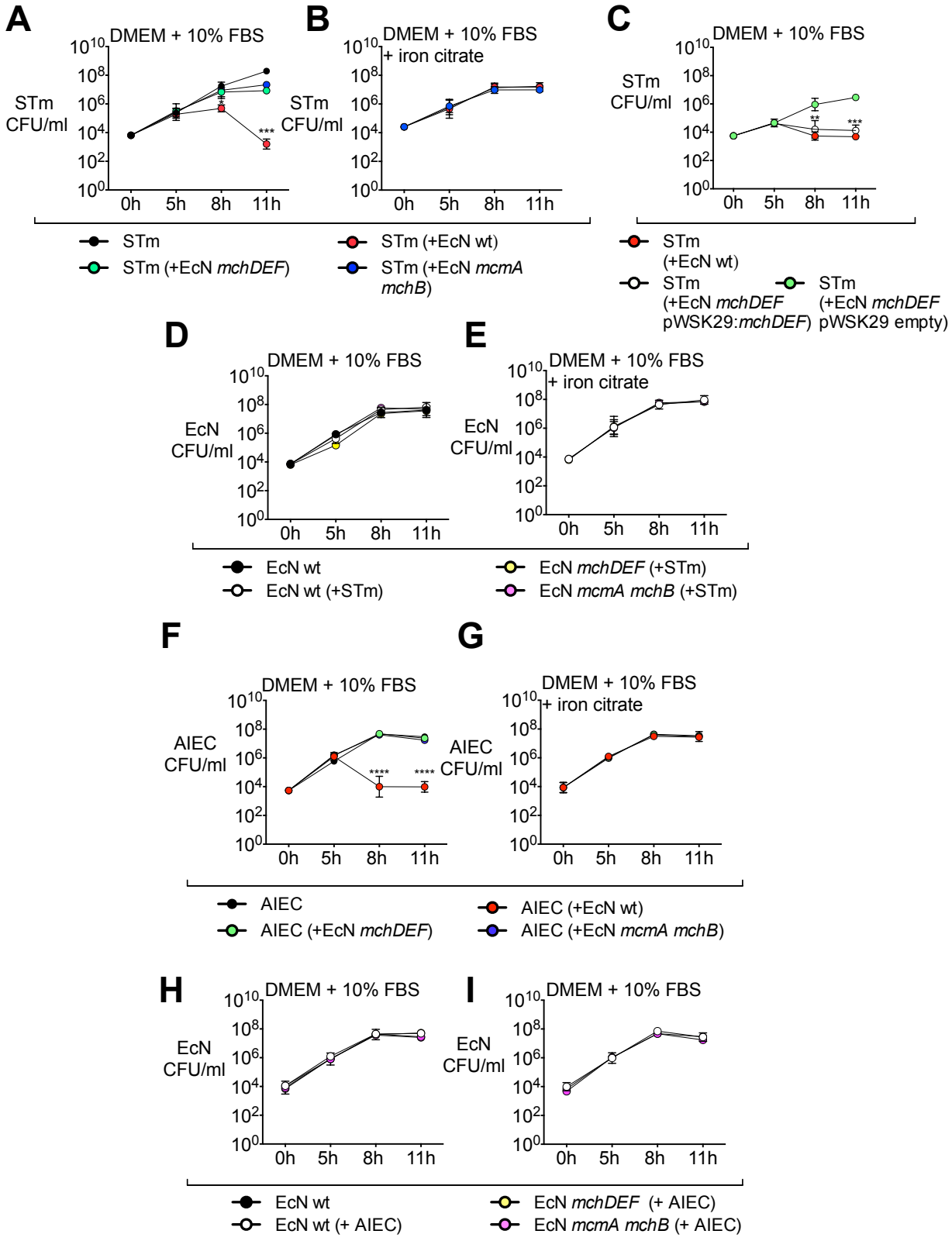

A
DMEM + 10% FBS
STm CFU/ml
B
DMEM + 10% FBS
+ iron citrate
STm CFU/ml
C
DMEM + 10% FBS
STm CFU/ml
0h 5h 8h 11h
STm
STm (+EcN mchDEF)
STm (+EcN wt)
STm (+EcN mcmA mchB)
STm (+EcN wt)
STm (+EcN mchDEF pWSK29:mchDEF)
STm (+EcN mchDEF pWSK29 empty)
D
DMEM + 10% FBS
EcN CFU/ml
E
DMEM + 10% FBS
+ iron citrate
EcN CFU/ml
EcN wt
EcN wt (+STm)
EcN mchDEF (+STm)
EcN mcmA mchB (+STm)
F
DMEM + 10% FBS
AIEC CFU/ml
G
DMEM + 10% FBS
+ iron citrate
AIEC CFU/ml
AIEC
AIEC (+EcN mchDEF)
AIEC (+EcN wt)
AIEC (+EcN mcmA mchB)
H
DMEM + 10% FBS
EcN CFU/ml
I
DMEM + 10% FBS
EcN CFU/ml
EcN wt
EcN wt (+ AIEC)
EcN mchDEF (+ AIEC)
EcN mcmA mchB (+ AIEC)

FIGURE 2.13

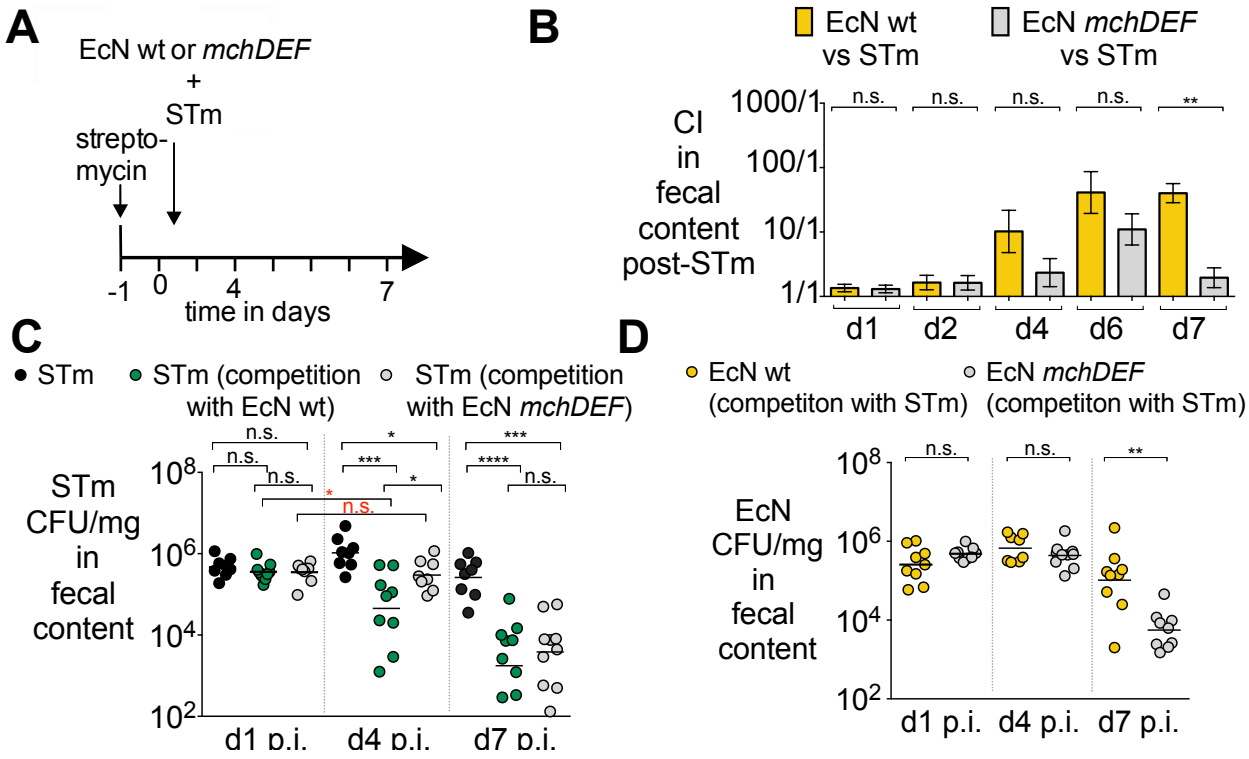


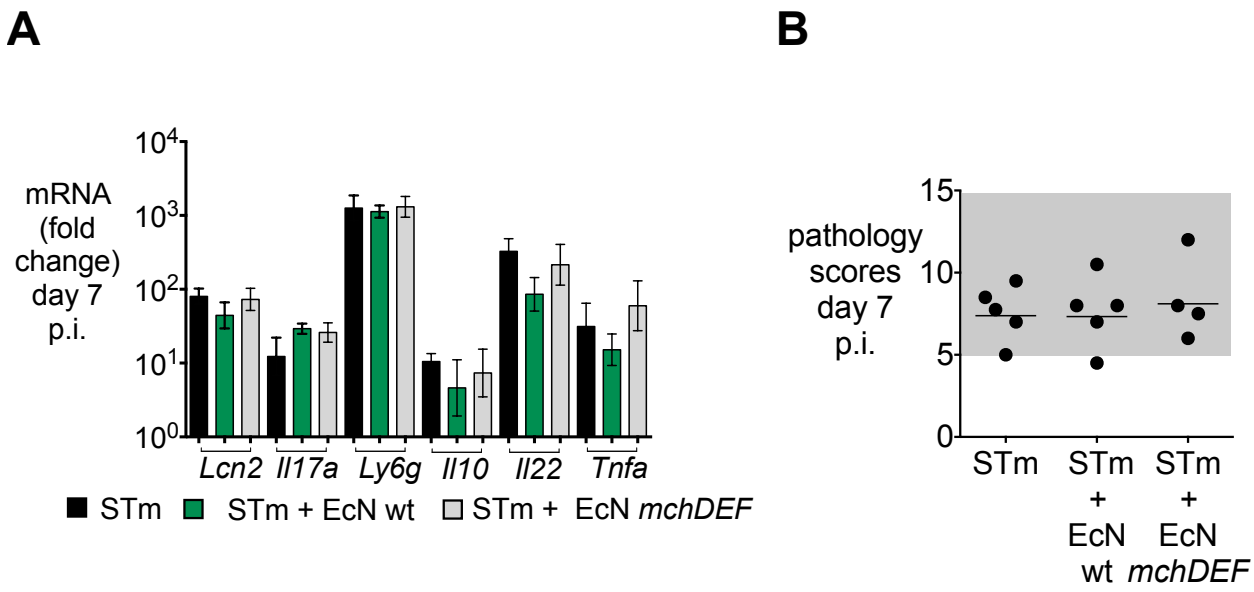
Figure 2.13 Microcins reduce colonization of enteric pathogens in the inflamed gut.

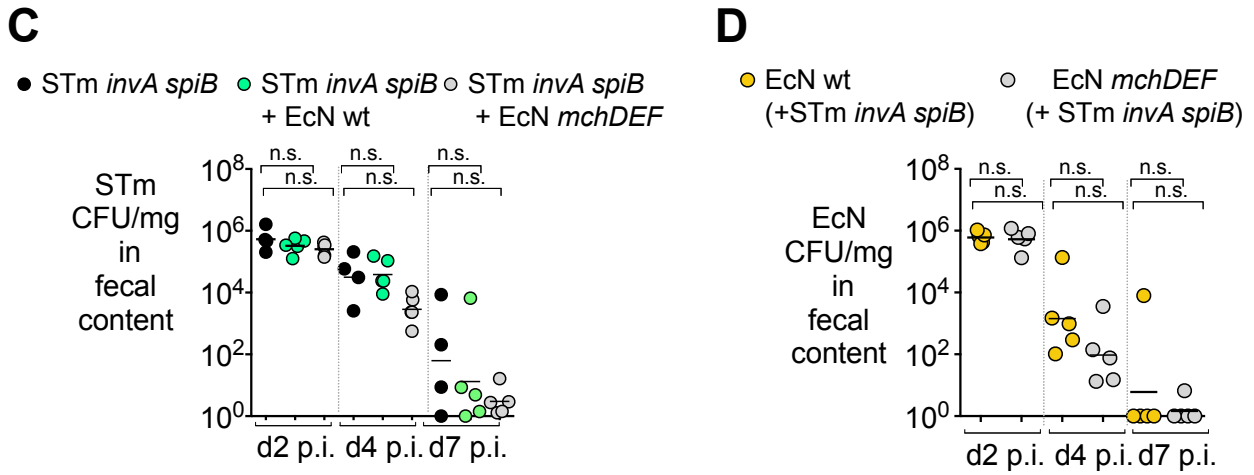
A, Schematic representation of the experimental design for (**B**-**D**). Groups of mice were treated with streptomycin one day prior to intragastric inoculation of *S*. Typhimurium (STm) alone, or STm in competition at a 1:1 ratio with either wild-type EcN or EcN *mchDEF*. **B**, Competitive index (CI) of wild-type EcN or EcN *mchDEF* over STm at day 1, 2, 4, 6, and 7 post-infection (n = 9 per group). **C**, CFU/mg of STm in mouse fecal content at day 1, 4 and 7 post-infection, either in single infection or in competition with wild-type EcN or with EcN *mchDEF*. **D**, CFU/mg of wild-type EcN and EcN *mchDEF* in the fecal content at day 1 , 4 and 7 post-infection. **B** Bars represents the mean ± standard error. **C**,**D** Each circle represents an individual mouse; bars represent the geometric mean. Data are representative of n = 2 experiments. * $P<0.05$ ** $P<0.01$ *** $P<0.001$; n.s.=not significant.

FIGURE 2.14

Figure 2.14 STm infection in competition with wild-type EcN and EcN *mchDEF*. **A,D**, C57BL/6 NRAMP1+ mice were treated with streptomycin 1 day prior infection. The following day, mice were orally inoculated with wild-type STm or with a 1:1 mixture of wild-type STm and either wild-type EcN or EcN *mchDEF*. **A,** Expression of *Lcn2*, *Il17a, Ly6g*, *Il22*, *Tnfa*, *Nos2* and *Il10* mRNA in caecal samples in mice infected with either wild-type STm alone, or STm + wild-type EcN, or STm + EcN *mchDEF* at day 7 post-infection (n = 5 per group). Bars represent the mean ± standard error. Data are expressed as fold increase over mock treated mice. **B**, Pathology scores in the caecum of mice infected with either wild-type STm alone, or STm in competition with either wild-type EcN or EcN *mchDEF* (day 7 post-infection, n = 5 mice per group). **C-E,** C57BL/6 NRAMP1+ mice were treated with streptomycin 1 day prior infection. The following day, mice were orally inoculated with STm *invA spiB* (a STm mutant unable to invade intestinal epithelial cells and trigger mucosal inflammation) or with a 1:1 mixture of STm *invA spiB* and either wild-type EcN or EcN *mchDEF*. **C,** CFU/mg of STm *invA spiB* mutant in fecal content when alone or in competition with either wild-type EcN or EcN *mchDEF* at day 2, 4 and 7 post-infection; **D**, CFU/mg of wild-type EcN and EcN *mchDEF* in fecal content when in competition with STm *invA spiB* at day 2, 4 and 7 post-infection. **E**, Competitive index (CI) of STm *invA spiB* mutant over the wild-type EcN or the EcN *mchDEF* mutant in fecal content at day 2, 4 and 7 post-infection (n = 5 per group). Bars represent the mean ± standard error. n.s.=not significant.

FIGURE 2.14


A
B
mRNA (fold change) day 7 p.i.
10^4
10^3
10^2
10^1
10^0
Lcn2
Il17a
Ly6g
Il10
Il22
Tnfa
STm
STm + EcN wt
STm + EcN mchDEF
pathology scores day 7 p.i.
15
10
5
0
STm
STm + EcN wt
STm + EcN mchDEF


C
D
STm invA spiB
STm invA spiB + EcN wt
STm invA spiB + EcN mchDEF
EcN wt (+STm invA spiB)
EcN mchDEF (+ STm invA spiB)
STm CFU/mg in fecal content
EcN CFU/mg in fecal content
10^8
10^6
10^4
10^2
10^0
n.s.
d2 p.i.
d4 p.i.
d7 p.i.

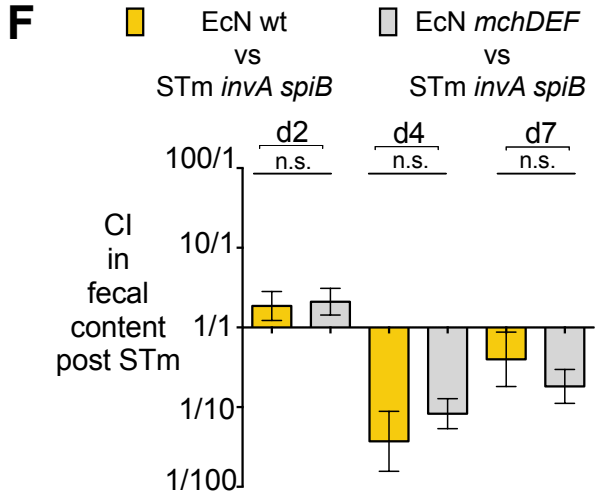
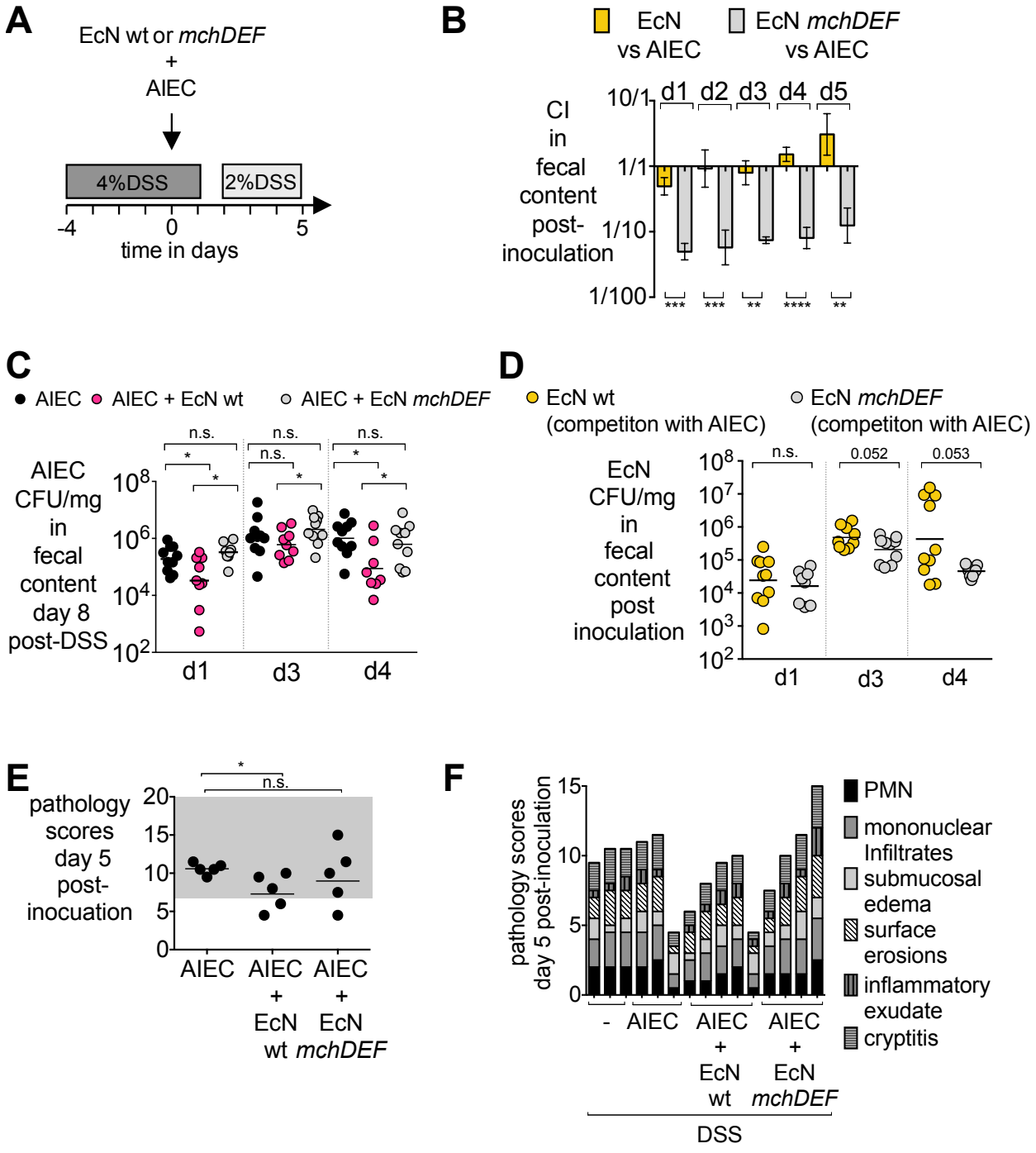

F
EcN wt vs STm invA spiB
EcN mchDEF vs STm invA spiB
d2
d4
d7
n.s.
CI in fecal content post STm
100/1
10/1
1/1
1/10
1/100

FIGURE 2.15

Figure 2.15 AIEC administration post-DSS treatment in competition with wild-type EcN and EcN *mchDEF*.
A, Schematic representation of the experimental design for (**B-F**). Mice were treated with 4% DSS in the drinking water for 4 days, then intragastrically inoculated with commensal AIEC alone or in competition at 1:1 with either wild-type EcN or *mchDEF* mutant. **B,** Competitive index (CI) of wild-type EcN or EcN *mchDEF* over AIEC at day 1-5 post inoculation (n = 10 per group). Bars represent the mean ± standard error. **C,** CFU/mg of AIEC in mouse fecal content at day 1, 3 and 4 post-inoculation, when alone or in competition with wild-type EcN or EcN *mchDEF*. **D**, CFU/mg of wild-type EcN and EcN *mchDEF* in mouse fecal content at day 1, 3 and 5 post-inoculation, when in competition with AIEC. **E**, Pathology scores in the caecum of mice inoculated with either AIEC alone, or AIEC in competition with either wild-type EcN or EcN *mchDEF* at day 5 post-inoculation. **F**, Detailed histopathology scoring of the animals shown in (**E**). **C-E**, Each circle represents one mouse. * $P \leq 0.05$; n.s.=not significant.

FIGURE 2.15


A
EcN wt or mchDEF
+
AIEC
4%DSS
2%DSS
-4
0
5
time in days
B
EcN vs AIEC
EcN mchDEF vs AIEC
CI in fecal content post-inoculation
10/1
1/1
1/10
1/100
d1
d2
d3
d4
d5
***
***
**
****
**
C
AIEC
AIEC + EcN wt
AIEC + EcN mchDEF
AIEC CFU/mg in fecal content day 8 post-DSS
n.s.
n.s.
n.s.
d1
d3
d4
D
EcN wt (competiton with AIEC)
EcN mchDEF (competiton with AIEC)
EcN CFU/mg in fecal content post inoculation
n.s.
0.052
0.053
d1
d3
d4
E
pathology scores day 5 post-inocuation
n.s.
AIEC
AIEC + EcN wt
AIEC + EcN mchDEF
F
pathology scores day 5 post-inoculation
PMN
mononuclear Infiltrates
submucosal edema
surface erosions
inflammatory exudate
cryptitis
-
AIEC
AIEC + EcN wt
AIEC + EcN mchDEF
DSS

Finally, we investigated whether microcin-producing EcN could be used as a therapeutic tool for treatment of infection with an enteric pathogen. We administered either wild-type EcN or EcN *mchDEF* as a treatment to mice previously infected with *S*. Typhimurium (**Fig. 2.16 A**). Compared to mock-treated mice, the group that received wild-type EcN at day 2 and day 5 after *S*. Typhimurium infection showed a dramatic reduction (up to 100,000 fold) of *S*. Typhimurium gut colonization (**Fig. 2.16 B**). This phenotype was dependent upon microcin secretion, as the EcN *mchDEF* mutant was unable to reduce *S*. Typhimurium intestinal burden in the presence of inflammation (**Fig. 2.16 B**). Moreover we found that the growth of a STm strain expressing the EcN *mchDEFmcmI* region (which includes the immunity gene *mcmI* for microcin M) was not impaired by the administration of the wild-type EcN (**Fig. 2.16 B)**. Indeed, *in vitro* studies suggested although both microcins target AIEC, only microcin M (produced by gene *mcmA*) has antibacterial activity against the commensal *E. coli*, and *Salmonella* strains we used (**Fig. 2.17**).

Finally, administration of wild-type EcN, but not of the EcN *mchDEF* mutant, to mice infected with *S*. Typhimurium wild-type but not STm expressing *mchDEF mcmI* genes provided additional benefits, indeed mice administered with EcN wild-type lost less weight and by reducing the expression of proinflammatory genes encoding for IFN-γ and lipocalin-2 (**Fig. 2.16 C, D**).

FIGURE 2.16

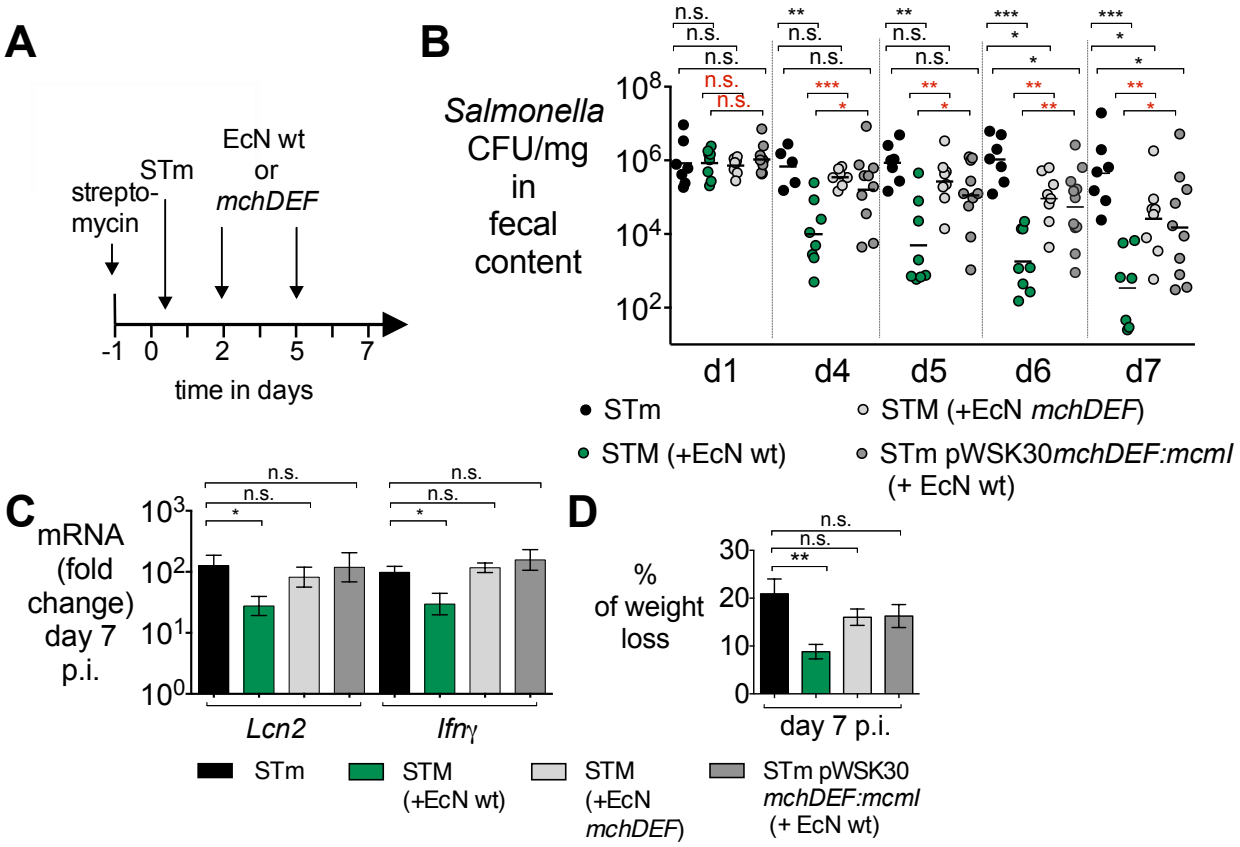
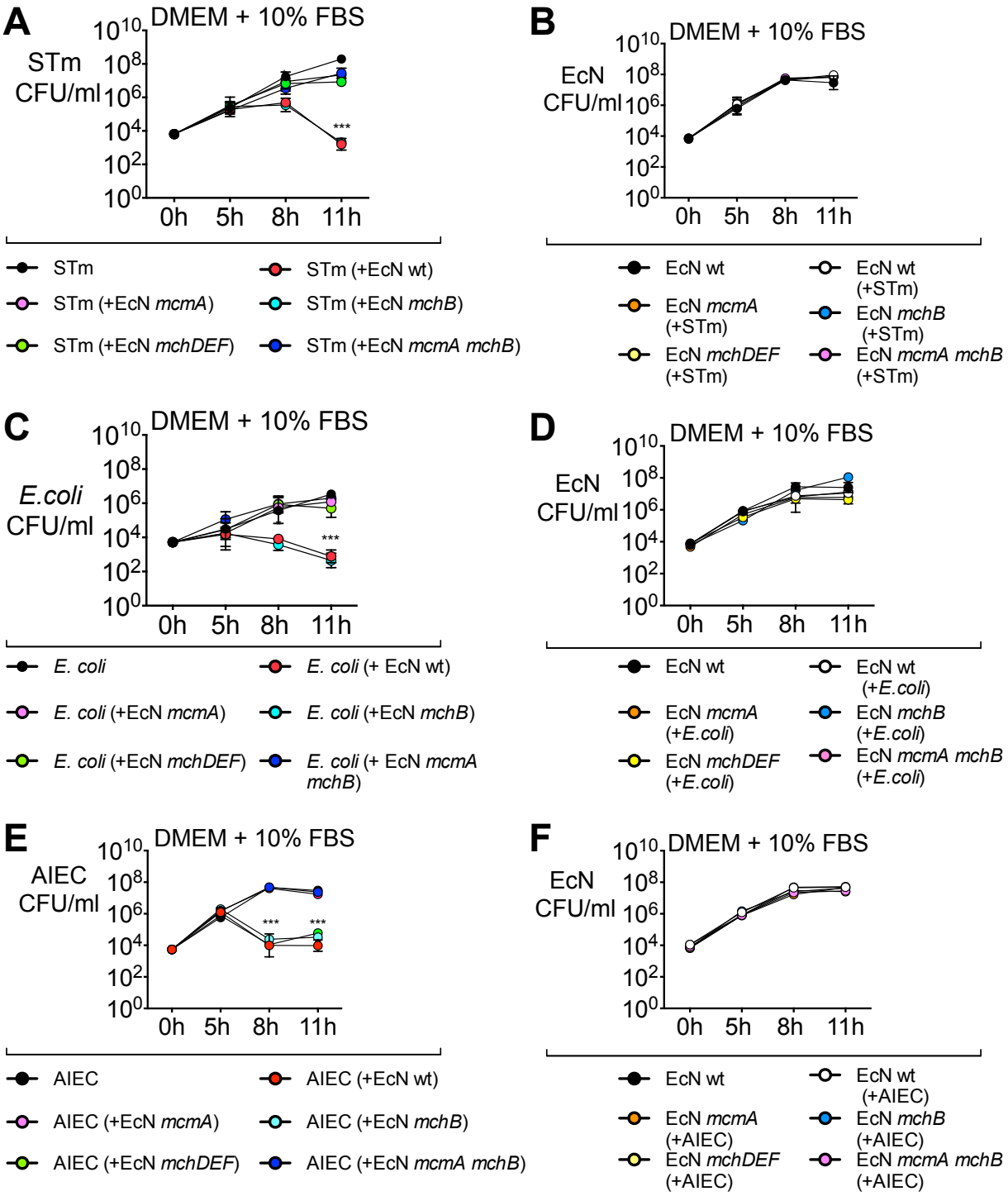


Figure 2.16 Therapeutic administration of wild-type EcN but not EcN *mchDEF* reduce colonization of enteric pathogens in the inflamed gut.
E, Schematic representation of the experimental design for **A-D**. Groups of mice were treated with streptomycin one day prior to intragastric inoculation of wild-type *S.* Typhimurium (STm) or STm transformed with pWSK30::*mchDEF mcmI*. Mice were then treated with wild-type EcN or EcN *mchDEF* at day 2 and 5 post-infection. **B**, CFU/mg of STm in mouse fecal content at day 1, 5, 6 and 7 post infection. Mice were either mock-treated or treated with wild-type EcN or with EcN *mchDEF* at day 2 and 5 after STm infection. **C**, Expression of *Lcn2*, *Ifng* mRNA in caecal samples of mice infected with STm, either untreated or treated with wild-type EcN or EcN *mchDEF,* at day 7 post-infection (n = 5 per group). D, Percentage of mouse weight loss at day 7 post-infection.
B, Each circle represents an individual mouse; bars represent the geometric mean. Data are representative of n = 2 experiments. * *P*<0.05 ***P*<0.001 ****P*<0.0001

FIGURE 2.17

Figure 2..17 *In vitro* activity of microcin M (*mcmA*) and microcin H47 (*mchB*) against STm, commensal *E.coli* and AIEC.
A-F*, In vitro* competition assays between wild-type EcN or microcin mutants (EcN *mchDEF* , EcN *mcmA mchB* or single mutants EcN *mcmA* and EcN *mchB*) against *Salmonella* Typhimurium (STm), commensal *E.coli* and AIEC. STm, commensal *E.coli*, AIEC, EcN wild-type and all EcN mutants were grown overnight in Nutrient Broth + 0.2 mM 2,2'-dipyridyl. Growth curves of strains in competition were performed in iron-limiting conditions (DMEM/F12 + 10%FBS) each time points at 0, 5, 8 and 11 hours post-inoculation were collected. **A**, STm CFU/mL at 5, 8, and 11 hours post inoculation when alone or in competition with either wild-type EcN or the indicated EcN mutants in iron-limiting conditions. **B**, wild-type EcN and mutants CFU/mL at 5, 8, and 11 hours post-inoculation when in competition with STm in iron-limiting conditions. **C**, commensal *E.coli* CFU/mL at 5, 8, and 11 hours post-inoculation when alone or in competition with either wild-type EcN or the indicated EcN mutants in iron-limiting conditions. **D**, wild-type EcN and mutants CFU/mL at 5, 8, and 11 hours post-inoculation when in competition with commensal *E.coli* in iron-limiting conditions. **E**, AIEC CFU/mL at 5, 8, and 11 hours post-inoculation when alone or in competition with either wild-type EcN or the indicated EcN mutants in iron-limiting conditions. **F**, wild-type EcN and mutants CFU/mL at 5, 8, and 11 hours post-inoculation when in competition with AIEC in iron-limiting conditions. Each symbol represents the geometric mean of three independent experiments ± standard error.* $P \leq 0.05$, *** $P \leq 0.0001$, **** $P \leq 0.00001$.

FIGURE 2.17


A
DMEM + 10% FBS
STm CFU/ml
0h 5h 8h 11h
***
STm
STm (+EcN wt)
STm (+EcN mcmA)
STm (+EcN mchB)
STm (+EcN mchDEF)
STm (+EcN mcmA mchB)
B
DMEM + 10% FBS
EcN CFU/ml
EcN wt
EcN wt (+STm)
EcN mcmA (+STm)
EcN mchB (+STm)
EcN mchDEF (+STm)
EcN mcmA mchB (+STm)
C
DMEM + 10% FBS
E.coli CFU/ml
***
E. coli
E. coli (+ EcN wt)
E. coli (+EcN mcmA)
E. coli (+EcN mchB)
E. coli (+EcN mchDEF)
E. coli (+ EcN mcmA mchB)
D
DMEM + 10% FBS
EcN CFU/ml
EcN wt
EcN wt (+E.coli)
EcN mcmA (+E.coli)
EcN mchB (+E.coli)
EcN mchDEF (+E.coli)
EcN mcmA mchB (+E.coli)
E
DMEM + 10% FBS
AIEC CFU/ml
***
***
AIEC
AIEC (+EcN wt)
AIEC (+EcN mcmA)
AIEC (+EcN mchB)
AIEC (+EcN mchDEF)
AIEC (+EcN mcmA mchB)
F
DMEM + 10% FBS
EcN CFU/ml
EcN wt
EcN wt (+AIEC)
EcN mcmA (+AIEC)
EcN mchB (+AIEC)
EcN mchDEF (+AIEC)
EcN mcmA mchB (+AIEC)

2.4 Discussion

Our work provides the first *in vivo* evidence that microcins linked to siderophore-like platforms are important for inter and intra-species competition among the Enterobacteriaceae in the inflamed gut. An interesting finding is that, although both microcins target AIEC in vitro, only microcin M (produced by gene *mcmA*) has antibacterial activity against the commensal *E. coli*, and *Salmonella* strains we used (**Fig 2.17**). Further studies will provide information on which of the two microcins can be employed to develop a possible therapeutic strategy against these and other strains. As this class of microcins specifically target microbes expressing particular siderophore receptors, microcins and other antimicrobial peptides linked to siderophore-like platforms could be used against enteric pathogens and pathobionts without affecting beneficial members of the microbiota . Indeed, we found that administration of EcN wild-type or the *mchDEF* mutant during DSS colitis yielded similar diversity and shifts in microbial communities, independent of EcN's ability to produce microcins (**Fig. 2.18**), which are thought to be resistant to these microcins. Indeed, we found that these microcins are employed by a probiotic bacterium (EcN) to compete with related species, efficiently colonize the inflamed gut, and displace an enteric pathogen from its niche, thereby contributing to its beneficial effects. Although mutants in siderophore receptors are resistant to microcins ((14) and **Fig. 2.19**), these mutants are also attenuated in the inflamed intestine (33) and thus are unlikely to be selected for *in vivo*. As these microcins specifically target microbes that express receptors for particular siderophores, microcins and other antimicrobial peptides linked to siderophores could be used against

enteric pathogens and pathobionts in the inflamed gut without broadly impacting the microbiota.

FIGURE 2.18

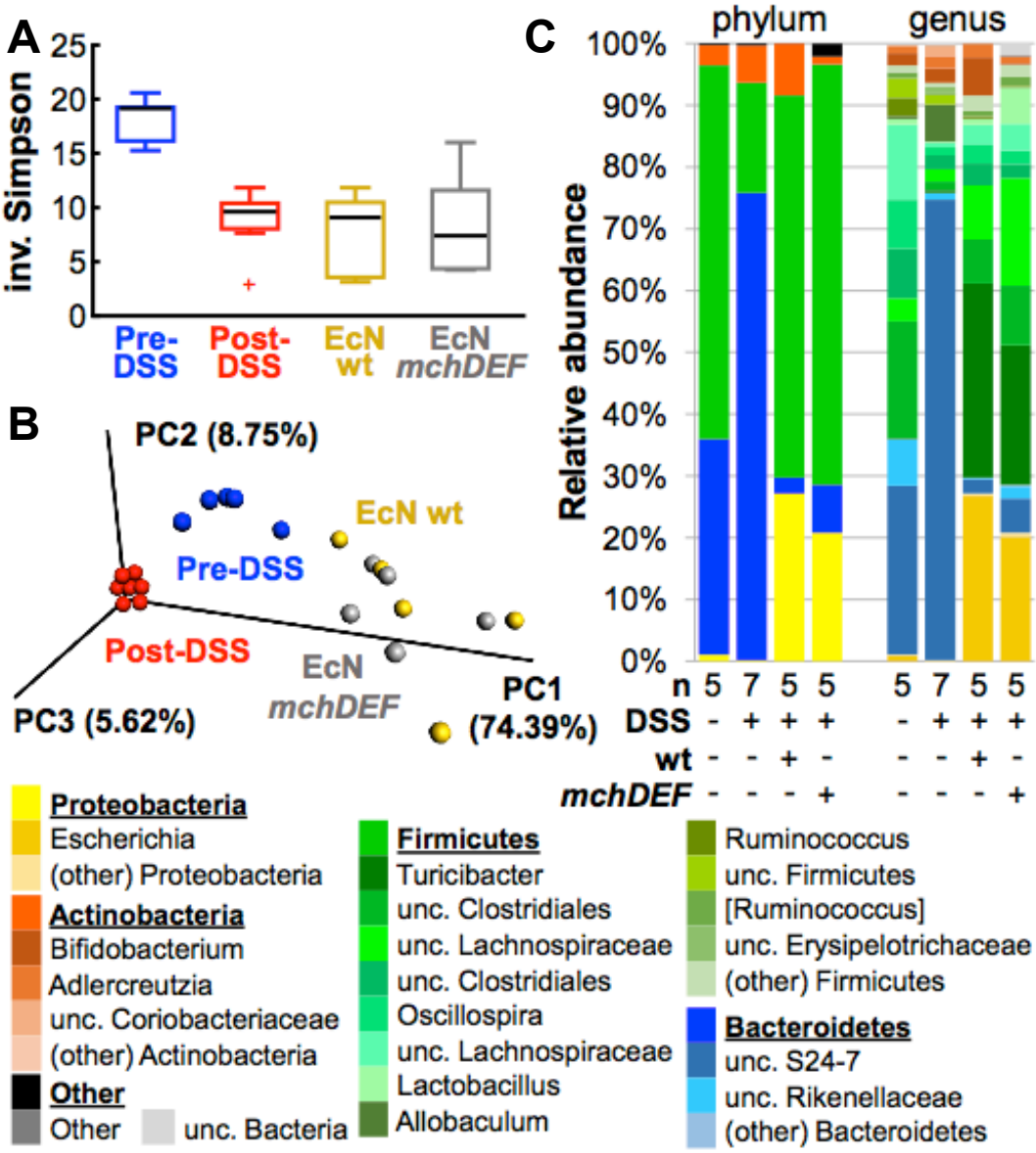


Figure 2.18 Microcins do not broadly impact composition of the gut microbiota during inflammation. Sequence analysis of fecal DNA from mice prior to DSS administration (pre-DSS; Day -4), after 4 days of 4% DSS in the drinking water (post-DSS; Day 0), and post-inoculation (Day 5) with a 1:1 ratio of commensal *E. coli* and either wild-type (wt) EcN or the EcN microcin exporter mutant (*mchDEF*). **a**, box plot of bacterial alpha diversity (inverse Simpson index); + = outlier, black lines = median. **b**, Emperor PCoA plot of bacterial beta diversity (weighted unifrac). **c**, Bar chart of group average bacterial relative OTU abundances at the phylum and genus level. OTUs with a relative abundance greater than 1% in at least one group are displayed; those with lower abundance are combined and displayed in entries marked “other”. Phylum names are in bold. n = mice per group.

FIGURE 2.19

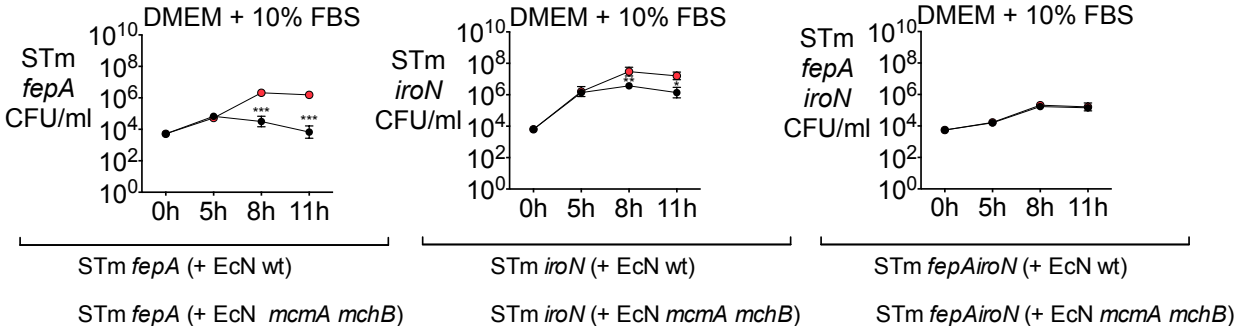


Figure 2.19 EcN microcins selectively target specific competitors through their iron receptor.
Competitive *in vitro* growth assays between STm *fepA* and/or *iroN* mutants and wild-type EcN or EcN *mcmA mchB* mutant. All strains were grown overnight in Nutrient broth + 0.2 mM 2,2'-dipyridyl prior to the competitive growth assay. CFU/ml of STm *fepA*, STm *iroN* and STm *fepA iroN* mutants were enumerated at 5, 8, and 11 hours post inoculation, when alone or in competition with either wild-type EcN or EcN *mcmA mchB.* Each symbol represents the geometric mean of three independent experiments ± standard error. * $P \leq 0.05$, ** $P \leq 0.01$, *** $P \leq 0.001$; n.s.=not significant.

2.5 Material and Methods

Bacterial Strains, culture conditions and chemicals

The *Escherichia coli* Nissle 1917 (EcN, Mutaflor, DSM 6601) wild-type and mutants, the pathogen *Salmonella enterica* serovar Typhimurium, the mouse commensal *Escherichia coli,* and the adherent invasive *E. coli* (AIEC) are listed in **Table 2.1** EcN was kindly provided by Ardeypharm Gmb, Herdecke, Germany. The AIEC strain is a human isolate from a patient with Crohn's disease (isolate NRG857c O83:H1)(34) and was kindly provided by Dr. Alfredo Torres. IR715 is a fully virulent, nalidixic acid-resistant derivative of *S*. Typhimurium wild-type isolate ATCC 14028. All strains were routinely grown aerobically in Luria-Bertani (LB) broth (10 g/L tryptone, 5 g/L yeast extract, 10 g/L NaCl) or in LB agar plates at 37 °C. When indicated, antibiotics were added to the media at the following concentrations: 0.03 mg/mL chloramphenicol (Cm), 0.1 mg/mL carbenicillin (Carb), 0.05 mg/mL kanamycin (Kan), and 0.01 mg/mL tetracycline (Tet). For animal infections or bacterial administration, all strains were grown in LB media aerobically at 37 °C overnight. For *in vitro* growth assays, strains were grown in iron limiting conditions (Nutrient Broth supplemented with 0.2 mM 2,2'-dipyridyl in ethanol, Sigma) aerobically at 37 °C overnight. All restrictions enzymes and *Phusion High Fidelity* DNA Polymerase were purchased from New England Biolabs. Oligonucleotides were synthesized by Fisher Scientific (**Table 2.3 and 2.4**).

Generation of bacterial mutants

Mutants in EcN and *S*. Typhimurium were constructed using the lambda red recombinase system(35). Briefly, primers (**Table 2.3**) homologous to sequences within the 5′ and 3′ ends of the target regions were designed (H1 and H2 primers, respectively; **Table 2.3**) and were used to replace the selected genes with chloramphenicol (derived from pKD3), kanamycin (derived from pKD4), or tetracycline resistance cassettes (**Table 2.2**). The name of the strains constructed is listed in **Table 2.1**. To verify whether the resistance cassettes recombined within the target gene site, primers that flank target sequence were designed for both upstream and downstream genes sequences (**Table 2.3**). Both wild-type and mutant genes sequences were amplified with genomic confirmation primers by PCR. Three PCRs were used to show that each mutant exhibited the correct structure. Three reactions were done by using nearby locus-specific primers with the respective common test primer (C1, C2, K1, K2 or primers for TetRA cassette) to test for both new junction fragments.

Complementation studies

The *mchDEF* fragment was amplified from EcN genomic DNA using primers listed in **Table 2.3**. A region of 4148 bp was amplified to ensure that all the regulatory elements were included. The PCR fragment was cloned into high copy number pCR ^{TM}- XL-TOPO vector using Invitrogen Zero Blunt TOPO PCR Cloning Kit's provided protocol and sub cloned into the multiple cloning site (MCS) of low copy number plasmid pWSK29. Sequencing analysis confirmed the correct insertion of the gene of interest. The *mchDEF mcmI* or *mchDEF mchI* fragments were amplified from EcN genomic DNA using primers listed in **Supplementary Table 3**. The PCR fragments of 4321bp

(*mchDEFmcmI*) and 4000bp (*mchDEF*) and 400bp (*mchI*) bp were directly assembled with the plasmid pWSK30 using the Gibson assembly method.

In vitro growth assays

The effect of EcN microcin secretion against commensal *E. coli,* AIEC, and *S*. Typhimurium was tested with *in vitro* competitive growth assays in iron-rich and iron-limiting conditions. Strains were grown in Nutrient Broth supplemented with 0.2mM 2,2'-dipyridyl aerobically at 37 °C overnight. Approximately $5x10^3$ CFU/mL from an overnight culture were inoculated into 0.1 mL of tissue culture medium (DMEM/F12 plus 10% fetal bovine serum (FBS), both Invitrogen), as previously described(32, 33). When indicated, 1 μM of ferric iron citrate (Sigma) was added to the media. Iron citrate was chosen as a source of iron because *E. coli* cannot utilize citrate as a carbon source. Wild-type EcN or mutants were inoculated in competition with wild-type *S*. Typhimurium or *S*. Typhimurium *fepA* and/or *iroN* mutants, commensal *E. coli*, or AIEC. CFUs of each strains were enumerated by plating serial dilution at 5h, 8h, and 11h after inoculation and fro some assays 16h post-inoculation.

Mice

The Institutional Animal Care at the University of California, Irvine, approved all mouse experiments. Eight to ten-week-old male and female C57BL/6 NRAMP1 functional mice were bred in our vivarium. For some experiments, mice were purchased from Jackson laboratory and upon arrival mice were allowed to the new environment for at least 1 week prior the start of the experiment. All mice were housed under specific pathogen-

free conditions. Mice were fed an irradiated 2920X teklad diet (Envigo). For one experimental procedure mice were fed an irradiated iron rich diet (1% Diet FeSO4 2020, teklad TD. 160234 Envigo). Fecal culture in MacConkey agar showed that mice from this line are free of *E. coli* and other enteric commensals. Five to eight mice were used per experimental group. The group sizes have been established empirically (based on previous studies) to detect a 10-fold difference with statistical significance. For one experiment 10 week old Swiss Webster germ-free mice were used. Swiss Webster germ-free mice were maintained in and were fed a double irradiated diet (Purina 5066, Charles River Rodent 18% Vac Pac). Only 3 mice per experimental group were used for this experimental procedure. Mice were randomly grouped in cages of a maximum five animals per cage. To avoid any sex phenotypic relationship, similar numbers of male and female mice were used in each experimental group. No blinding was performed, with the exception of the histopathology.

Dextran sodium sulfate induced colitis mouse model

To induce colitis, the following procedure was followed. The drinking water was replaced with either filter-sterilized water (mock-treatment) or with a filter-sterilized solution of 4% (w/v) dextran sulfate sodium (DSS; relative molecular mass 36,000 – 50,000; MP Biomedicals, Santa Ana) in water as indicated. For DSS- treated mice, the drinking water was switched for 24h to regular, filter-sterilized water 3 days prior the end of the experiment. The remaining days the drinking water was replaced with either filter-sterilized water (mock-treatment) or with a filter-sterilized solution of 2% (w/v) DSS. 4 days after the start of the DSS treatment, animals were orally inoculated with 1:1 ratio of

$5x10^8$ CFU of each wild-type EcN and mutants in competition with the commensal *E. coli* or AIEC strains (resuspended in 0.1 mL LB broth). Fecal material was collected each day after bacterial administration and was harvested in sterile PBS and the bacterial load for the EcN wt and mutants or commensal *E. coli* strains was determined by plating serial 10-fold dilutions on selective agar plates. Animals were euthanized 5 days after inoculation. Cecal tissue was collected for isolation of mRNA and protein and for histopathological analysis, flash frozen and stored at -80 °C. Fecal material, cecal content, and colonic content was harvested in sterile PBS and the bacterial load for the *E. coli* strains was determined by plating serial 10-fold dilutions on selective agar plates. To differentiate EcN from other *E. coli* strains in biological samples, the strains were differentially marked with the low-copy number pACYomega (Cm) or pHP45omega (Carb) (**Table 2.2**). Plasmids were stable throughout the infection and similar colonies were counted in other differential media such as MacConkey agar (not shown). When noted, the competitive indices were calculated by dividing the output ratio (EcN CFU/ commensal *E. coli* or AIEC CFU) by the input ratio (EcN CFU/ commensal *E. coli* or AIEC CFU).

Salmonella Typhimurium-induced colitis

C57BL/6 NRAMP1 functional mice were treated with streptomycin (100 μL of a 200 mg/mL solution in sterile water) one day prior infection. The following day, mice were orally inoculated with $1x\ 10^9$ CFU of *S.* Typhimurium (resuspended in 0.1 mL LB broth) or with a 1:1 ratio of $5x10^8$ CFU each of *S.* Typhimurium and wild-type EcN, or EcN *mchDEF* strain for competitive colonization experiments. For therapeutic administration

of EcN after *S.* Typhimurium infection, C57BL/6 NRAMP1 functional mice were treated with streptomycin (100 μL of a 200 mg/mL solution in sterile water) one day prior to *S.* Typhimurium infection. The following day, mice were orally inoculated with 1x 10^9 CFU of *S.* Typhimurium. At day 2 and 5 after *S.* Typhimurium infection, mice were either mock-treated or treated with 1x 10^9 CFU of wild-type EcN, or EcN *mchDEF.* Fecal material was collected each day after bacterial administration and was harvested in sterile PBS, and the bacterial load for *S.* Typhimurium and EcN strains was determined by plating serial 10- fold dilutions on selective agar plates. At day 7 post infection, mice were euthanized and one portion of the cecum was collected for isolation of mRNA and protein and flash frozen and stored at -80 °C. A second portion of the caecum was fixed in formalin for histopathology. Bacteria were enumerated in the colon content, terminal ileum, Peyer's patches and by plating serial dilutions on LB agar plates containing the appropriate antibiotics. To selectively identify *S*. Typhimurium from EcN strain in the colon content, the strains were differentially marked with the low-copy number pACYomega (Cm) or pHP45omega (Carb). Plasmids were stable throughout the infection and similar colonies were counted in other differential media such as MacConkey agar (not shown). The recovered bacteria were then plated on LB agar containing respective antibiotics. When noted, the competitive indices were calculated by dividing the output ratio (EcN CFU/ *S*. Typhimurium CFU) by the input ratio (EcN CFU/ *S*. Typhimurium CFU).

Bacterial RNA extraction

A bacterial RNA mini kit (Bio-Rad Aurum Total) was used to extract RNA from bacterial cultures. Both wild-type EcN and the EcN *mchB mcmA* mutant were grown in Nutrient Broth supplemented with 0.2 mM 2,2'-dipyridyl aerobically at 37 °C overnight. Approximately 10^4 CFU/mL from an overnight culture were inoculated into 5ml of tissue culture medium (DMEM/F12 plus 10% fetal bovine serum, Invitrogen), as previously described(32, 33). When indicated, 1μM of iron citrate was added to the media. At 7h post-inoculation, $2x10^9$ bacteria were used to extract RNA. An additional DNAse treatment (Ambion) was done prior to the generation of cDNA with reverse transcription reagents (Roche).

Quantitative Real-Time PCR

For analysis of gene expression by quantitative real-time PCR, total RNA was extracted from cecal tissues with TRI Reagent (Molecular Research Center; Cincinnati, OH). RNA from DSS treated mice was further purified using the dynabeads mRNA direct kit (Life Technologies) according to the recommendations of the manufacturer. Reverse transcription reagents (Roche) were employed to generate cDNA from all RNA samples. Real-time PCR was performed using SYBR Green (Roche, Indianapolis, IN) and the Roche Lightcycler 480 system (Roche, Indianapolis, IN). The data were analyzed using the comparative ΔΔ-Ct method. Target gene transcription of each sample was normalized to the respective levels of mRNA *β-actin*. For qPCR analysis of bacterial transcripts, transcription of *mchB* and *mcmA* was normalized to the respective levels of

bacterial *gapA* mRNA. DNA contamination was less than 1% for all bacterial amplicons, as determine by separate RT-PCR mock reactions lacking reverse transcriptase. All primers used are listed in **Table 2.4**.

Histopathology analysis

Tissue samples were fixed in formalin, processed according to standard procedures for paraffin embedding, sectioned at 5 mm, and stained with hematoxylin and eosin. The pathology score of cecal samples was determined by blinded examinations of cecal sections from a board-certified pathologist using previously published methods(20). Each section was evaluated for the presence of neutrophils, mononuclear infiltrate, submucosal edema, surface erosions, inflammatory exudates, and cryptitis. Inflammatory changes were scored from 0 to 4 according to the following scale: 0 = none; 1 = low; 2 = moderate; 3 = high; 4 = extreme. The inflammation score was calculated by adding up all the scores obtained for each parameter and interpreted as follows 0–2 = within normal limit; 3–5 = mild; 6–8 = moderate; 8+ = severe.

Analysis of microbiota

DNA extracted from fecal samples was amplified (UC Davis HMSB Facility) by a two-step PCR enrichment of 16S rDNA (V4 region) with primers 515F and 806R modified by addition of barcodes for multiplexing, then sequenced on an Illumina MiSeq system. After quality filtering, demultiplexing and trimming, sequences were processed and analyzed by employing the QIIME pipeline v1.9.1. In brief: paired-end sequences were joined, quality filtered, and chimera filtered (usearch61 option; RDP gold database),

then assigned (usearch61 option) to operational taxonomic units (OTUs), assigned taxonomy (confidence threshold = 0.8) with the RDP classifier, aligned with PyNAST ,then relative abundance, alpha diversity and beta diversity were assessed. Greengenes database v13_8 was utilized in the open-reference OTU picking workflow.

Statistical analysis of data

We used the Graphpad Prism 6 software for statistical analysis. To compare bacterial CFUs in feces and tissue content and mRNA expression in different experimental conditions, we applied a non-parametric Mann-Whitney-Wilcoxon test. We chose this test because it can be applied to data with normal or unknown distribution.

TABLE 2.1 **Strains used in this study**

Designation	**Genotype**	**Source or Reference**
STRAINS (*Escherichia coli*)		
EcN	*E. coli* Nissle 1917, wild-type	(Ardeypharm, Germany)
MSC30	*EcN* Δ*mchDEF::kan* Kan^R	This study
MSC66	*EcN* Δ*mchB::scar* Δ*mcmA*::Kan Kan^R	This study
MSC86	*EcN* Δ*mchDEF::kan* Δ*mchI::cat* Kan^R Cm^R	This study
MSC87	*EcN* Δ*mchDEF::kan* Δ*mcmI::tetRA* Kan^R Tet^R	This study
MSC108	*EcN* Δ*mchDEF::kan* Δ*mcmI::cat* Δ*mchI::tetRA* Kan^R Cm^R Tet^R	This study
MSC136	*EcN* Δ*mchDEF::kan* (pWSK29) Kan^R Ap^R	This study
MSC140	*EcN* Δ*mchDEF::kan* (pWSK29*::mchDEF*) restored Kan^R Ap^R	This study
E. coli JB2	mouse commensal *E. coli* (our vivarium)	(20)

AIEC	Adherent invasive *E. coli* isolate (NRG857c, O83:H1) $Carb^R$ Cm^R	(34)
DH5αMCR	F- *mcrA* Δ(*mrr-hsdRMS-mcrBC*) Φ80d*lacZ*M15 (*lacZYA-argF*)*U169 deoR recA1 endA1 phoA supE44*l- *thi-1 gyrA*96 *relA*1	Gibco BRL
One Shot® TOP10 Chemically Competent *E. coli*	F- *mcr*A Δ(*mrr-hsd*RMS-*mcr*BC) φ80*lacZ*ΔM15 Δ*lac*X74 *rec*A1 *ara*D139 Δ(*ara, leu*) 7697 *gal*U *gal*K *rps*L (StrR) *end*A1 *nup*G I	Invitrogen
MSC 46	EcN Δ*mcmA*::kan Kan^R	This study
MSC 31	EcN Δ*mchB*::kan Kan^R	This study
MSC 172	EcN Δ*mchDEF::kan* Δ*mchI::cat* (pWSK30*::mchDEFmchI*) restored Kan^R Tet^R Ap^R	This study
MSC 173	EcN Δ*mchDEF::kan* Δ*mcmI::cat* (pWSK30*::mchDEFmcmI*) restored Kan^R Cm^R Ap^R	This study
STRAINS (*Salmonella* Typhimurium)		
IR715	*Salmonella* Typhimurium ATCC 14028, Nal^R	(36)
SPN452	IR715, Δ*invA::tetRA* Δ*spiB*::KSAC	(33)
MSC50	IR715, Δ*fepA::kan* Kan^R	This study
MSC74	IR715, Δ*iroN::tetRA* Tet^R	This study
MSC75	IR715, Δ*fepA::kan* Δ*iroN::tetRA* Kan^R	This study
MSC75	IR715, Δ*fepA::kan* Δ*iroN::tetRA* Kan^R Tet^R	This study

MSC 168	IR715, pWSK30*::mchDEFmcmI* Ap^R	This study
MSC 170	IR715, pWSK30*::mchDEFmchI* Ap^R	This study

TABLE 2.2 **Plasmids used in this study**

Designation	**Genotype**	**Source or Reference**
pJK611	Ap^R, temperature-sensitive, λ Red recombinase system	(35)
pKD3	Ap^R, Cm^R	(35)
pkD4	Ap^R, Kan^R	(35)
pCP20	Ap^R, temperature-sensitive, FLP system	(35)
pHP45 Ω	$Strep^R$, $Carb^R$	(37)
pACY Ω	PHP45Ω derivative, $Strep^R$, Cm^R	Takeshi Haneda and Andreas Bäumler
pWSK29	Ap^R, MCS *lacZ*	(38)
pWSK29:*mchDEF*	*mchDEF* under control of native promoter in pWSK29	This study
pWSK30::*mchDEF mchI*	*mchDEF mchI* under control of native lacZ promoter	This study
pCR2.1	TOPO Cloning Vector ($Carb^R$, Kan^R)	Invitrogen

TABLE 2.3 **Primers for targeted mutagenesis**

Designation	**Purpose**	**Sequence**
H1P1 *mchDEF*	Flanking region 1 deletion of EcN *mchDEF*	5'AGAAACACAGTGTAATAAATATATAAGGGAAATAGTAA TGTGTAGGCTGGAGCTGCTTC3'
H2P2 *mchDEF*	Flanking region 2 deletion of EcN *mchDEF*	5'CCATCGACAAAACTCCTTACAAAGTTACACCAGTGGA TTTCATATGAATATCCTCCTTA3'
Check *mchDEF*	Check for *mchDEF* deletion	5'GGCATAATCAAAAGCAGG3' 5'CCATAGTAATAACTAAGAT3'
H1P1 *mchB*	Flanking region 1 deletion of EcN *mchB*	5'TCAGGCTGGAAAAACGGAAGTTAAATATGATGGAGTT TATGTGTAGGCTGGAGCTGCTTC3'
H2P2 *mchB*	Flanking region 2 deletion of EcN *mchB*	5'GGTACTACCGAAAAAGTACCTGTAAAATAAATAAAAAT ATCATATGAATATCCTCCTTA3'
Check *mchB*	Check for *mchB* deletion	5'GGTCCTCACTGGTTATGA3' 5'GATCCACAAGCTGCCAGGAT3'
H1P1 *mcmA*	Flanking region 1 deletion of EcN *mcmA*	5'CTTAAAGCGTTACATAGGCACCATTATCATATAATGAA GCACCGATTGTGTAGGCTGGAGCTGCTTC3'

H2P2 *mcmA*	Flanking region 2 deletion of EcN *mcmA*	5'GAATTTTTACTTCTTCACAAATCTTATAGCGAAGGTGT TGAAATGGTCCATATGAATATCCTCCTTA3'
Check *mcmA*	Check for *mcmA* deletion	5'GCCACAGTCGATGAATCC3' 5'CCTGTGTCTACTATTGGT3'
H1P1 *mchI*	Flanking region 1 deletion of EcN *mchI*	5'GTAACTTTTCATAATGAAAATAAAGCAACAGGTAGGTA TTGTGTAGGCTGGAGCTGCTTC3'
H2P2 *mchI*	Flanking region 2 deletion of EcN *mchI*	5'CTGTGATTCTGTTATTTCTCGCATATAAACTCCATCAT ATCATATGAATATCCTCCTTA3'
Check *mchI*	Check for *mchI* deletion	5'CATTCTTATGCCTCCTCAC3' 5'ATCCTGGCAGCTTGTGGATC3'
H1P1 *mcmI*	Flanking region 1 deletion of EcN *mcmI*	5'TCCCATAATCCACTGGTGTAACTTTGTAAGGAGTTTTG TCTTAAGACCCACTTTCACATT3'
H2P2 *mcmI*	Flanking region 2 deletion of EcN *mcmI*	5'TCATTTCAACACCTTCGCTATAAGATTTGTGAAGAAGT AACTAAGCACTTGTCTCCTG3'

Check *mcmI*	Check for *mcmI* deletion	5'CATTCTTATGCCTCCTCAC3' 5' TCAATGTTTACTTTATCAT3'
K1	pkD4 Kanamycin cassette for PCR confirmation	5'GCCACAGTCGATGAATCC3'
K2	pkD4 Kanamycin cassette for PCR confirmation	5'CGGTGCCCTGAATGAACTGC3'
C1	pkD3 Chloramphenicol cassette for PCR confirmation	5'TTATACGCAAGGCGACAAGG3'
C2	pkD3 Chloramphenicol cassette for PCR confirmation	5'GATCTTCCGTCACAGGTAGG3'

T1	*tetRA* cassette for PCR confirmation	5'TCATACTGTTTTTCTGTA3'
T2	*tetRA* cassette for PCR confirmation	5'TGATAATACAGATACCGAAG3'
*mchDEF*_compl	restoration *mchDEF*	5'TAATGAGCTCCCTGCTGGATAATCATGGC3' 5'TGGTTCTAGACTCCTTACAAAGTTACAC3'
*mchDEF*_ *mchI* compl	restoration *mchDEF mchI*	*mchDEF* construct (GIBSON ASEMBLY) 5'ACTCACTATAGGGCGAATTGGAGCTCCTGCTGGATAATCATGG3' 5' TCAAAAAAAGTGTCTCCTTACAAAGTTACACCAG3' *mchI* construct 5'ACTTTGTAAGGAGACACTTTTTTTGAAAAGTAAATAAC3' 5'CTGCAGCCCGGGGGATCCACTAGTTACTCCATCATATTTAACTTCCG3'
*mchDEF*_ *mcmI* compl	restoration *mchDEF mcmI*	*mchDEFmcmI* construct (GIBSON ASEMBLY) 5'ATACGACTCACTATAGGGCGAATTGGAGCTACCGATAAGAAACACAGTGTAATAAATATATAAG3' 5'AATTCCTGCAGCCCGGGGGATCCACTAGTTTCCCGTCACCTCCAGATAT3'

TABLE 2.4 **Primers for quantitative Real-Time PCR**

Species	**Target**	**Primer Pairs**
Mus musculus	*Lcn2*	5'ACATTTGTTCCAAGCTCCAGGGC3' 5'CATGGCGAACTGGTTGTAGTCCG3'
Mus musculus	*Il17a*	5'GCTCCAGAAGGCCCTCAGA3' 5'AGCTTTCCCTCCGCATTGA3'
Mus musculus	*Ly6g*	5'TGCGTTGCTCTGGAGATAGA3' 5'CAGAGTAGTGGGGCAGATGG3'
Mus musculus	*Il22*	5'GGCCAGCCTTGCAGATAACA3' 5'GCTGATGTGACAGGAGCTGA3'
Mus musculus	*Tnfa*	5'CATCTTCTCAAAATTCGAGTGACAA3' 5'TGGGAGTAGACAAGGTACAACCC3'
Mus musculus	*Nos2*	5'TTGGGTCTTGTTCACTCCACGG3' 5'CCTCTTTCAGGTCACTTTGGTAGG3'
Mus musculus	*Il10*	5'GGTTGCCAAGCCTTATCGGA3' 5'ACCTGCTCCACTGCCTTGCT3'
Mus musculus	*Actb*	5'GGCTGTATTCCCCTCCATCG3' 5'CCAGTTGGTAACAATGCCATGT3'
E. coli Nissle 1917	*mchB*	5'CAGCTATTGTTGGAGCTCTCG3' 5'ACTTGGGGTTGTAGTTGGAGC3'
E. coli Nissle 1917	*mcmA*	5'ATATCTGGAGGTGACGGGAA-3' 5'TGATAAAGTACATTCATGGG-3'
E. coli Nissle 1917	*gapA*	5'CTGACTGGTATGGCGTTCCG3' 5'TGTAACCCAGCCGCCTTTC3'

2.6 References

1. Winter SE & Bäumler AJ (2014) Why related bacterial species bloom simultaneously in the gut: principles underlying the 'Like will to like' concept. *Cell. Microbiol.* 16(2):179-184.
2. Stecher B (2015) The Roles of Inflammation, Nutrient Availability and the Commensal Microbiota in Enteric Pathogen Infection. *Microbiol. Spectr.* 3(3).
3. Winter SE, Lopez CA, & Bäumler AJ (2013) The dynamics of gut-associated microbial communities during inflammation. *EMBO Rep.* 14(4):319-327.
4. Rebuffat S (2012) Microcins in action: amazing defence strategies of Enterobacteria. *Biochem. Soc. Trans.* 40(6):1456-1462.
5. Yang SC, Lin CH, Sung CT, & Fang JY (2014) Antibacterial activities of bacteriocins: application in foods and pharmaceuticals. *Front. Microbiol.* 5:241.
6. Kamada N, Chen GY, Inohara N, & Nunez G (2013) Control of pathogens and pathobionts by the gut microbiota. *Nat. Immunol.* 14(7):685-690.
7. Buffie CG & Pamer EG (2013) Microbiota-mediated colonization resistance against intestinal pathogens. *Nat. Rev. Immunol.* 13(11):790-801.
8. Donaldson GP, Lee SM, & Mazmanian SK (2016) Gut biogeography of the bacterial microbiota. *Nat. Rev. Microbiol.* 14(1):20-32.
9. Spees AM*, et al.* (2013) Streptomycin-induced inflammation enhances *Escherichia coli* gut colonization through nitrate respiration. *mBio* 4(4).
10. Hill DA*, et al.* (2010) Metagenomic analyses reveal antibiotic-induced temporal and spatial changes in intestinal microbiota with associated alterations in immune cell homeostasis. *Mucosal. Immunol.* 3(2):148-158.
11. Winter SE*, et al.* (2013) Host-derived nitrate boosts growth of *E. coli* in the inflamed gut. *Science* 339(6120):708-711.
12. Behnsen J, Deriu E, Sassone-Corsi M, & Raffatellu M (2013) Probiotics: properties, examples, and specific applications. *Cold Spring Harb. Perspect. Med.* 3(3):10074.
13. Jacobi CA & Malfertheiner P (2011) *Escherichia coli* Nissle 1917 (Mutaflor): new insights into an old probiotic bacterium. *Dig. Dis.* 29(6):600-607.
14. Patzer SI, Baquero MR, Bravo D, Moreno F, & Hantke K (2003) The colicin G, H and X determinants encode microcins M and H47, which might utilize the catecholate siderophore receptors FepA, Cir, Fiu and IroN. *Microbiology* 149(Pt 9):2557-2570.
15. Kommineni S*, et al.* (2015) Bacteriocin production augments niche competition by enterococci in the mammalian gastrointestinal tract. *Nature* 526(7575):719-722.
16. Nolan EM & Walsh CT (2008) Investigations of the MceIJ-catalyzed posttranslational modification of the microcin E492 C-terminus: linkage of ribosomal and nonribosomal peptides to form "trojan horse" antibiotics. *Biochemistry* 47(35):9289-9299.
17. Asensio C & Perez-Diaz JC (1976) A new family of low molecular weight antibiotics from enterobacteria. *Biochemical and biophysical research communications* 69(1):7-14.
18. F. Baquero FM (1978) The microcins. *FEMS Microbiology Letters* 23(2-3):117-124.
19. Sassone-Corsi M & Raffatellu M (2015) No vacancy: how beneficial microbes cooperate with immunity to provide colonization resistance to pathogens. *Journal of immunology* 194(9):4081-4087.

20. Behnsen J*, et al.* (2014) The cytokine IL-22 promotes pathogen colonization by suppressing related commensal bacteria. *Immunity* 40(2):262-273.
21. Vassiliadis G, Destoumieux-Garzon D, Lombard C, Rebuffat S, & Peduzzi J (2010) Isolation and characterization of two members of the siderophore-microcin family, microcins M and H47. *Antimicrob. Agents Chemother.* 54(1):288-297.
22. Azpiroz MF & Lavina M (2004) Involvement of enterobactin synthesis pathway in production of microcin H47. *Antimicrob. Agents Chemother.* 48(4):1235-1241.
23. Rodriguez E & Lavina M (1998) Genetic analysis of microcin H47 immunity. *Can. J. Microbiol.* 44(7):692-697.
24. Rodriguez E, Gaggero C, & Lavina M (1999) The structural gene for microcin H47 encodes a peptide precursor with antibiotic activity. *Antimicrob. Agents Chemother.* 43(9):2176-2182.
25. Vassiliadis G*, et al.* (2007) Insight into siderophore-carrying peptide biosynthesis: enterobactin is a precursor for microcin E492 posttranslational modification. *Antimicrob. Agents Chemother.* 51(10):3546-3553.
26. Nolan EM, Fischbach MA, Koglin A, & Walsh CT (2007) Biosynthetic tailoring of microcin E492m: post-translational modification affords an antibacterial siderophore-peptide conjugate. *J. Am. Chem. Soc.* 129(46):14336-14347.
27. Azpiroz MF, Rodriguez E, & Lavina M (2001) The structure, function, and origin of the microcin H47 ATP-binding cassette exporter indicate its relatedness to that of colicin V. *Antimicrob. Agents Chemother.* 45(3):969-972.
28. Braun V, Patzer SI, & Hantke K (2002) Ton-dependent colicins and microcins: modular design and evolution. *Biochimie* 84(5-6):365-380.
29. Duquesne S, Destoumieux-Garzon D, Peduzzi J, & Rebuffat S (2007) Microcins, gene-encoded antibacterial peptides from enterobacteria. *Nat. Prod. Rep.* 24(4):708-734.
30. Rebuffat S, Blond A, Destoumieux-Garzon D, Goulard C, & Peduzzi J (2004) Microcin J25, from the macrocyclic to the lasso structure: implications for biosynthetic, evolutionary and biotechnological perspectives. *Curr. Protein Pept. Sci.* 5(5):383-391.
31. Fischbach MA, Lin H, Liu DR, & Walsh CT (2006) How pathogenic bacteria evade mammalian sabotage in the battle for iron. *Nat. Chem. Biol.* 2(3):132-138.
32. Deriu E*, et al.* (2013) Probiotic bacteria reduce *salmonella* typhimurium intestinal colonization by competing for iron. *Cell host & microbe* 14(1):26-37.
33. Raffatellu M*, et al.* (2009) Lipocalin-2 resistance confers an advantage to *Salmonella* enterica serotype Typhimurium for growth and survival in the inflamed intestine. *Cell host & microbe* 5(5):476-486.
34. Eaves-Pyles T*, et al.* (2008) *Escherichia coli* isolated from a Crohn's disease patient adheres, invades, and induces inflammatory responses in polarized intestinal epithelial cells. *Int. J. Med. Microbiol.* 298(5-6):397-409.
35. Datsenko KA & Wanner BL (2000) One-step inactivation of chromosomal genes in *Escherichia coli* K-12 using PCR products. *Proc. Natl. Acad. Sci. USA* 97(12):6640-6645.
36. Stojiljkovic I, Bäumler AJ, & Heffron F (1995) Ethanolamine utilization in *Salmonella* typhimurium: nucleotide sequence, protein expression, and mutational analysis of the *cchA cchB eutE eutJ eutG eutH* gene cluster. *J. Bacteriol.* 177(5):1357-1366.

37. Prentki P & Krisch HM (1984) In vitro insertional mutagenesis with a selectable DNA fragment. *Gene* 29(3):303-313.
38. Wang RF & Kushner SR (1991) Construction of versatile low-copy-number vectors for cloning, sequencing and gene expression in Escherichia coli. *Gene* 100:195-199.

CHAPTER 3

A novel mucosal immunization strategy to reduce *Salmonella* gastroenteritis by targeting iron acquisition

3.1 Summary

Infections with Gram-negative pathogens pose a serious threat to public health. This scenario is exacerbated by increases in antibiotic resistance and the limited availability of vaccines and therapeutic tools to combat these infections. Here we report a new immunization approach that targets siderophores, small molecules exported by enteric Gram-negative pathogens to acquire iron, an essential nutrient, in the host. Because siderophores are non-immunogenic, we designed and synthesized conjugates of a native siderophore and the immunogenic carrier protein cholera toxin subunit B (CTB). Mice immunized with the CTB-siderophore conjugate developed anti-siderophore antibodies in the gut mucosa, and when infected with the enteric pathogen *Salmonella*, exhibited reduced intestinal colonization and reduced systemic dissemination of the pathogen. Moreover, analysis of the gut microbiota revealed that reduction of *Salmonella* colonization in the inflamed gut was accompanied by expansion of *Lactobacillus* spp., beneficial commensal organisms that thrive in similar locales as

Enterobacteriaceae. Collectively, our results demonstrate that anti-siderophore antibodies inhibit *Salmonella* colonization. Because siderophore-mediated iron acquisition is a virulence trait shared by many bacterial and fungal pathogens, blocking microbial iron acquisition by siderophore-based immunization or other siderophore-targeted approaches may represent a novel strategy to prevent and ameliorate a broad range of infections.

3.2 Introduction

Gram-negative pathogens cause a range of human diseases, including foodborne illness, urinary tract infections, and sepsis. Infections with these organisms pose a serious global public health threat that is exacerbated by increasing antibiotic resistance, the dearth of new antibiotics in the drug pipeline, and the limited availability of vaccines (1). To slow the emergence of antibiotic resistance and to reduce the incidence of secondary infections, narrow-spectrum therapeutic strategies are needed; specifically, ones that limit disruption of the gut microbiota, which comprises beneficial microbes that provide colonization resistance to pathogens (2). Many studies have elucidated molecular mechanisms by which pathogens thrive in the host, thus indicating potential targets for the prevention and treatment of infection. In recent years, bacterial metabolism has been proposed to be a key factor in promoting pathogenicity (3).

The vast majority of bacterial pathogens have a metabolic requirement for iron. Because the vertebrate host tightly controls the concentration of free iron (e.g., $\approx 10^{-24}$ M in serum), many microbes biosynthesize and export secondary metabolites called siderophores to scavenge iron from the host (4). These small molecules chelate ferric iron (Fe^{3+}) with high affinity (e.g., enterobactin, (**Fig. 1*A***), $K_d \approx 10^{-25}$ M at neutral pH) (5-8). Once a siderophore coordinates iron in the extracellular space, the iron-bound siderophore is recognized and transported into a microbial cell by a dedicated membrane receptor. Following cellular uptake, the iron is released from the siderophore to support microbial metabolism and replication. Siderophores are regarded as major

virulence factors during infection with bacterial and fungal pathogens, examples for which include *Salmonella enterica*, uropathogenic *Escherichia coli*, *Klebsiella pneumoniae*, *Pseudomonas aeruginosa*, *Mycobacterium tuberculosis*, *Staphylococcus aureus*, and *Aspergillus fumigatus* (9).

Enterobactin (Ent, **Fig. 1A**) is a siderophore biosynthesized and deployed by commensal and pathogenic Enterobacteriaceae (10). In a process known as “nutritional immunity”, the host responds to microbial infection and inflammation by limiting the availability of essential nutrient metals, including iron (11). To prevent Ent-mediated microbial iron acquisition, epithelial cells and neutrophils secrete the host-defense protein lipocalin-2 (LCN2). This protein inhibits siderophore-mediated iron uptake by capturing ferric Ent in the extracellular milieu (12). By inhibiting the growth of Enterobacteriaceae that rely on Ent-mediated iron acquisition, LCN2 plays an essential role in preventing lethal infection by these organisms (12, 13). Nevertheless, various Gram-negative pathogens evade LCN2 by producing and utilizing “stealth siderophores” that cannot be captured by this host-defense protein. For example, *Salmonella* spp. and strains of pathogenic *E. coli* overcome LCN2 by biosynthesizing a family of C-glucosylated Ent derivatives named salmochelins (GlcEnt, **Fig. 1A**) (14, 15). These stealth siderophores cannot be captured by LCN2, thus allowing the pathogen to thrive in the inflamed gut in the presence of LCN2 and outcompete the microbiota (14-16). Indeed, *Salmonella* mutants that lack the GlcEnt receptor IroN are susceptible to the LCN2-mediated host response; these mutants exhibit reduced colonization in the inflamed intestine and cannot outcompete the microbiota (17, 18). In the absence of

intestinal inflammation or LCN2 expression, iron is more readily available and mutants in siderophore receptors are not attenuated (19).

Inspired by seminal studies exemplifying the importance of siderophore-mediated iron acquisition during infection with *Salmonella* as well as other pathogens (18, 20), we hypothesized that boosting host nutritional immunity by blocking siderophore-based iron acquisition would reduce microbial burden and improve the outcome of infection. To address this hypothesis, we designed and synthesized conjugates of a native siderophore employed by *Salmonella* and an immunogenic carrier protein, then immunized mice with the compounds to induce an antibody response against siderophores. Herein, we show that immunization of mice with the siderophore-carrier protein conjugate elicited an antibody response to siderophores in the intestinal mucosa, and significantly reduced *Salmonella* colonization of the inflamed gut.

3.3 Results

Immunization with siderophore-conjugates elicits a mucosal antibody response.

To induce the development of an antibody response against siderophores, we selected cholera toxin subunit B (CTB) as the immunogenic carrier protein because it induces a strong mucosal immune response (21). We reasoned that immunizing mice with a CTB-siderophore conjugate should result in the production of anti-siderophore antibodies in the gut mucosa, which is the primary site of *Salmonella* infection. Because Ent **1** and GlcEnt **2** share several structural features, including the catechol moieties and trilactone ring (**Fig. 3.1 A**), and GlcEnt is a derivative of Ent, we hypothesized that immunization with CTB-Ent would elicit an antibody response against both Ent and GlcEnt. We reasoned that it could be difficult to elicit a specific antibody response to only one of these siderophores, given the shared structural attributes. Although Ent is captured by LCN2 in the inflamed gut, we also reasoned that the development of antibodies that capture both Ent and GlcEnt would be advantageous, especially if LCN2 levels are low in response to infection (for instance, in immunocompromised patients (22).

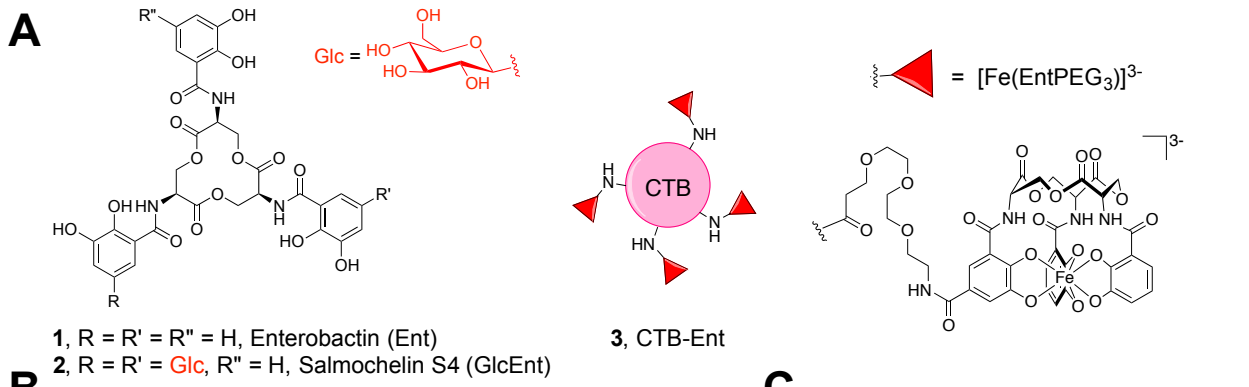
We thus designed and prepared a CTB-Ent conjugate that harbors the native Ent scaffold. We assembled CTB-Ent **3** from CTB and intermediate **8** (**Fig. 3.2**), an Ent derivative monofunctionalized with a polyethylene glycol (PEG_3) linker using standard amide coupling methods (**Fig. 3.1 A*; Fig. 3.2 and 3.3)***. This procedure results in the Ent haptens covalently attached to surface-exposed lysine residues of CTB via the PEG_3 linker (**Fig. 3.1 A**). The average number of Ent-labeled lysine residues is ≈4 out of 9 surface-exposed lysine residues in one subunit of CTB. We selected a PEG_3 linker

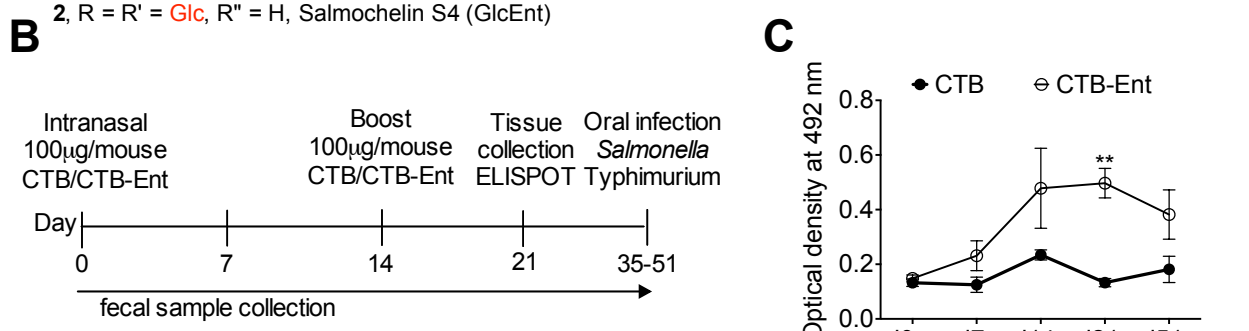
because it is stable and affords both flexibility and enhanced solubility in aqueous solution (23). In prior work, we modified the native Ent scaffold with a PEG_3 linker and established that these molecules coordinate Fe^{3+} and are recognized and transported by the Ent receptor FepA (23, 24). From these prior studies, we reasoned that antibodies that bind the Ent moiety of CTB-Ent will also recognize and bind unmodified Ent.

FIGURE 3.1

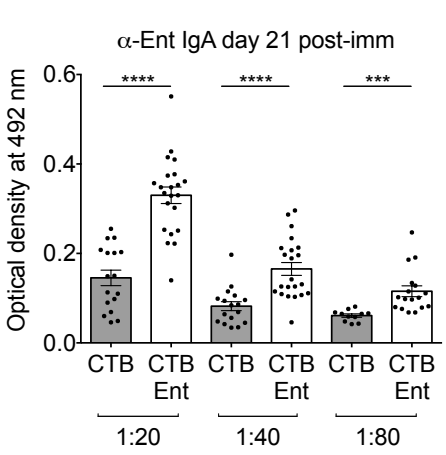
Figure 3.1. Detection of mucosal IgA anti-siderophores(A) Chemical structures of enterobactin (Ent, **1**), salmochelin S4 (GlcEnt, **2**), and a cartoon depicting CTB-Ent **3** conjugate. Ent and GlcEnt are cyclic trimers of *N*-2,3-dihydroxylbenzoyl-L-serine. **(B)** Description and timeline of the immunization protocol. Timing of intranasal immunization (day 0 and day 14) and dosage of antigen (100 μg/mL) are indicated. Feces were collected weekly. ELISPOT assay was carried out at day 21 post-immunization. Mice were infected with *Salmonella enterica* serovar Typhimurium *per os* between day 35 and day 51 post-immunization. **(C)** Anti-Ent IgA antibodies were quantified by using an in-house ELISA in fecal samples from mice immunized with either CTB (n = 5) or CTB-Ent (n = 7) during the indicated time course. **(D)** Two-fold dilution for detection of fecal anti-Ent IgA by ELISA in mice immunized with either CTB (n = 15-20) or CTB-Ent (n = 15-20) at day 21 post-immunization. **(E)** Representative ELISPOT images of supernatant from B cells producing anti-Ent IgA isolated from Peyer's patches of mice immunized with either CTB or CTB-Ent at day 21 post-immunization. Average number of spots detected in CTB- or CTB-Ent-immunized mice per million Peyer's patches cells (n = 7). **(F)** Two-fold dilution for detection of fecal anti-GlcEnt IgA by ELISA in mice immunized with either CTB (n = 15-20) or CTB-Ent (n = 15-20) at day 21 post-immunization. **(G)** Representative ELISPOT images of supernatant from B cells producing anti-GlcEnt IgA isolated from Peyer's patches of mice immunized with either CTB or CTB-Ent at day 21 post-immunization. Average number of spots detected in CTB- or CTB-Ent-immunized mice per million Peyer's patches cells (n = 5). **(C**-**G)** Bars represents the mean ± standard error. Immunization experiments were repeated three times. Each time, a different batch of CTB/CTB-Ent was used **** $P < 0.0001$, *** $P < 0.001$,** $P < 0.01$.

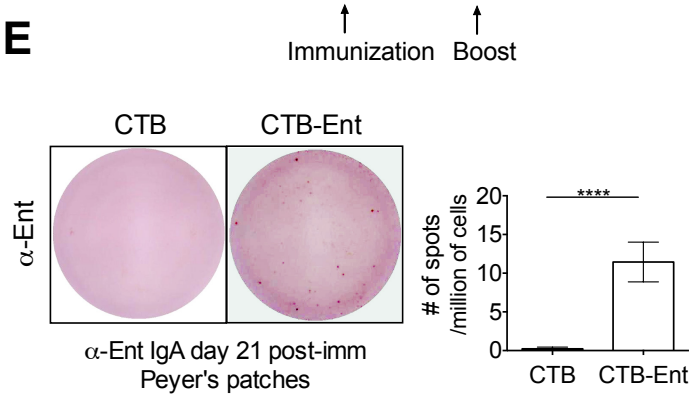
FIGURE 3.1

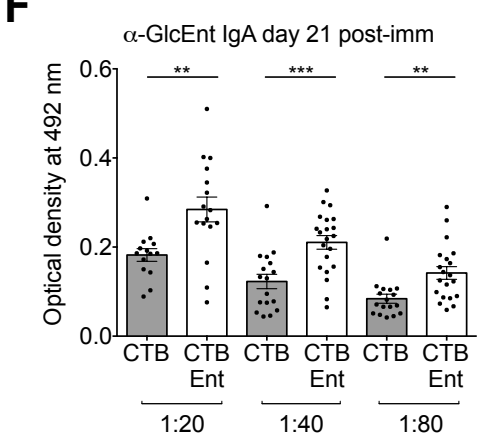

A
Glc =
= [Fe(EntPEG3)]3-
CTB
1, R = R' = R" = H, Enterobactin (Ent)
2, R = R' = Glc, R" = H, Salmochelin S4 (GlcEnt)
3, CTB-Ent

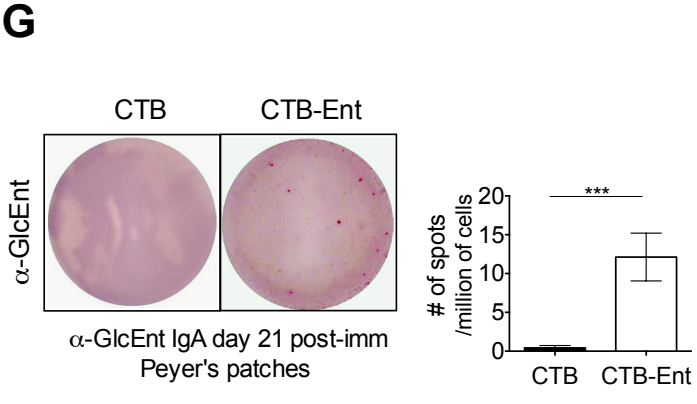

B
Intranasal 100μg/mouse CTB/CTB-Ent
Boost 100μg/mouse CTB/CTB-Ent
Tissue collection ELISPOT
Oral infection Salmonella Typhimurium
Day
0
7
14
21
35-51
fecal sample collection

C
CTB
CTB-Ent
Optical density at 492 nm
0.0
0.2
0.4
0.6
0.8
**
d0
d7
d14
d21
d51
Immunization
Boost


D
α-Ent IgA day 21 post-imm
Optical density at 492 nm
0.0
0.2
0.4
0.6
****
****
***
CTB
CTB Ent
1:20
1:40
1:80


E
CTB
CTB-Ent
α-Ent
α-Ent IgA day 21 post-imm
Peyer's patches
# of spots /million of cells
0
5
10
15
20
****
CTB
CTB-Ent

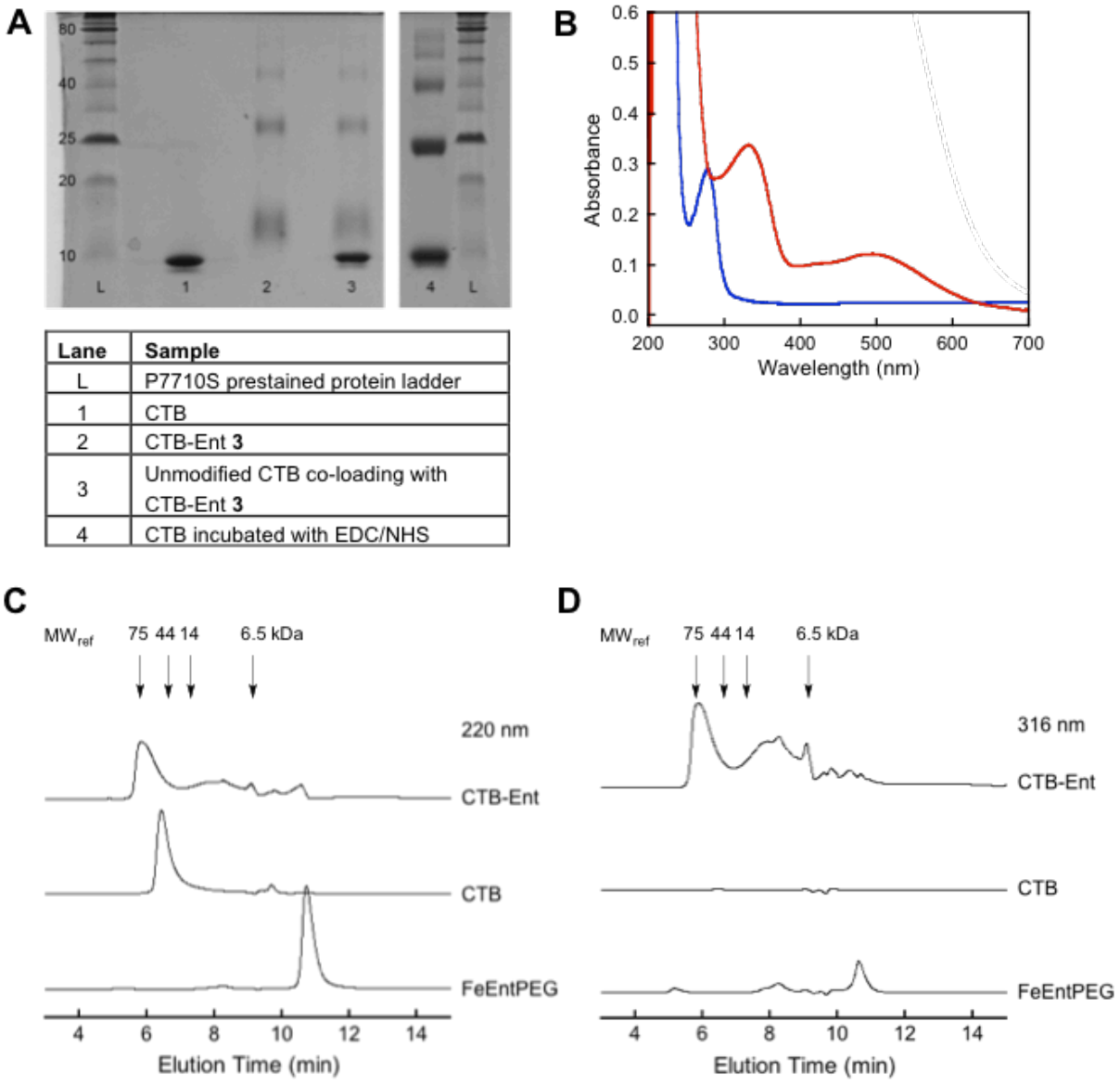

F
α-GlcEnt IgA day 21 post-imm
Optical density at 492 nm
0.0
0.2
0.4
0.6
**
***
**
CTB
CTB Ent
1:20
1:40
1:80


G
CTB
CTB-Ent
α-GlcEnt
α-GlcEnt IgA day 21 post-imm
Peyer's patches
# of spots /million of cells
0
5
10
15
20
***
CTB
CTB-Ent

We immunized mice at day 0 and boosted at day 14 (**Fig. 3.1 B**) by intranasal administration of either unmodified CTB (100 μg/mouse, mock-immunization) or CTB-Ent (100 μg/mouse). To determine whether mice immunized with CTB-Ent developed a specific antibody response against Ent, blood and fecal samples were collected weekly for detection of anti-Ent antibodies by using an in-house ELISA and dot-blot. As expected, the amount of total fecal IgA was similar between the two groups of mice (**Fig. 3.4 A**). However, only mice immunized with CTB-Ent developed specific fecal IgA antibodies that recognized Ent (**Fig. 3.1 D; Fig. 3.4 B**). The production of fecal anti-Ent IgA significantly increased at day 21 post-immunization in mice immunized with CTB-Ent (**Fig. 3.1 C and D**) in conjunction with the detection of specific fecal anti-CTB IgA (**Fig. 3.4 C**). The latter antibodies were also found in mice immunized with unmodified CTB, as expected (**Fig. 3.4 C**). An ELISPOT assay confirmed that mice immunized with CTB-Ent developed B cells secreting antigen-specific antibodies against Ent in the Peyer's patches (**Fig. 3.1 E**). In contrast, IgA that recognized unmodified CTB were secreted by B cells isolated from the Peyer's patches in both groups of mice (**Fig. 3.4 D**).

.

FIGURE 3.2



Lane	Sample
L	P7710S prestained protein ladder
1	CTB
2	CTB-Ent **3**
3	Unmodified CTB co-loading with CTB-Ent **3**
4	CTB incubated with EDC/NHS

Figure 3.2. Characterization of CTB-Ent. (A) SDS-PAGE (16% tricine gel) of samples from conjugation reactions. Unmodified CTB is 11.6 kDa, Ent-PEG$_3$-CO$_2$H **8** is approximately 900 Da. All samples were run on the same gel and the image was formatted to facilitate comparison of lane 4 with lanes 1-3. **(B)** Optical absorption spectra of CTB (30 μM, blue) and iron-bound CTB-Ent **3** (20 μM, red). The samples were prepared in PBS pH 7.2. **(C, D)** SEC HPLC traces of CTB, CTB-Ent **3**, and Ent-PEG$_3$-CO$_2$H **8** in 50 mM sodium phosphate buffer, pH 7.2. The Ent moieties present in these samples are in the Fe^{3+}-bound form. The arrow indicates the elution time and the molecular weight of the standard.

FIGURE 3.3

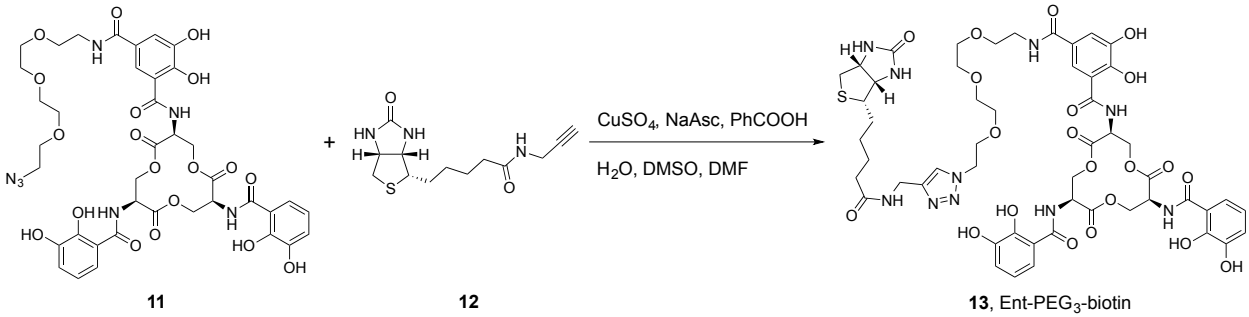


Figure 3.3 Synthesis of Ent-PEG$_3$-biotin conjugate 13.

We next investigated whether the mucosal IgA elicited by CTB-Ent immunization would also recognize GlcEnt. Consistent with our expectation based on the structural attributes shared by Ent and GlcEnt (**Fig. 3.1 A**), fecal IgA from mice immunized with CTB-Ent also recognized GlcEnt (**Fig. 3.1 F and G; Fig. 3.4 B**). This immunization appeared to specifically trigger mucosal immunity to Ent and GlcEnt. We found no evidence for the production of anti-Ent/GlcEnt IgG in the spleen or blood of mice immunized with CTB-Ent, even though we detected IgG and IgA recognizing unmodified CTB in the spleen (**Fig. 3.4 E**). Additionally, the mucosal response to the CTB-Ent antigen was independent of the route of immunization. Mice immunized intraperitoneally with CTB-Ent also developed B cells secreting anti-Ent/GlcEnt IgA in the Peyer's patches, but not antibodies recognizing these antigens in the spleen (**Fig. 3.5 A and B**). We thus conclude that our immunization strategy generates mucosal IgA that recognize Ent and GlcEnt. These results are in agreement with the known effects of CTB in boosting mucosal immunity (25).

FIGURE 3.4

Figure 3.4. Detection and characterization of antibodies in response to CTB/CTB-Ent immunization.
(A) Total fecal IgA detected at day 0, day 14 and day 21 post-immunization in CTB (n = 6) and CTB-Ent (n = 6). **(B)** Representative dot blot image for detection of anti-siderophore antibodies. Ent (1 μg) or of Glc-Ent (1 μg) was spotted on a PVDF membrane and CTB-Ent fecal extract (day 21 post-immunization) was used to detect specific IgA anti-Ent and anti-Glc-Ent. **(C)** anti-CTB fecal IgA detected in CTB (n = 6) and CTB-Ent (n = 6) by in-house ELISA. **(D)** Representative ELISPOT images of CTB-IgA from Peyer's patches of mice immunized with either CTB or CTB-Ent at day 21 post-immunization. Bar graph represent number of spots detected in the CTB or CTB-Ent immunized mice per million Peyer's patches cells (n = 3). **(E)** Representative ELISPOT images of Ent-IgG or Ent-IgA and CTB-IgG or CTB-IgA from spleen of mice immunized with either CTB or CTB-Ent at day 21 post-immunization. Bar graph represent number of spots detected in the CTB or CTB-Ent immunized mouse per million splenocytes (n = 3). **(A-C)** Bars represent the mean ± standard error.

FIGURE 3.4

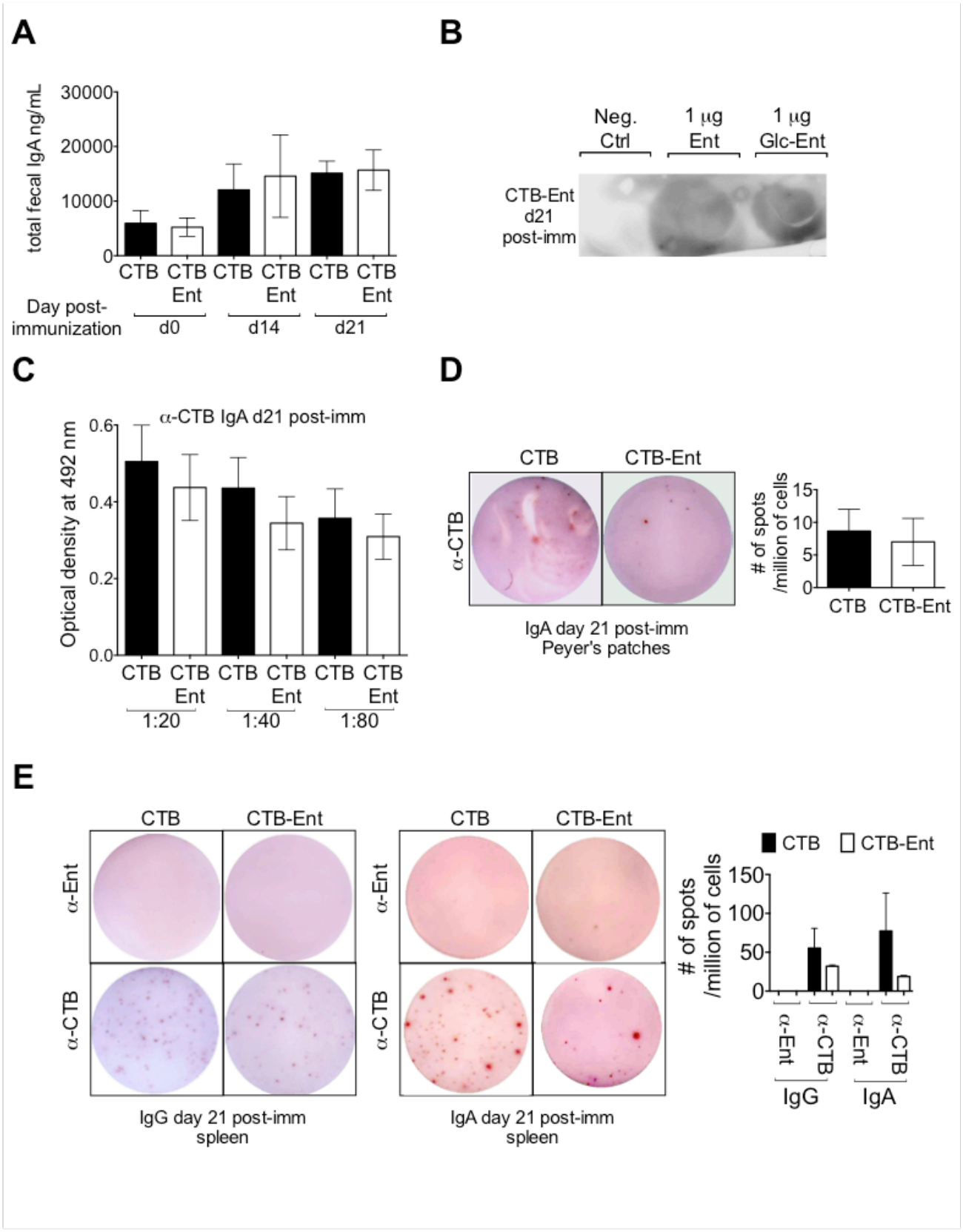

A
total fecal IgA ng/mL
30000
20000
10000
0
CTB
CTB Ent
Day post-immunization
d0
d14
d21
B
Neg. Ctrl
1 μg Ent
1 μg Glc-Ent
CTB-Ent d21 post-imm
C
α-CTB IgA d21 post-imm
Optical density at 492 nm
0.6
0.4
0.2
0.0
1:20
1:40
1:80
D
CTB
CTB-Ent
α-CTB
IgA day 21 post-imm Peyer's patches
# of spots /million of cells
15
10
5
0
E
α-Ent
α-CTB
IgG day 21 post-imm spleen
IgA day 21 post-imm spleen
150
100
50
IgG
IgA

FIGURE 3.5

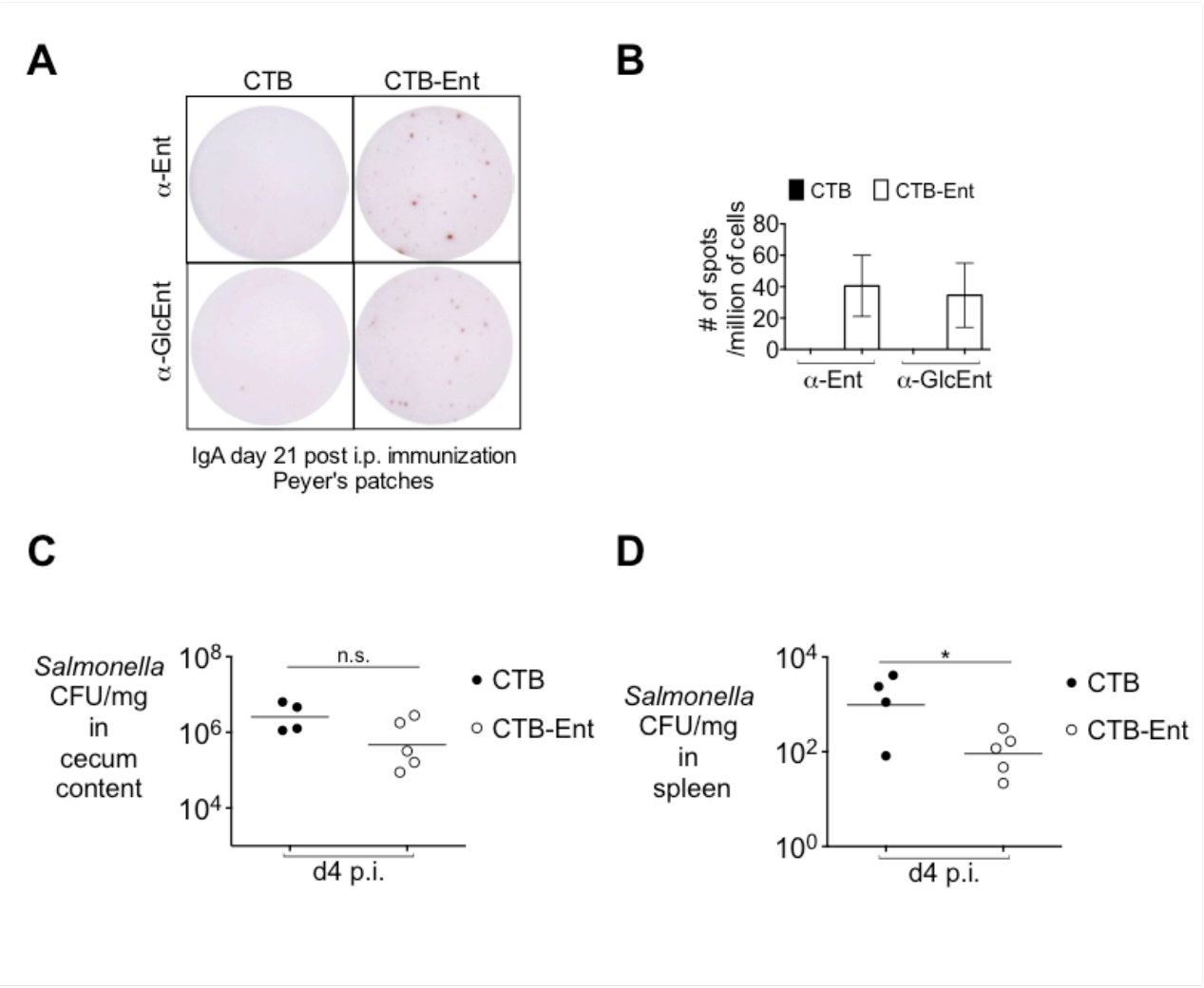


Figure 3.5. Intraperitoneal immunization with CTB-Ent induces the development anti-siderophores IgA antibodies.
(A) Representative ELISPOT images of Ent-IgA of GlcEnt-IgA from Peyer's patches of mice immunized by intraperitoneal injection with either CTB or CTB-Ent at day 21 post-immunization and boosted with 100 μg/mouse of CTB or CTB-Ent. **(B)** Average number of spots detected with ELISPOT assay in CTB and CTB-Ent immunized mice per million Peyer's patches cells (n = 3). **(C)** Bacterial load in the caecum of C57BL/6 immunized by intraperitoneal injection with CTB or CTB-Ent and infected with *Salmonella.* CTB (n = 4) and CTB-Ent immunized mice (n = 5) at day 4 post-infection. **(D)** Bacterial load in the spleen of C57BL/6 immunized by intraperitoneal injection with CTB or CTB-Ent and infected with *Salmonella.* CTB immunized mice (n = 4) and CTB-Ent immunized mice (n = 5) at day 4 post-infection. **(B)** Bars represent the mean ± standard error. **(C and D)** Each circle represents an individual mouse. Bars represent the geometric mean. * $P < 0.05$.

Immunization with siderophore-conjugates results in lower intestinal colonization and dissemination of an enteric pathogen

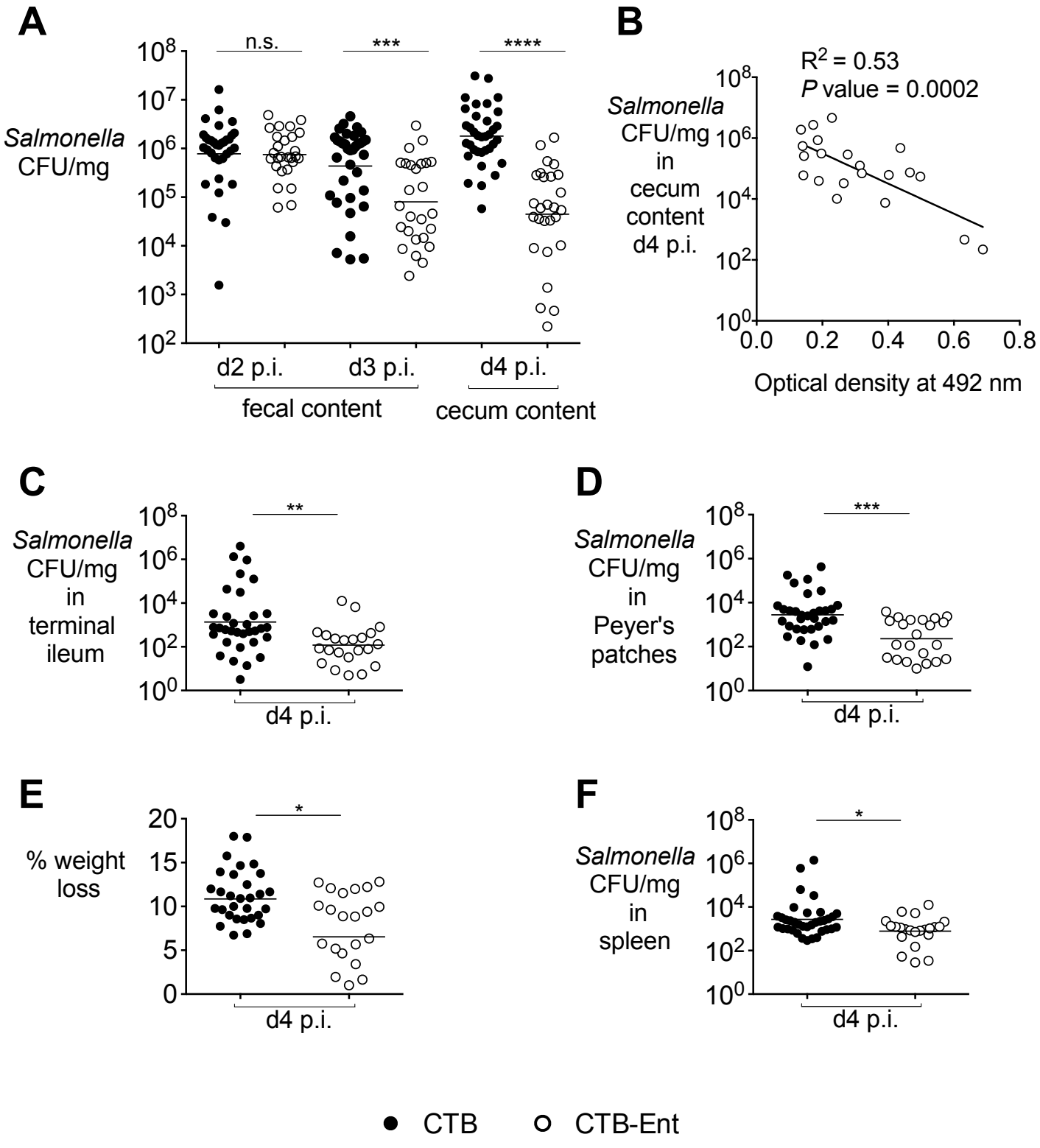
Once we established the antibody response, we investigated whether the production of anti-Ent/GlcEnt IgA would limit gut colonization and systemic dissemination of *Salmonella*. We employed the mouse model of *Salmonella* colitis and infected mice (C57BL/6) that are highly susceptible to the pathogen (26). Groups of 10-20 C57BL/6 mice were purchased from Taconic Biosciences and immunized with either CTB or CTB-Ent. Subsequently, the mice were treated with a single oral dose of streptomycin, followed by infection with 10^9 CFU/mouse of *Salmonella enterica* serovar Typhimurium. In the mouse model, pre-treatment with streptomycin is necessary for development of cecal and colonic inflammation during *Salmonella* infection (27). The transient alteration of the microbiota (28), accompanied by the increase in iNOS production (29), renders mice more prone to colitis. In this model, the development of intestinal inflammation and the recruitment of neutrophils to the gut peak at day 3-4 post-infection. We previously demonstrated that iron is limited in the inflamed gut at these time points (18, 19), and that *Salmonella* utilizes Glc-Ent to evade iron sequestration by LCN2 to thrive in this environment and outcompete the microbiota (18).

At both days 1 and 2 post-infection, when levels of inflammation are low and iron is more abundant, we observed similar levels of *Salmonella* colonization in the feces of mice immunized with CTB or with CTB-Ent (**Fig. 3.6 A**; data for day 1 not shown).

FIGURE 3.6

Figure 3.6. Immunization of mice with CTB-Ent reduces *Salmonella* gut colonization and systemic dissemination.
(A) *Salmonella* colonization in the colon content of mice immunized intranasally with either CTB (n = 35) or CTB-Ent (n = 27), then infected with 10^9 CFU of *Salmonella* by oral gavage. **(B)** Scatter plot showing an inverse correlation between *Salmonella* CFU in the colon content at day 4 post-infection and anti-Ent IgA detected by ELISA assay in individual mice that were immunized with CTB-Ent prior to infection (n = 21). **(C and D)**, *Salmonella* CFU/mg in the terminal ileum **(C)** and Peyer's patches **(D)** of mice immunized with CTB (n = 33) or CTB-Ent (n = 22) at day 4 post-infection. **(E)** Weight loss of mice immunized with either CTB or CTB-Ent at day 4 post-infection (n = 15 per group). **(F)** *Salmonella* CFU/mg in the spleen of mice immunized with either CTB (n = 33) or CTB-Ent (n = 22 at day 4 post-infection. (**A**,**C**,**D**,**F)**, Each circle represents an individual mouse. Bars represent the geometric mean. **e**, Bars represents the mean ± standard error. Immunization with challenge experiments were repeated 6 times. Each time a different batch of CTB/CTB-Ent was used **** $P < 0.0001$, *** $P < 0.001$, ** $P < 0.01$, * $P < 0.05$, n.s. = not significant.

FIGURE 3.6


A
n.s.
***
****
Salmonella CFU/mg
d2 p.i.
d3 p.i.
d4 p.i.
fecal content
cecum content
B
R2 = 0.53
P value = 0.0002
Salmonella CFU/mg in cecum content d4 p.i.
Optical density at 492 nm
C
**
Salmonella CFU/mg in terminal ileum
d4 p.i.
D
***
Salmonella CFU/mg in Peyer's patches
d4 p.i.
E
*
% weight loss
d4 p.i.
F
*
Salmonella CFU/mg in spleen
d4 p.i.
CTB
CTB-Ent

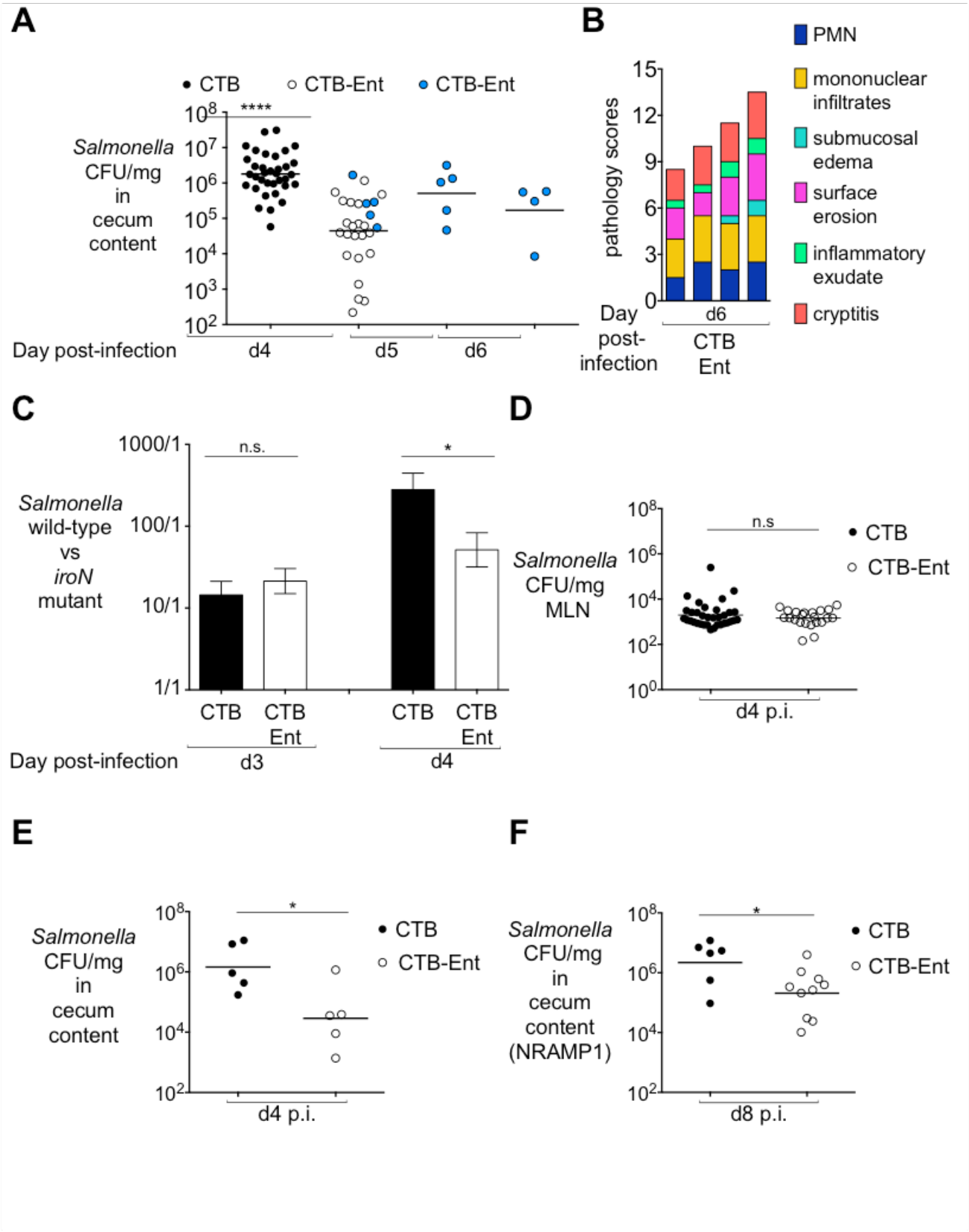
In contrast, we found a significant reduction of *Salmonella* in the feces of mice immunized with CTB-Ent at day 3, and especially in the caecum content at day 4, post-infection (**Fig. 3.6 A**). These time points correspond to the peak of inflammatory response and of iron limitation during *Salmonella* infection (18, 19). *Salmonella* colonization was lower in mice with the highest anti-Ent antibody titer, with some mice showing a 20,000-fold reduction of *Salmonella* in the cecal content (**Fig. 3.6 B**). These results demonstrate that our immunization strategy successfully hindered the growth advantage of *Salmonella* in the inflamed gut.

Salmonella colonization of the terminal ileum and Peyer's patches (**Fig. 3.6 C and D**), but not of the mesenteric lymph nodes (**Fig. 3.7 D**), was also reduced in mice immunized with CTB-Ent. Moreover, mice immunized with CTB-Ent exhibited reduced weight loss (**Fig. 3.6 E**) and reduced *Salmonella* dissemination to the spleen (**Fig. 3.6 F**) compared to mock-immunized mice, indicating that CTB-Ent immunization also slows disease progression. Because C57BL/6 mice are very susceptible to lethal infection by *Salmonella,* all mock-immunized mice had to be euthanized at day 4 because of marked weight loss and high bacterial burden (**Fig. 3.7 A**)**.** In contrast, mice immunized with CTB-Ent exhibited less severe weight loss (**Fig. 3.6 E**) and could survive infection for two additional days (**Fig. 3.7 A**). Moreover, when mice were immunized intraperitoneally with CTB-Ent, we observed similar reductions of *Salmonella* gut colonization and dissemination to the spleen (**Fig. 3.6 F and E**).

FIGURE 3.7

Figure 3.7 (Related to Figure 3.6) Immunization with CTB-Ent reduces *Salmonella* gut colonization.
(A) Bacterial load in colon content of immunized mice infected with *Salmonella.* CTB immunized mice (n = 35) and CTB-Ent (n = 27) immunized mice at day 4, 5 and 6 post-infection. Light blue dots (n = 5) represent CTB-Ent immunized mice that survived after day 4 post-infection. **(B)** Blinded histopathology scores of mice immunized with CTB-Ent that survived up to day 6 post-infection. **(C)** Competitive index (CI) of *S.* Typhimurium wild-type over *S*. Typhimurium *iroN* mutant in CTB or CTB-Ent immunized mice at day 3 and day 4 post-infection. **(D)** *Salmonella* CFU/mg in mesenteric lymph nodes (MLN) of CTB (n = 33) and CTB-Ent (n = 22) immunized mice at day 4 post-infection. **(E)** Bacterial load in the colon of C57BL/6 bred in our vivarium immunized with CTB or CTB-Ent at day 4 post *Salmonella* infection. **(F)** *Salmonella* colon content in C57BL/6 NRAMP1 CTB (n = 6) and CTB-Ent immunized mice (n = 10) at day 8 post *Salmonella* infection. **(A,D,E,F)** Each circle represents an individual mouse. Bars represent the geometric mean. **(B)** Bars represent the mean ± standard error. **** $P < 0.0001$, * $P < 0.05$, n.s. = not significant.

FIGURE 3.7


A
CTB
CTB-Ent
CTB-Ent
****
Salmonella CFU/mg in cecum content
Day post-infection
d4
d5
d6
B
PMN
mononuclear infiltrates
submucosal edema
surface erosion
inflammatory exudate
cryptitis
pathology scores
Day post-infection
d6
CTB
Ent
C
n.s.
*
Salmonella wild-type vs iroN mutant
1000/1
100/1
10/1
1/1
CTB
CTB Ent
CTB
CTB Ent
Day post-infection
d3
d4
D
n.s
Salmonella CFU/mg MLN
CTB
CTB-Ent
d4 p.i.
E
*
Salmonella CFU/mg in cecum content
CTB
CTB-Ent
d4 p.i.
F
*
Salmonella CFU/mg in cecum content (NRAMP1)
CTB
CTB-Ent
d8 p.i.

To ensure that the success of our immunization strategy was independent of housing conditions and differences in the gut microbiota, we immunized and infected mice from two colonies bred in our vivarium. The first colony consisted of conventional C57BL/6 mice, and the second colony consisted of C57BL/6 mice engineered to express functional Natural Resistance-Associated Macrophage Protein 1 (NRAMP1) (30). In our hands, these C57BL/6 NRAMP1+ mice survive up to 8-9 days post-infection (data not shown). Analogous to the mice purchased from Taconic, the C57BL/6 mice from the first colony produced anti-Ent IgA in the Peyer's patches (data not shown) and exhibited reduced *Salmonella* colonization in the feces at day 4 post-infection (**Fig. 3.7 E)**. Moreover, in the C57BL/6 NRAMP1+ mice, we observed a significant reduction in *Salmonella* burden in the caecum at day 8 post-infection as a result of CTB-Ent immunization (**Fig. 3.7 F**). Taken together, these results indicate that our immunization strategy was reproducible in different mouse lines.

Based on our findings suggesting that anti-Ent/GlcEnt IgA produced in response to CTB-Ent immunization sequester GlcEnt in the gut lumen, we evaluated whether the competitive advantage of wild-type *Salmonella* over a mutant in the GlcEnt receptor IroN is reduced in mice immunized with CTB-Ent. We have previously shown that the *iroN* mutant is defective in colonization of the inflamed gut, where LCN2 is highly induced (18). Moreover, the *iroN* mutant is outcompeted by *Salmonella* wild-type 10- to 100-fold during intestinal inflammation (18). We reasoned that anti-Ent/GlcEnt IgA produced in response to CTB-Ent immunization would bind to GlcEnt in the gut lumen, thereby inhibiting growth of wild-type *Salmonella*. Consistent with our hypothesis, the

competitive advantage of wild-type *Salmonella* over the *iroN* mutant was significantly reduced by approximately 10-fold in mice immunized with CTB-Ent (**Fig. 3.7 C**). These results further support the model that sequestration of GlcEnt by specific IgA contributes to the reduction of *Salmonella* colonization in mice immunized with CTB-Ent.

Pathology and inflammation are similar in mice immunized with either carrier proteins or siderophore-conjugates

Because *Salmonella* thrives in the inflamed gut and benefits from inflammatory responses from the host during infection (31), we questioned whether the lower *Salmonella* levels in the colon content resulted from reduced inflammation in mice immunized with CTB-Ent (32, 33). Blinded histological analysis ruled out this possibility because similar levels of intestinal inflammation were observed in mock-immunized and CTB-Ent-immunized mice upon *Salmonella* infection (**Fig. 3.8 A and B; Fig. 3.7 B**). Moreover, several inflammatory markers, including genes encoding LCN2, interleukin (IL)-17A, IL-22, CXCL1, Ly-6G, and iNOS, were similarly upregulated in both groups of mice after infection (**Fig. 3.8 C and D**). Taken together, these results demonstrate that lower levels of *Salmonella* gut colonization occurred in mice immunized with CTB-Ent despite similarly high levels of intestinal inflammation.

FIGURE 3.8

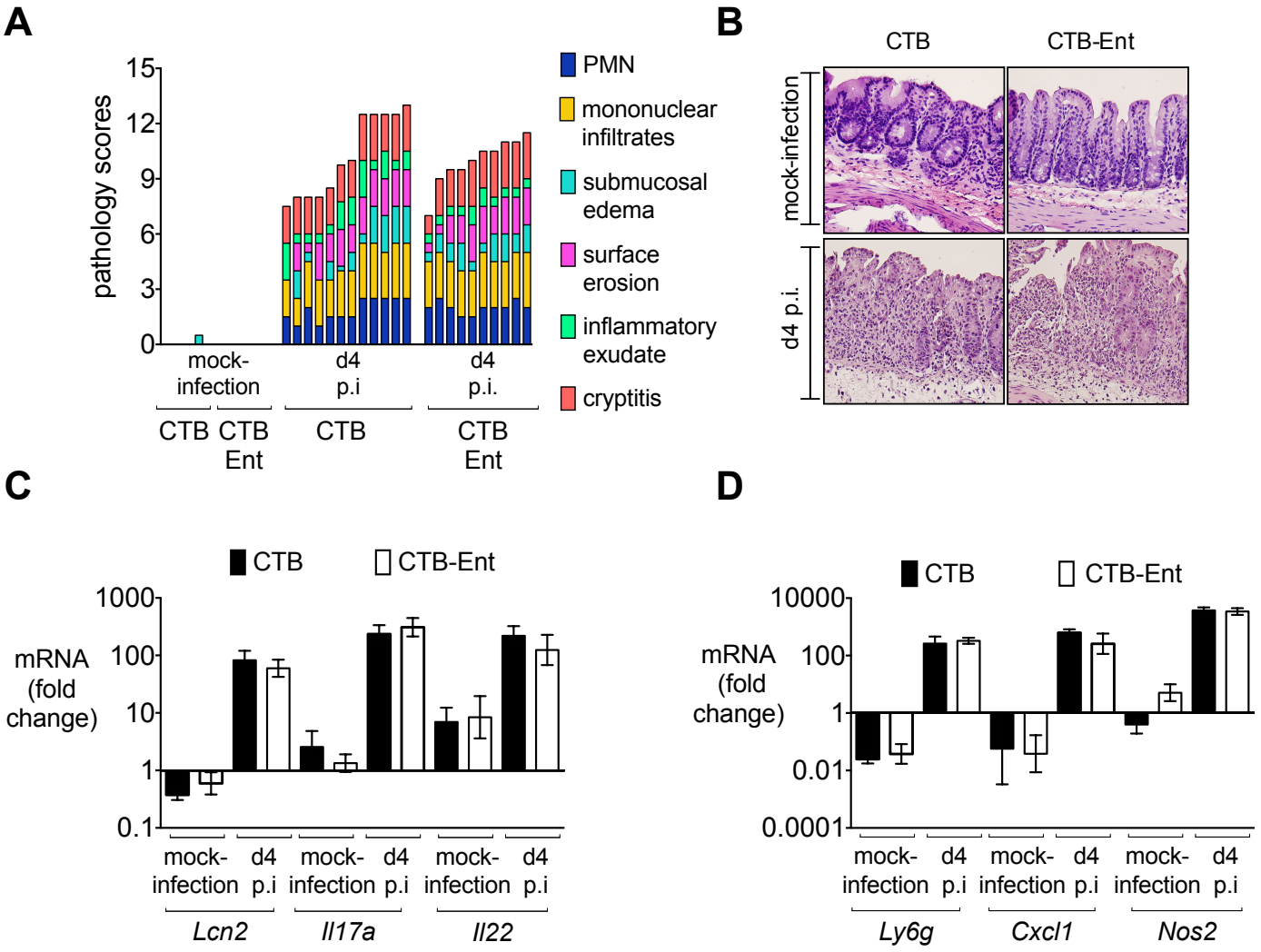


Figure 3.8. Mice immunized with CTB-Ent show similar pathology and inflammation as CTB-immunized mice.
(A) Blinded histopathology scores of mice immunized with CTB or CTB-Ent at day 4 post-infection. **(B)** H&E stained sections from representative animals for each group. **(C)** Relative expression of *Lcn2*, *Il17a,* and *Il22* in cecal samples of mice immunized with CTB (n = 7) or CTB-Ent (n = 7) then mock-infected (n = 12) or infected (n = 12) with *Salmonella* for 4 days. **(D)** Relative expression of *Ly6g*, *Cxcl1* and *Nos2* in cecal samples of mice immunized with CTB (n = 7) or CTB-Ent (n = 7) then mock-infected (n = 12) or infected (n= 12) with *Salmonella* for 4 days. **(C and D)** Bars represent the mean ± standard error.

Lactobacillus spp. expand in the context of diminished *Salmonella* intestinal colonization

One consequence of intestinal inflammation, whether induced by *Salmonella* infection or by other infectious and non-infectious etiologies, is a profound alteration of the gut microbiota, termed “dysbiosis”. The highly oxidative environment in the inflamed gut (34) reduces the growth of obligate anaerobes such as Bacteroidetes and Clostridiales, which constitute approximately 99% of microbes in the normal, non-inflamed gut. In contrast, inflammation promotes the bloom of Enterobacteriaceae, which usually constitute less than 1% of the microbiota in the absence of intestinal inflammation (35). Commensal and pathogenic facultative anaerobes, including *Salmonella*, can respire novel electron acceptors (e.g., nitrate, tetrathionate) that only become available in the inflamed gut, thus outcompeting the resident microbiota (36, 37). Moreover, acquisition of metal ions including iron in the inflamed gut enhances capability of *Salmonella* to thrive in this environment (38). Because we observed lower levels *Salmonella* in mice immunized with CTB-Ent, we questioned the impact of our immunization strategy on the microbiota in the inflamed gut (**Fig. 3.6 A**). In particular, we sought to identify which bacterial species thrive in the inflamed gut when *Salmonella* growth was hindered by CTB-Ent immunization.

The composition of the gut microbiota was not significantly different in mice that were immunized with either CTB or CTB-Ent at 36-51 days post-immunization (**Fig. 3.9 A; Tables 3.1 and 3.2**). The microbiota in these mice was largely comprised of Bacteroidetes and Firmicutes, whereas Proteobacteria (*Proteus* and *Desulfovibrio*)

constituted only a small fraction of the gut microbiota (**Fig. 3.9 A; Table 3.1**). Overall, the microbiota composition in these mice was comparable to prior studies in naïve mice in the absence of intestinal inflammation (32).

Also consistent with earlier studies in naïve mice (32), we found that *Salmonella* infection induced a significant decrease in bacterial diversity at day 4 post-infection in mice immunized with either CTB or CTB-Ent (**Fig. 3.9 A; Table 3.2**). As observed previously in naïve mice (32), *Salmonella* constituted an average of 50% of the gut microbes in mock-immunized mice (**Fig. 3.9 B and C)**. Notably, this value dropped to an average of 15% in mice immunized with CTB-Ent (**Fig. 3.9 B and C)**, which was in agreement with the observed reduction of *Salmonella* cecal CFUs in these mice (**Fig. 3.6 A**). Commensal Enterobacteriaceae (e.g. *Proteus* spp.) increased only slightly in CTB-immunized mice during *Salmonella* infection. This result agrees with prior studies (32), which showed that *Salmonella* outcompetes other Proteobacteria in the inflamed gut. Moreover, commensal Enterobacteriaceae did not expand in the inflamed gut of mice immunized with CTB-Ent 4 days after *Salmonella* infection. Because all Enterobacteriaceae that experience conditions of iron limitation deploy Ent to acquire this nutrient, we reason that the production of anti-Ent IgA limits the expansion of this family in the inflamed gut by sequestering this common siderophore.

Because of the similarly high levels of intestinal inflammation (**Fig. 3**), most other bacterial genera were equally affected during *Salmonella* infection in both groups of mice (**Fig. 3.9 C; Table 3.1)**. However, we detected a significant expansion of

Lactobacillus spp. in the inflamed gut of mice immunized with CTB-Ent (50% of the microbiota), but not in CTB-immunized mice (15% of the microbiota) (**Fig. 3.9 B and C**). These results are in agreement with previous findings showing that *Lactobacillus* spp. also replicate in a similar inflamed environment as Enterobacteriaceae and also benefit from inflammation, albeit by unknown mechanisms (32). Consistent with this idea, *Lactobacillus* was recently shown to expand during non-infectious colitis and to up-regulate TonB-dependent receptor components in the inflamed gut, suggesting that this genus can also acquire essential metal nutrients in this environment (39). Importantly, *Lactobacillus* spp. are considered beneficial microbes, and a few species are even administered as therapeutic agents (40). By reducing *Salmonella* colonization without reducing intestinal inflammation, it appears that our immunization strategy indirectly promoted the expansion of beneficial microbes that also thrive in the inflamed gut, thereby providing additional benefits to the host.

FIGURE 3.9

Figure 3.9. Analysis of the gut microbiota in mice immunized with CTB or CTB-Ent before and after infection with *Salmonella.*
(A) Gut bacterial diversity, measured by the Shannon diversity index, in mice immunized with CTB or CTB-Ent, before infection and 4 days after infection with *Salmonella* (n = 8 per group). **(B)** Analysis of the relative abundance of *Salmonella* and *Lactobacillus* in individual mice (n = 8 per group), measured by Illumina MiSeq in mice immunized with CTB or CTB-Ent, before infection and 4 days after infection with *Salmonella*. **(C)** Relative abundance of order/family/genus 16S rDNA sequence assignments (Illumina MiSeq) in fecal samples from mice immunized with CTB or CTB-Ent, collected before infection (mock, n = 8) and at day 4 post-infection (infected, n = 8). **(A)** Bars represent the mean ± standard error. **(B)** Each circle represents an individual mouse. Bars represent the geometric mean. ** $P < 0.01$, n.s.= not significant.

FIGURE 3.9

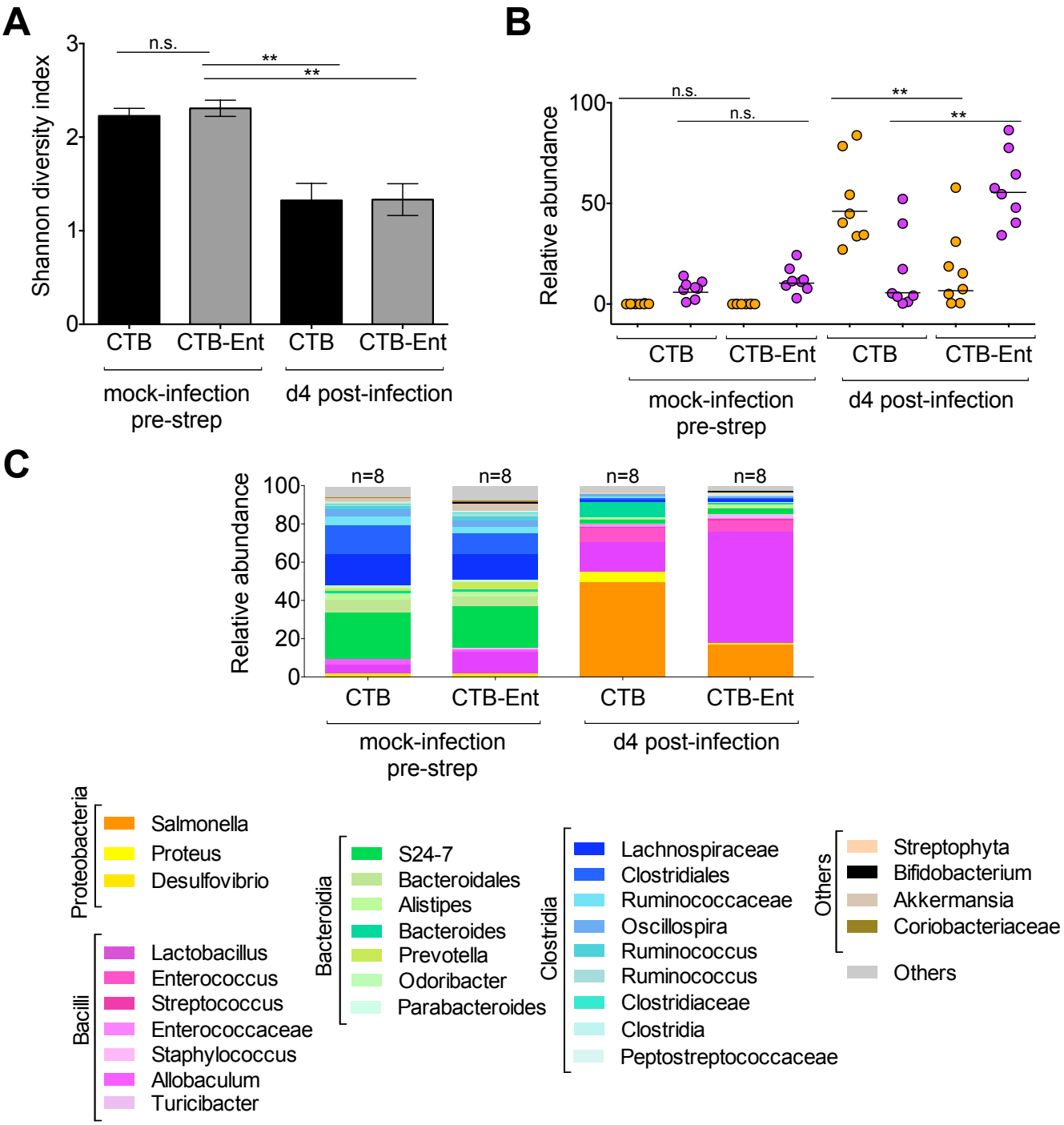

A
Shannon diversity index
n.s.
**
**
CTB
CTB-Ent
CTB
CTB-Ent
mock-infection pre-strep
d4 post-infection
B
Relative abundance
n.s.
n.s.
**
**
CTB
CTB-Ent
CTB
CTB-Ent
mock-infection pre-strep
d4 post-infection
C
Relative abundance
n=8
n=8
n=8
n=8
CTB
CTB-Ent
CTB
CTB-Ent
mock-infection pre-strep
d4 post-infection
Proteobacteria
Salmonella
Proteus
Desulfovibrio
Bacilli
Lactobacillus
Enterococcus
Streptococcus
Enterococcaceae
Staphylococcus
Allobaculum
Turicibacter
Bacteroidia
S24-7
Bacteroidales
Alistipes
Bacteroides
Prevotella
Odoribacter
Parabacteroides
Clostridia
Lachnospiraceae
Clostridiales
Ruminococcaceae
Oscillospira
Ruminococcus
Ruminococcus
Clostridiaceae
Clostridia
Peptostreptococcaceae
Others
Streptophyta
Bifidobacterium
Akkermansia
Coriobacteriaceae
Others

TABLE 3.1

Analysis of the microbiota of CTB-Ent/CTB immunized mice before and after *Salmonella* infection.

Means and standard deviation of assigned genus operational taxonomic units (OTUs). Each taxon was compared between groups by Tukey's multiple comparison test ($P < 0.1$)

TABLE 3.1

Phylum. Family. Genus	CTB mock	CTB-Ent mock	CTB d4 p.i.	CTB-Ent d4 p.i	CTB mock vs CTB-Ent mock	CTB mock vs CTB d4 p.i	CTB-Ent mock vs CTB-Ent d4 p.i	CTB d4 p.i. vs CTB-Ent d4 p.i
Proteobacteria. Enterobacteriaceae. Salmonella	0.075+/-0.139	0.0142+/-0.038	49.637+/-21.125	17.012+/-19.458	NS	****	****	****
Proteobacteria. Enterobacteriaceae. Proteus	0+/-0.0	0+/-0.0	5.2875+/-8.222	0.7+/-1.333	NS	NS	NS	NS
Proteobacteria. Enterobacteriaceae. Desulfovibrio	1.8625+/-1.625	2.0571+/-2.084	0+/-0/0	0.0125+/-0.036	NS	NS	NS	NS
Firmicutes. Lactobacillaceae. Lactobacillus	4.425+/-2.367	9.4285+/-4.482	15.525+/-19.857	57.887+/-17.815	NS	****	****	****
Firmicutes. Lactobacillaceae. Enterococcus	0+/- 0.0	0+/-0.0	7.375+/-8.105	5.95+/-6.448	NS	*	NS	NS
Firmicutes. Lactobacillaceae. Streptococcus	0.0125+/-0.035	0.0285+/-0.049	0.4125+/-0.429	0.9625+/-0.717	NS	NS	NS	NS
Firmicutes. Lactobacillaceae. Enterococcaceae	0+/-0.0	0+/-0.0	0.5875+/-0.664	0.45+/-0.809	NS	NS	NS	NS
Firmicutes. Erysipelotrichaceae. Allobaculum	3.15+/-3.3615	0.9428+/-0.927	0.262+/-0.665	0.0625+/-0.052	NS	NS	NS	NS
Firmicutes. Staphylococcaceae. Staphylococcus	0+/-0.0	0+/-0.0	0.3625+/-0.684	0.25+/-0.298	NS	NS	NS	NS
Firmicutes. Erysipelotrichaceae. Turicibacter	0.35+/-0.251	0.9714+/-0.732	0.5375+/-0.802	1.9375+/-1.903	NS	NS	NS	NS
Bacteroidetes. Bacteroidaceae. S24-7	23.987+/-4.726	23.571+/-9.676	2.3125+/-6.180	2.825+/-4.389	NS	****	****	NS
Bacteroidetes. Bacteroidaceae	6.825+/-2.094	5.5714+/-2.078	0.1625+/-0.385	0.325+/-0.369	NS	*	NS	NS

Bacteroidetes. Rikenellaceae. Alistipes	3.0875+/ 1.360	2.385714 +/-1.568	0.8875+/- 2.350	1.8375+/- 3.491	NS	NS	NS	NS
Bacteroidetes. Bacteroidaceae. Bacteroides	1.525+/-0 .991	1.44+/-1. 066	7.825+/-1 2.682	0.6+/-0.6 17	NS	NS	NS	*
Bacteroidetes. Prevotellaceae. Prevotella	1.1+/-0.5 05	3.871429 +/-7.331	0.0125+/- 0.035	0.35+/-0. 463	NS	NS	NS	NS
Bacteroidetes. Porphyromonadaceae. Odoribacter	1.2375+/- 0.818	0.6+/-0.4 00	0.025+/-0 .071	0.0375+/- 0.052	NS	NS	NS	NS
Bacteroidetes. Porphyromonadaceae. Parabacteroides	0.7125+/- 0.494	0.585714 3+/-0.430	0.2375+/- 0.478	0.0625+/- 0.106	NS	NS	NS	NS
Firmicutes. Lachnospiraceae	16.225+/- 18.288	9.900001 +/-0.10.7 96	0.9625+/- 1.817	1.9125+/- 2.357	NS	****	*	NS
Firmicutes. Clostridiales	14.9875+/ -12.161	12.12857 +/-9.875	0.875+/-2 .275	0.15+/-0. 169	NS	****	****	NS
Firmicutes. Ruminococcaceae	4.4125+/- 1.418	3.957143 +/-1.860	0.9125+/- 1.817	0.35+/-0. 153	NS	NS	NS	NS
Firmicutes. Oscillospiraceae. Oscillospira	3.85+/-1. 575	3.314286 +/-1.292	1.2625+/- 2.461	0.425+/-0 .539	NS	NS	NS	NS
Firmicutes. Ruminococcaceae. Ruminococcus	1.6875+/- 0.638	1.971429 +/-0.834	0.05+/-0. 107	0.225+/-0 .328	NS	NS	NS	NS
Firmicutes. Ruminococcaceae. Ruminococcus	1.0625+/- 0.619	1.685714 +/-2.080	0.2875+/- 0.736	0.1+/-0.1 41	NS	NS	NS	NS
Firmicutes. Clostridiaceae	0.2375+/- 0.177	0.44285+/ -0.29972	0.1125+/- 0.173	0.3875+/- 0.666	NS	NS	NS	NS

Firmicutes. Clostridia	0.8625+/--1.215	0.2718+/-0.4726	0.075+/-0.212	0.175+/-0.255	NS	NS	NS	NS
Firmicutes. Peptostreptococcaceae	0.1+/-0.193	0.214+/-0.449	0.05+/-0.093	0.75+/-0.927	NS	NS	NS	NS
Streptophyta	0.075+/-0.1164	0.1285+/-0.26276	0.2875+/-0.533	0.75+/-0.74641	NS	NS	NS	NS
Verrucomicrobia. Akkermansiaceae. Akkermansia	1.8625+/--4.914392	4.3719+/-4.8541	0.6125+/-1.73241	0.000+/-0.000	NS	NS	NS	NS
Actinobacteria. Bifidobacteriaceae. Bifidobacterium	0.275+/-0.265	0.8428572+/-1.53	0.025+/-0.046291	0.8375+/-2.05	NS	NS	NS	NS
Actinobacteria. Coriobacteriaceae	0.35+/-0.791	1.028+/-1.23	0.3+/-0.848	0+/-0	NS	NS	NS	NS
Others	5.3+/-2.239898	7.45+/-4.178516	2.2375+/-3.4146	2.15+/-1.9964	NS	NS	NS	NS

TABLE 3.2

Bray Curtis dissimilarities test of the microbiota of CTB-Ent/CTB-immunized mice before and after *Salmonella* infection.

Quantification of compositional dissimilarities between each group, where 0 means that the two groups have the same composition and 1 that do not share any species.

	CTB mock-infection	CTB-Ent d21 mock-infection	CTB day 4 post-infection	CTB-Ent day 4 post-infection
CTB mock-infection	0			
CTB-Ent d21 mock-infection	0.159897	0		
CTB day 4 post-infection	0.830200	0.780001	0	
CTB-Ent day 4 post-infection	0.828175	0.768892	0.506063	0

3.4 Discussion

For many years, siderophores as well as the biosynthetic and transport machineries for these virulence factors have garnered significant interest as targets for new antibiotics. Reported efforts include the design and application of siderophore-antibiotic conjugates for targeted drug delivery, the identification of small-molecule inhibitors of siderophore biosynthesis, and the inhibition of siderophore uptake by immunization against siderophore receptors or siderophores (9, 41-43). A prior study described the development of antibodies against vibriobactin; however, this study did not evaluate whether the vaccination provided protection to the host during infection with *Vibrio cholerae* (44). Our work establishes that immunization against bacterial siderophores results in the production of anti-siderophore antibodies and affords reduced intestinal colonization (up to 20,000-fold) during infection with the enteric pathogen *Salmonella*. These results are particularly significant because *Salmonella* is known to thrive in the inflamed gut and outcompete the microbiota in this environment. Our immunization shifted the balance in favor of the microbiota, promoting the expansion of beneficial microbes (e.g. *Lactobacillus*) that thrive in a similar environment. Moreover, as only mice that shed the highest level of *Salmonella* (the so-called “super-shedders”) are able to achieve successful transmission of the pathogen to naïve hosts (45), we reason that our strategy, which reduces fecal shedding, could be employed to hinder *Salmonella* transmission. Because *Salmonella* intestinal colonization was most highly reduced in mice that developed the highest antibody titers, future studies will address further optimization of the immunization strategy to increase antibody production.

We expect that our immunization strategy may be advanced as a therapeutic for infections caused by pathogens that utilize siderophores to thrive in the mammalian host. Because the biosynthesis and uptake of new siderophores by a microbe would require horizontal acquisition of new and diverse gene clusters, we predict that resistance against our antibody-based strategy would not readily develop. Our immunization strategy can in principle be applied to every siderophore, which would be useful in the event that resistance develops, or to target pathogens that utilize more than one siderophore. Moreover, the development of anti-siderophore antibodies will likely provide narrow-spectrum antimicrobial activity by targeting only microbes that utilize that subset of siderophores, while minimally impacting the microbiota (in contrast to broad- and even narrow-spectrum antibiotics). Broadly, our work indicates that new preventive and therapeutic strategies for microbial infections should target siderophore-mediated iron acquisition, a virulence trait shared by almost all bacterial and fungal pathogens (9). As recent studies demonstrate additional, non-classical roles for siderophores (46, 47), including protection from oxidative stress (48), inhibition of myeloperoxidase activity (49), and modulation of gene expression (50), antibody-mediated sequestration of siderophores may provide additional benefits to the host.

3.5 Materials and Methods

General Materials and Methods for Chemical Synthesis and the Preparation of CTB-Ent.

Dimethylformamide (DMF) and dichloromethane (DCM) were dried using a VAC solvent purification system (Vacuum Atmospheres). Anhydrous dimethyl sulfoxide (DMSO) was purchased from Sigma and used as received. Enterobactin acid **6**(23), Ent-azide **11**(24), and biotin-alkyne **12**(51) were synthesized by following literature procedures. All other solvents, reagents, and chemicals were purchased from commercial suppliers and used as received unless noted otherwise. EMD TLC silica gel 60 F254 plates were used for analytical thin-layer chromatography (TLC). EMD PLC sillica gel 60 F254 plates of 1-mm thickness were used for preparative TLC. Column chromatography was carried out on Zeoprep 60HYD silica gel (40-63 μm) from Zeochem using a positive pressure of nitrogen. For procedures requiring mixtures of solvents, the reported ratios are by volume.

Analytical and semi-preparative high-performance liquid chromatography (HPLC) were performed on an Agilent 1200 instrument equipped with a thermostatted autosampler set at 4 °C and thermostatted column compartment generally set at 20 °C, and a multi-wavelength detector set at 220, 280, and 316 nm (500-nm reference wavelength with 100-nm bandwidth). A Clipeus C18 column (5-μm pore, 4.6 x 250 mm, Higgins Analytical, Inc.) set at a flow rate of 1 mL/min was employed for all analytical HPLC experiments. A ZORBAX C18 column (5-μm pore, 9.4 x 250 mm, Agilent Technologies,

Inc.) set at a flow rate of 4 mL/min was employed for all semi-preparative-scale HPLC purification. A Luna 100 Å C18 LC column (10-μm particle size, 21.2 x 250 mm, Phenomenex) set at a flow rate of 10 mL/min was utilized for all preparative-scale HPLC purification. HPLC-grade acetonitrile (MeCN) and HPLC-grade trifluoroacetic acid (TFA) were routinely purchased from EMD and Alfa Aesar, respectively. For all HPLC runs, solvent A was 0.1% TFA/H_2O and solvent B was 0.1% TFA/MeCN.

Size-exclusion chromatography (SEC) was performed on an Agilent 1200 instrument equipped with a thermostatted autosampler set at 4 °C and thermostatted column compartment set at 20 °C, and a multi-wavelength detector set at 220, 280, and 316 nm (500-nm reference wavelength with 100-nm bandwidth). An Agilent Bio SEC-3 HPLC column (3-μm pore, 4.6 x 300 mm, Agilent) set at a flow rate of 0.35 mL/min was employed for all SEC HPLC experiments. The running solvent was 50 mM sodium phosphate buffer, pH 7.2.

An Agilent Bio SEC-3 HPLC column was calibrated with a 20-μL mixture of aprotinin (6.5 kDa, 3 mg/mL), ribonuclease A (13.7 kDa, 3 mg/mL), ovalbumin (44 kDa, 4 mg/mL) and conalbumin (75 kDa, 3 mg/mL) obtained from GE Lifesciences. The mixture was buffered at pH 8.0 (20 mM HEPES, 150 mM NaCl). The dead volume of the column was determined with Blue Dextran 2000 (1 mg/mL, GE Lifesciences). The partition coefficient, K_{av}, for each species was determined by the equation:

$$K_{av} = (V_e - V_0) / (V_t - V_0)$$

where V_0 is the dead volume, V_e is the elution volume of the analyte, and V_t is the bed volume. K_{av} was plotted against the log of the molecular mass of each standard to

obtain a linear calibration curve.

Solutions of the conjugate (50 μL x 20 μM) were injected onto the SEC column. The column was pre-equilibrated with at least one volume of running buffer (50 mM sodium phosphate buffer, pH 7.2) and the samples were eluted at a flow rate of 0.35 mL/min.

All 1-D ^{1}H and ^{13}C NMR spectra were recorded at ambient probe temperature using a Varian 500 MHz spectrometer. Chemical shifts are quoted as parts per million (ppm) relative to the internal signal of the solvent ($CDCl_3$/DMSO/MeOD), coupling constants (*J*) are quoted in Hertz (Hz) and are accurate to ± 0.2 Hz.

High-resolution mass spectrometry was performed by using an Agilent LC-MS system comprised of an Agilent 1260 series LC system outfitted with an Agilent Poroshell 120 EC-C18 column (2.7-μm pore size) and an Agilent 6230 TOF system housing an Agilent Jetstream ESI source. For all LC-MS analyses, solvent A was 0.1% formic acid/H_2O and solvent B was 0.1% formic acid/MeCN. The samples were analyzed by using a gradient of 5−95% B over 5 min with a flow rate of 0.4 mL/min. The MS profiles were analyzed and deconvoluted by using Agilent Technologies Quantitative Analysis 2009 software version B.03.02.

The extinction coefficient (10,095 $M^{-1}cm^{-1}$ at 280 nm) of CTB was calculated by using ExPASy ProtParam. Concentrations of CTB solutions were determined by using a calibrated Bio-Tek Take3 micro volume plate and the calculated extinction coefficient.

To determine the extinction coefficients of $[FeEnt]^{3-}$ in PBS pH 7.2, a stock solution of Ent (20 mM) in MeOH was prepared and its concentration was confirmed by using the reported extinction coefficient of Ent (9500 $M^{-1}cm^{-1}$ at 316 nm in MeOH(52)). Next, 5 μL of the 20-mM Ent stock solution was added into 95 μL of PBS pH 7.2 to achieve a 1-mM solution of Ent. One equivalent of $FeCl_3$ (4 μL, 25 mM in Chelex-treated Milli-Q water and 0.3 M HCl) was then added. The solution turned dark red and was incubated at room temperature for 15 min. The solution was diluted with PBS pH 7.2 (10-90 μM), and the optical absorption spectra of the resulting solutions were recorded. These experiments were done in triplicate with two different synthetic batches of Ent. The corresponding extinction coefficients of $[FeEnt]^{3-}$ in PBS pH 7.2 were determined to be 8,260 and 5480 $M^{-1}cm^{-1}$ at 280 and 498 nm, respectively.

Solution and buffer pH values were verified by using a Mettler Toledo S20 SevenEasy pH meter.

Optical absorption spectra were recorded on a Beckman Coulter DU800 spectrophotometer (1-cm path-length quartz cuvettes, Starna).

1-(3,4-Bis(benzyloxy)-5-(((3*S*,7*S*,11*S*)-7,11-bis(2,3-bis(benzyloxy)benzamido) -2,6,10-trioxo-1,5,9-trioxacyclododecan-3-yl)carbamoyl)phenyl)-1-oxo-5,8,11-trioxa-2-azatetradecan-14-oic acid (7)

To a 10-mL round-bottom flask, *tert*-butyl 12-amino-4,7,10-trioxadodecanoate **4** (32.2

mg, 116 μmol), triethylsilane (27.7 μL, 290 μmol), and 1 mL of DCM were added. Trifluoroacetic acid (TFA, 350 μL) was added to this mixture and the solution was stirred at room temperature for 3 h. The solution was concentrated under reduced pressure to obtain PEG_3•TFA **5** as yellow oil, which was used in the next step without further purification.

Ent acid **6** (96.3 mg, 76.8 μmol), 1-[bis(dimethylamino)methylene]-1H-1,2,3-triazolo[4,5-*b*]pyridinium 3-oxid hexafluorophosphate (HATU, 29.2 mg, 76.8 μmol), and 1-hydroxy-7-azabenzotriazole (HOAt, 10.5 mg, 76.8 μmol) were dissolved in 1 mL of anhydrous DMSO and the mixture was purged with N_2 three times. Diisopropylethylamine (DIPEA, 83.0 μL, 464 μmol) was slowly added and the reaction was stirred at room temperature for 5 min. To the resulting bright yellow solution, a 500-μL pre-mixed solution of PEG_3•TFA **5** and DIPEA (40.4 μL, 232 μmol) in DMSO was added dropwise and the reaction was stirred at room temperature. After 1 h, the reaction was partitioned in water (20 mL) and DCM (20 mL). The organic layer was washed with 1 M HCl (3 x 10 mL) and brine (1 x 10 mL), and dried over anhydrous Na_2SO_4. The solvents were removed by rotary evaporation. The crude product was purified by preparative TLC (EtOAc, dried and then 7% MeOH/DCM) to yield **7** as a white solid (67.7 mg, 61%). TLC R_f = 0.5 (10% MeOH/DCM). ^{1}H NMR (500 MHz, $CDCl_3$) δ 2.59 (t, J = 6.0 Hz, 2H), 3.58-3.72 (m, 12H), 3.77 (t, J = 6.5 Hz, 2H), 3.97-4.07 (m, 3H), 4.08-4.17 (m, 3H), 4.85-4.94 (m, 3H), 5.01-5.22 (m, 12H), 7.06-7.46 (m, 31H), 7.65 (dd, J = 6.8, 2 Hz, 2H), 7.79 (br, 1H), 7.90 (d, J = 1.6 Hz, 1H), 8.16 (d, J = 1.6 Hz, 1H), 8.49 (d, J = 6.8 Hz, 2H), 8.66 (d, J = 6.8 Hz, 1H). ^{13}C NMR (125 MHz, $CDCl_3$) δ 30.0, 40.0, 51.4, 63.8, 66.7, 69.7, 69.9, 70.2, 71.2, 76.3,

117.5, 121.0, 123.0, 124.3, 126.2, 127.6, 127.7, 128.0, 128.2, 128.4, 128.5, 128.5, 128.6, 128.8, 128.9, 128.9, 129.0, 135.4, 135.9, 136.0, 136.2, 146.8, 146.9, 149.0, 151.6, 165.0, 168.9, 169.1. HRMS (ESI): $[M+H]^+$ *m/z* calcd, 1479.5213; found, 1479.5500.

1-(3-(((3*S*,7*S*,11*S*)-7,11-Bis(2,3-dihydroxybenzamido)-2,6,10-trioxo-1,5,9-trioxacyclododecan-3-yl)carbamoyl)-4,5-dihydroxyphenyl)-1-oxo-5,8,11-trioxa-2-azatetra decan-14-oic acid (8)

In a 10-mL round-bottom flask, compound **7** (49.6 mg, 34.1 μmol) was dissolved in 4 mL of 1:1 EtOH/EtOAc. The flask was purged with N_2 three times, and 50 mg of Pd/C (10% wt, Sigma) was added. A balloon of H_2 was attached and the reaction was stirred under an atmosphere H_2 (1 atm) at room temperature for 3 h. The flask was purged with N_2 and the reaction was transferred to a centrifuge tube. The Pd/C was removed by centrifuging at 13,000 rpm for 10 min. The supernatant was transferred to a round-bottom flask and concentrated by rotary evaporation. The resulting crude product was dissolved in 2:2:1 H_2O/MeCN/DMSO, purified by semi-preparative HPLC (25–34% B over 15 min, 4 mL/min), and lyophilized to yield **8** as white powder (24.6 mg, 78%). The product eluted at 17.5 min (0–100% B over 30 min, 1 mL/min, **Fig. 3.10**). ^{1}H NMR (500 MHz, MeOD) δ 2.49 (t, *J* = 6.2 Hz, 2H), 3.50-3.56 (m, 4H), 3.57-3.64 (m, 8H), 3.66 (t, *J* = 6.3 Hz, 2H), 4.58-4.72 (m, 6H), 5.04 (t, *J* = 4.9 Hz, 3H), 6.70 (t, *J* = 8.0 Hz, 2H), 6.94 (ddd, *J* = 7.9, 2.4, 1.6 Hz, 2H), 7.23 (ddd, *J* = 8.2, 5.3, 1.6 Hz, 2H), 7.44 (d, *J* = 2.2 Hz, 1H), 7.86 (d, *J* = 2.2 Hz, 1H). ^{13}C NMR (125 MHz, MeOD) δ 35.7, 41.0, 53.6, 65.8, 67.8, 70.5, 71.2, 71.3, 71.4, 71.5, 116.6, 116.7, 118.6, 119.5, 119.7, 120.1, 126.5, 143.1,

147.2, 149.4, 152.2, 169.3, 170.0, 175.4. HRMS (ESI): $[M+Na]^+$ *m/z* calcd, 939.2396; found, 939.2395.

FIGURE 3.10

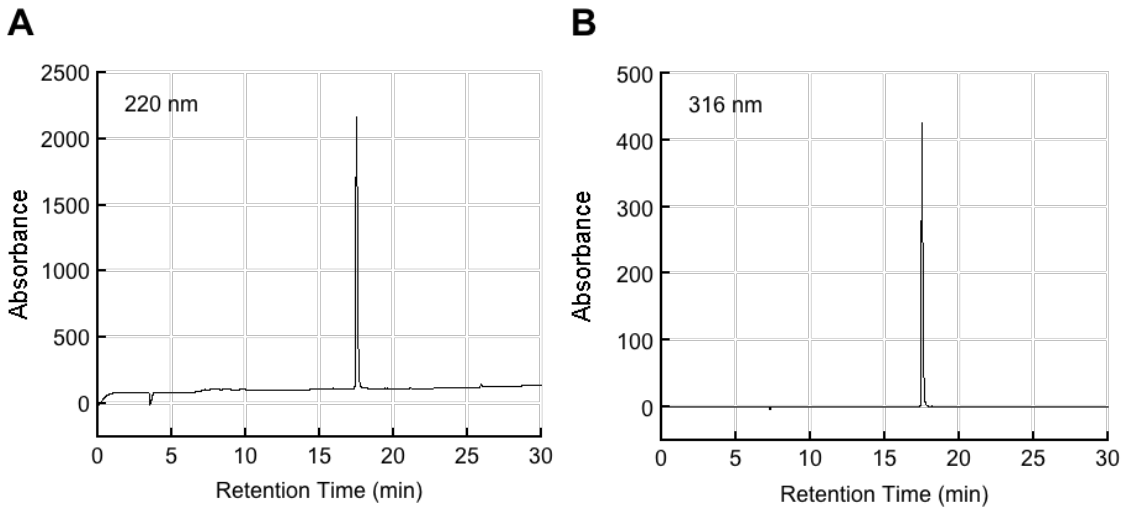


Figure 3.10. Analytical HPLC traces of Ent-PEG_3-CO_2H **8** at **(A)** 220 nm and **(B)** 316 nm (Method: 0–100% B over 30 min, 1 mL/min).

CTB-Ent (3)

The conjugation procedure was adapted from literature procedures for the attachment of haptens to carrier proteins.(53) Cholera toxin subunit B (1 mg, CTB, Sigma-Aldrich) was dissolved in 1 mL of Milli-Q water. The solution was divided into two 500-μL aliquots and each aliquot was transferred to an Amicon ultra-0.5 centrifugal filter unit with an ultracel-10 membrane (3 kDa MWCO, EMD Millipore) and buffer exchanged into phosphate buffered saline (PBS) pH 7.2 (5 x 500 μL, 13,000 rpm x 15 min, 4 °C), and then buffer exchanged into 100 mM sodium phosphate (NaP) pH 8.0 (3 x 500 μL, 13,000 rpm x 15 min, 4 °C). Following buffer exchange, the concentration of CTB was quantified by the calculated extinction coefficient (*vide supra*), and the concentration of CTB was adjusted to 2 mg/mL by addition of NaP pH 8.0.

To activate the carboxylate group of Ent-PEG_3-CO_2H **8**, stock solutions of *N*-(3-dimethylaminopropyl)-*N'*-ethylcarbodiimide *hydrochloride (EDC,* 100 μg/μL*) and N-hydroxysuccinimide (NHS,* 60 μg/μL) were prepared in anhydrous DMSO. A 12.5-μL aliquot of the EDC solution was added to the powder of Ent-PEG_3-CO_2H **8** (2 mg, 0.2 μmol) followed by the addition of a 12.5-μL aliquot of the NHS solution. The progress of the reaction was monitored by analytical HPLC (0-100% B over 30 min, 1 mL/min), and the new peak at 18.9 min was identified as the product Ent-PEG_3-NHS **9** by LC-MS. The reaction was complete after 2 h. Iron(III) ethylacetoacetate ($Fe(acac)_3$, 10 μL, 212 mM in DMSO, 0.95 equiv) was then added to Ent-PEG_3-NHS **9** to afford the iron-bound form. The colorless solution turned dark purple within 5 min after addition of $Fe(acac)_3$. Without any further purification, Fe-Ent-PEG_3 **10** was added to a solution of CTB (500

μL, 1 mg in NaP pH 8.0). The reaction was incubated for 3 h at room temperature. At this time, 500 μL of PBS pH 7.2 was added to the reaction and the resulting solution was subjected to eight rounds of spin filtration (13,000 rpm x 15 min) with PBS pH 7.2 by using an Amicon ultra-0.5 centrifugal filter unit with an ultracel-10 membrane (3 kDa MWCO, EMD Millipore) to remove coupling reagents and any unreacted **9**. Following buffer exchange, the concentration of CTB-Ent **3** was determined by employing a Bradford protein assay and the concentration was adjusted to 2 mg/mL by adding PBS pH 7.2. CTB-Ent **3** was stored in PBS pH 7.2 as a dark red solution at 4 °C up to one month prior to immunization. The ratio of Ent to CTB was determined to be ≈ 4 based on the absorbance at 280 (CTB and Fe-Ent) and 495 nm (Fe-Ent only). Unmodified CTB is a pentamer, and analytical SEC revealed that CTB-Ent is a mixture composed of CTB-Ent pentamers and lower-order oligomers.

Ent-PEG$_3$-biotin (13)

DMSO solutions of Ent-PEG$_3$-azide **11** (26 mM, 125 μL) and biotin-alkyne **12** (13 mM, 250 μL), a DMF solution of benzoic acid (450 mM, 500 μL), and an aqueous solution of $CuSO_4$ (10 mg/mL, 45 mM, 500 μL) were combined, and 400 μL of DMSO was added to yield a clear yellow-brown solution. An aqueous solution of sodium ascorbate (NaAsc, 90 mM, 500 μL) was subsequently added. The reaction turned light yellow and was stirred at room temperature for 15 min, at which time another 500 μL of aqueous NaAsc was added. After stirring for an additional 15 min, the reaction was flash frozen in liquid N_2 and lyophilized to give a yellow oil. The oil was dissolved in a 1:1 mixture of H_2O/MeCN, purified by semi-preparative HPLC (20% B for 5 min followed by 20–50% B

over 11 min, 4 mL/min), and lyophilized to yield **13** as white powder (1.8 mg, 46%). The product eluted at 17.4 min (0–100% B over 30 min, 1 mL/min, **Fig. 3.11**). HRMS (ESI): $[M+Na]^+$ *m/z* calcd., 1217.3704; found, 1217.3711.

FIGURE 3.11

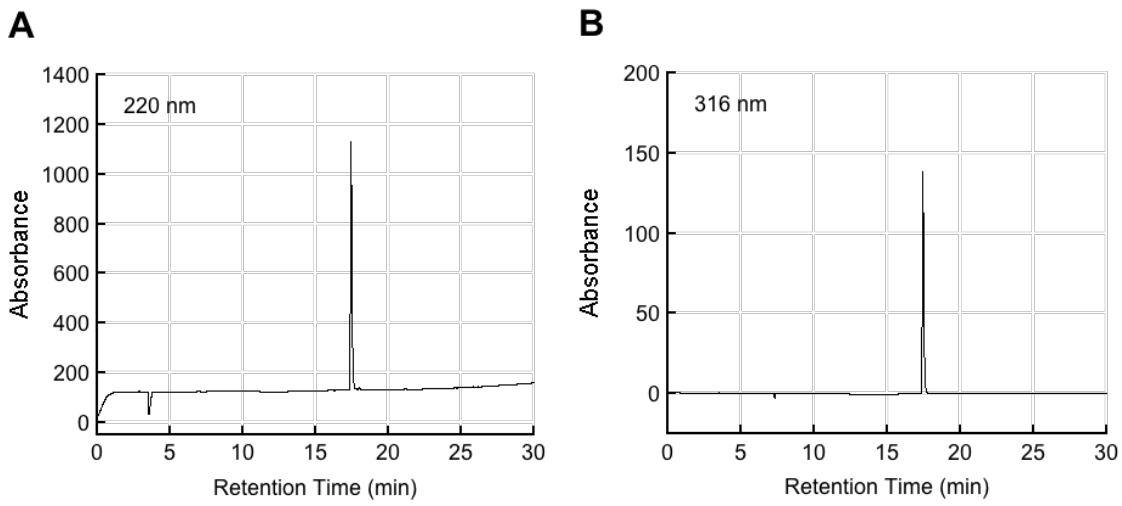


Figure 3.11. Analytical HPLC traces of Ent-PEG_3-biotin **13** at **(A)** 220 nm and **(B)** 316 nm (Method: 0–100% B over 30 min, 1 mL/min).

Gel Electrophoresis

Solutions of the conjugate (1 mg/mL) were prepared in SDS-PAGE sample buffer (10 mM Tris, 1 mM EDTA, 2.5% SDS, 5% mercaptoethanol, pH 8.0) and heated to 100 °C for 3 min. Gels (16% tricine(54)) were loaded with 5 μL of sample and run under denaturing conditions for 90 min at 120 V using a Bio-Rad electrophoresis apparatus and stained with Coomassie blue (Amresco).

Mice

Six-to-eight weeks-old C57BL/6 females were purchased from Taconic. When indicated, six-to-eight weeks old males or females C57BL/6 or C57BL/6 NRAMP1+ mice bred in our vivarium were also used for the experiments. Eight to ten mice per experimental group were used for each experiment. The group sizes have been established empirically (based on previous studies) to detect a 10-fold difference with statistical significance. Mice were randomly grouped in cages of maximum five animals per cage. No blinding was performed, with the exception of the histopathology and the phylogenetic analysis of the microbiota. Each mouse experiment was repeated a minimum of three times, and a maximum of six. Mouse colonies were maintained in pathogen-free barrier facilities for the duration of the immunization studies. The Institutional Animal Care and Use Committee at University of California Irvine approved all of the mouse experiments.

Mucosal immunization with CTB/CTB-Ent conjugates

C57BL/6 mice were immunized by intranasal administration of either 100 μg of CTB-Ent or CTB (Sigma). CTB-Ent (2 mg/mL) was prepared in PBS pH 7.2 as described above. CTB (2 mg/mL) was dissolved in ultrapure water. Mice were briefly anesthetized with isolflourane and injected intranasally with 25-50 μL of CTB-Ent/CTB. Mice were boosted 14 days later with the same amount. To monitor the health of the animals during the immunization period, mice were weighed weekly. When indicated, mice were immunized by intraperitoneal injection with same timing and doses. For our immunization followed by challenge experiments, mice that did not developed an anti-Ent antibody response, indicated by an OD_{442} < 0.2, were excluded from further analysis. Mice that did not develop a specific anti-Ent response after immunization were approximately 20% of the total number of immunized mice.

Preparation of fecal samples for ELISA and dot blot

Fresh fecal samples were collected weekly before and after immunization. Fecal pellets were weighed and 50-60 mg of fecal pellets were resuspended in 400 μL of sterile PBS containing a protease cocktail inhibitor (Roche) and incubated at RT shaking for 30 minutes. Samples were centrifuged at 7,200x g for 20 minutes and the supernatants were collected individually and stored at -20 °C until further use.

ELISA

To measure anti-Ent and anti-GlcEnt IgA antibodies by ELISA, 96-well plates (NUNC MAXIsorp) were incubated overnight at 4 °C or 2 h at 37 °C with 1 μg/mL of Ent-PEG_3-biotin **13** (**Fig. S3**) or Glu-Ent diluted in sterile PBS pH 7.4. The plates were then

blocked for 1h at 37 °C with 5% non-fat dry milk. Serial 2-fold dilutions of fecal extracts from CTB-immunized mice and mice immunized with CTB-Ent were added to the wells, starting from 1:10 dilution. To evaluate the presence of specific IgA, we added a goat anti-mouse IgA conjugated with horseradish peroxidase (1:5,000; Catalog number 1040-05 Southern Biotechnology Associates, Inc., Birmingham, AL, USA) and incubated for 1h at 37 °C. This step was followed by detection with horseradish peroxidase substrate. Briefly, o-phenylediamine dihydro-chloride 3 mg tablets (Sigma) were dissolved in 1x phosphate-citrate buffer and 60 μL of hydrogen peroxide 3 wt. % (Sigma) was added. The reaction was quenched with 2 N hydrogen sulfate.

ELISPOT

A multi-screen ELISPOT PVDF (Millipore) membrane plate was washed with 35% ethanol and then coated with 1 μg/mL of the antigen (Ent/GlcEnt) diluted in sterile PBS. The plate was then blocked by the addition of RPMI with 10% FBS (Gibco, Life technology) and incubated for 1h at room temperature with shaking. Cells isolated from the intestinal mucosa (Peyer's patches, mesenteric lymph nodes) and as a control, a non-mucosal site (spleen) from CTB-immunized (mock) and CTB-Ent-immunized mice were resuspended in RPMI with 10% FBS and seeded at a density of 2.5 x 10^5 cells/well or lower in duplicates. Then, the plate was incubated at 37 °C 5% CO_2 for at least 18 h. The cells were washed out and specific antibodies were detected after incubation with 0.5 g/mL goat anti-mouse IgA secondary antibody for 2 h at room temperature with shaking (Southern Biotechnology Associates, Inc., Birmingham, AL,

USA), and addition of 3-amino-9-ethylcarbazole (AEC), then visualized and counted with the CTL Immunospot software (Cellular Technology Limited).

Bacterial strains and growth conditions

IR715 is a fully virulent, nalidixic acid-resistant derivative of *Salmonella enterica* serovar Typhimurium wild-type isolate ATCC 14028. The *S*. Typhimurium mutant strain lacking the salmochelin receptor IroN was also used in this study(16). The strains were grown aerobically in Luria-Bertani (LB) broth (10 g/L tryptone, 5 g/L yeast extract, 10 g/L NaCl) or on LB agar plates at 37 °C. When needed, antibiotics were added to the media at the following concentrations: 0.03 mg/mL chloramphenicol (Cm), 0.1 mg/mL carbenicillin (Carb), 0.05 mg/mL kanamycin (Kan). For animal infections, all strains were grown in LB media aerobically at 37 °C overnight.

***Salmonella* acute model of gastrointestinal infection**

Between 36-51 days post-immunization, immunized mice were inoculated intragastrically with streptomycin (100 μL of a 200 mg/mL solution in sterile water) 1 day prior to infection. The following day, the mice were inoculated intragastrically with 10^9 CFU of *S.* Typhimurium (resuspended in 0.1 mL LB broth) or with 1:1 ratio of 5 x 10^8 CFU each of *S.* Typhimurium wild-type and the *iroN* mutant for competitive colonization experiments. Fecal samples were collected daily after bacterial administration and were harvested in sterile PBS. The bacterial load was determined by plating serial 10-fold dilutions on selective agar plates. Between 4-6 days post infection, mice were euthanized. Each mouse caecum was collected and one portion was fixed in formalin

for histopathology, whereas a second portion was flash frozen in liquid nitrogen and stored at -80 °C for isolation of mRNA and protein. Bacteria were enumerated in the colon content, terminal ileum, Peyer's patches, mesenteric lymph nodes, and spleen by plating serial dilutions on LB agar plates containing the appropriate antibiotics. When noted, the competitive indices were calculated by dividing the output ratio (*S*. Typhimurium wild-type CFU/ *S*. Typhimurium *iroN* CFU) by the input ratio (*S*. Typhimurium wild-type CFU/ *S*. Typhimurium *iroN* CFU).

Quantitative Real-time PCR

For analysis of gene expression by quantitative real-time PCR, total RNA was extracted from cecal tissues with TRI Reagent (Molecular Research Center; Cincinnati, OH). Reverse transcription reagents were employed to generate cDNA from all RNA samples. Real-time PCR was performed using SYBR Green (Roche, Indianapolis, IN) and the Roche Lightcycler 480 system (Roche, Indianapolis, IN). The data were analyzed using the comparative $\Delta\Delta$-C_t method. Target gene transcription of each sample was normalized to the respective levels of mRNA β-actin (Table 3.3).

TABLE 3.3
Primers for quantitative Real-Time PCR

Species	**Target**	**Primer Pairs**
Mus musculus	*Lcn2*	5'-ACATTTGTTCCAAGCTCCAGGGC-3' 5'-CATGGCGAACTGGTTGTAGTCCG-3'
Mus musculus	*Il17a*	5'-GCTCCAGAAGGCCCTCAGA-3' 5'-AGCTTTCCCTCCGCATTGA-3'
Mus musculus	*Ly6g*	5'-TGCGTTGCTCTGGAGATAGA-3' 5'-CAGAGTAGTGGGGCAGATGG-3'
Mus musculus	*Il22*	5'-GGCCAGCCTTGCAGATAACA-3' 5'- GCTGATGTGACAGGAGCTGA-3'
Mus musculus	*Cxcl-1*	5'-TGCACCCAAACCGAAGTCAT-3' 5'-TTGTCAGAAGCCAGCGTTCAC-3'
Mus musculus	*Nos2*	5'-TTGGGTCTTGTTCACTCCACGG-3' 5'-CCTCTTTCAGGTCACTTTGGTAGG-3'
Mus musculus	*ActB*	5'-GGCTGTATTCCCCTCCATCG-3' 5'-CCAGTTGGTAACAATGCCATGT-3'

Histopathological analysis

Tissue samples were fixed in formalin, processed according to standard procedures for paraffin embedding, sectioned at 5 mm, and stained with hematoxylin and eosin. The pathology score of cecal samples was determined by blinded examinations of cecal sections from a board-certified pathologist using previously published methods. Each section was evaluated for the presence of neutrophils, mononuclear infiltrate, submucosal edema, surface erosions, inflammatory exudates, and cryptitis. Inflammatory changes were scored from 0 to 4 according to the following scale: 0 = none; 1 = low; 2 = moderate; 3 = high; 4 = extreme. The inflammation score was calculated by adding up all the scores obtained for each parameter and interpreted as follows: 0–2 = within normal limit; 3–5 = mild; 6–8 = moderate; 8+ = severe.

Microbiota analysis

DNA from the colon content was extracted with the QIAamp DNA stool kit (QIAGEN). Bacterial DNA was amplified by a two-step PCR enrichment of the 16S rDNA (V4 region) encoding sequences from each sample with primers 515F and 806R modified by addition of barcodes for multiplexing. Libraries were sequenced using an Illumina MiSeq system. Uncalled bases, incorrect primer sequence, and runs of ≥ 12 identical nucleotides sequences were removed. Phylogenetic analysis of the microbiota composition was performed by a blinded investigator. Following quality filtering, the sequences were demultiplexed and trimmed before performing sequence alignments,

identification of operational taxonomic units (OTU), clustering, and phylogenetic analysis using QIIME open-source software.

Statistical analysis

Statistical analysis was performed by using Graphpad Prism 6. In most cases, we applied the non-parametric Mann-Whitney-Wilcoxon test. We chose this test because it can be applied to data with normal or unknown distribution. Analysis of the microbiota was performed with a 2-way ANOVA and Tukey's multiple comparison test.

3.6 References

1. Anonymous (2014) Antimicrobial resistance: global report on surveillance. *World Health Organization*.
2. Anonymous (2013) The antibiotic alarm. *Nature* 495(7440):141.
3. Rohmer L, Hocquet D, & Miller SI (2011) Are pathogenic bacteria just looking for food? Metabolism and microbial pathogenesis. *Trends in microbiology* 19(7):341-348.
4. Crosa JH & Walsh CT (2002) Genetics and assembly line enzymology of siderophore biosynthesis in bacteria. *Microbiol. Mol. Biol. Rev.* 66(2):223-249.
5. Fischbach MA, Lin H, Liu DR, & Walsh CT (2006) How pathogenic bacteria evade mammalian sabotage in the battle for iron. *Nat. Chem. Biol.* 2(3):132-138.
6. Leong J & Neilands JB (1976) Mechanisms of siderophore iron transport in enteric bacteria. *J. Bacteriol.* 126(2):823-830.
7. Miethke M & Marahiel MA (2007) Siderophore-based iron acquisition and pathogen control. *Microbiol. Mol. Biol. Rev.* 71(3):413-451.
8. Ratledge C (2007) Iron metabolism and infection. *Food Nutr. Bull.* 28(4 Suppl):S515-523.
9. Cassat JE & Skaar EP (2013) Iron in infection and immunity. *Cell host & microbe* 13(5):509-519.
10. Raymond KN, Dertz EA, & Kim SS (2003) Enterobactin: an archetype for microbial iron transport. *Proc. Natl. Acad. Sci. USA* 100(7):3584-3588.
11. Weinberg ED (1975) Nutritional immunity. Host's attempt to withold iron from microbial invaders. *Jama* 231(1):39-41.
12. Goetz DH, *et al.* (2002) The neutrophil lipocalin NGAL is a bacteriostatic agent that interferes with siderophore-mediated iron acquisition. *Mol. Cell* 10(5):1033-1043.
13. Flo TH, *et al.* (2004) Lipocalin 2 mediates an innate immune response to bacterial infection by sequestrating iron. *Nature* 432(7019):917-921.
14. Fischbach MA, Lin H, Liu DR, & Walsh CT (2005) *In vitro* characterization of IroB, a pathogen-associated C-glycosyltransferase. *Proc. Natl. Acad. Sci. USA* 102(3):571-576.
15. Hantke K, Nicholson G, Rabsch W, & Winkelmann G (2003) Salmochelins, siderophores of *Salmonella enterica* and uropathogenic *Escherichia coli* strains, are recognized by the outer membrane receptor IroN. *Proc. Natl. Acad. Sci. USA* 100(7):3677-3682.
16. Bäumler AJ, *et al.* (1998) IroN, a novel outer membrane siderophore receptor characteristic of *Salmonella enterica*. *J. Bacteriol.* 180(6):1446-1453.
17. Fischbach MA, *et al.* (2006) The pathogen-associated *iroA* gene cluster mediates bacterial evasion of lipocalin 2. *Proc. Natl. Acad. Sci. USA* 103(44):16502-16507.
18. Raffatellu M, *et al.* (2009) Lipocalin-2 resistance confers an advantage to *Salmonella enterica* serotype Typhimurium for growth and survival in the inflamed intestine. *Cell host & microbe* 5(5):476-486.
19. Deriu E, *et al.* (2013) Probiotic bacteria reduce *Salmonella typhimurium* intestinal colonization by competing for iron. *Cell host & microbe* 14(1):26-37.

20. Bachman MA, *et al.* (2011) *Klebsiella pneumoniae* yersiniabactin promotes respiratory tract infection through evasion of lipocalin 2. *Infect. Immun.* 79(8):3309-3316.
21. Sanchez J & Holmgren J (2011) Cholera toxin - a foe & a friend. *Indian J. Med. Res.* 133:153-163.
22. Landro L, *et al.* (2008) Decreased serum lipocalin-2 levels in human immunodeficiency virus-infected patients: increase during highly active anti-retroviral therapy. *Clinical and experimental immunology* 152(1):57-63.
23. Zheng T, Bullock JL, & Nolan EM (2012) Siderophore-mediated cargo delivery to the cytoplasm of *Escherichia coli* and *Pseudomonas aeruginosa*: syntheses of monofunctionalized enterobactin scaffolds and evaluation of enterobactin-cargo conjugate uptake. *J. Am. Chem. Soc.* 134(44):18388-18400.
24. Zheng T & Nolan EM (2014) Enterobactin-mediated delivery of beta-lactam antibiotics enhances antibacterial activity against pathogenic *Escherichia coli*. *J. Am. Chem. Soc.* 136(27):9677-9691.
25. Holmgren J & Czerkinsky C (2005) Mucosal immunity and vaccines. *Nat. Med.* 11(4 Suppl):S45-53.
26. Hapfelmeier S & Hardt WD (2005) A mouse model for *S*. typhimurium-induced enterocolitis. *Trends Microbiol.* 13(10):497-503.
27. Barthel M, *et al.* (2003) Pretreatment of mice with streptomycin provides a *Salmonella* enterica serovar Typhimurium colitis model that allows analysis of both pathogen and host. *Infection and immunity* 71(5):2839-2858.
28. Stecher B, *et al.* (2007) *Salmonella* enterica serovar typhimurium exploits inflammation to compete with the intestinal microbiota. *PLoS biology* 5(10):2177-2189.
29. Spees AM, *et al.* (2013) Streptomycin-induced inflammation enhances *Escherichia coli* gut colonization through nitrate respiration. *mBio* 4(4):e00430-00413.
30. Barton CH, Biggs TE, Baker ST, Bowen H, & Atkinson PG (1999) Nramp1: a link between intracellular iron transport and innate resistance to intracellular pathogens. *J. Leukoc. Biol.* 66(5):757-762.
31. Santos RL, *et al.* (2009) Life in the inflamed intestine, *Salmonella* style. *Trends Microbiol.* 17(11):498-506.
32. Behnsen J, *et al.* (2014) The cytokine IL-22 promotes pathogen colonization by suppressing related commensal bacteria. *Immunity* 40(2):262-273.
33. Winter SE, Lopez CA, & Bäumler AJ (2013) The dynamics of gut-associated microbial communities during inflammation. *EMBO Rep.* 14(4):319-327.
34. Rigottier-Gois L (2013) Dysbiosis in inflammatory bowel diseases: the oxygen hypothesis. *The ISME journal* 7(7):1256-1261.
35. Winter SE & Bäumler AJ (2014) Why related bacterial species bloom simultaneously in the gut: principles underlying the 'Like will to like' concept. *Cellular microbiology* 16(2):179-184.
36. Winter SE, *et al.* (2013) Host-derived nitrate boosts growth of *E. coli* in the inflamed gut. *Science* 339(6120):708-711.
37. Thiennimitr P, *et al.* (2011) Intestinal inflammation allows *Salmonella* to use ethanolamine to compete with the microbiota. *Proc. Natl. Acad. Sci. USA* 108(42):17480-17485.

38. Raffatellu M & Bäumler AJ (2010) *Salmonella*'s iron armor for battling the host and its microbiota. *Gut microbes* 1(1):70-72.
39. Ilott NE*, et al.* (2016) Defining the microbial transcriptional response to colitis through integrated host and microbiome profiling. *The ISME journal*.
40. Behnsen J, Deriu E, Sassone-Corsi M, & Raffatellu M (2013) Probiotics: properties, examples, and specific applications. *Cold Spring Harbor perspectives in medicine* 3(3):a010074.
41. Ji C, Juarez-Hernandez RE, & Miller MJ (2012) Exploiting bacterial iron acquisition: siderophore conjugates. *Future medicinal chemistry* 4(3):297-313.
42. Bolin CA & Jensen AE (1987) Passive immunization with antibodies against iron-regulated outer membrane proteins protects turkeys from Escherichia coli septicemia. *Infection and immunity* 55(5):1239-1242.
43. Clifton-Hadley FA*, et al.* (2002) A laboratory study of an inactivated bivalent iron restricted Salmonella enterica serovars Enteritidis and Typhimurium dual vaccine against Typhimurium challenge in chickens. *Veterinary microbiology* 89(2-3):167-179.
44. Bergeron RJ*, et al.* (2009) Vibriobactin antibodies: a vaccine strategy. *J. Med. Chem.* 52(12):3801-3813.
45. Gopinath S, Carden S, & Monack D (2012) Shedding light on *Salmonella* carriers. *Trends in microbiology* 20(7):320-327.
46. Holden VI & Bachman MA (2015) Diverging roles of bacterial siderophores during infection. *Metallomics : integrated biometal science* 7(6):986-995.
47. Johnstone TC & Nolan EM (2015) Beyond iron: non-classical biological functions of bacterial siderophores. *Dalton transactions* 44(14):6320-6339.
48. Adler C*, et al.* (2014) The alternative role of enterobactin as an oxidative stress protector allows *Escherichia coli* colony development. *PloS one* 9(1):e84734.
49. Singh V*, et al.* (2015) Interplay between enterobactin, myeloperoxidase and lipocalin 2 regulates *E. coli* survival in the inflamed gut. *Nature communications* 6:7113.
50. Holden VI*, et al.* (2014) Bacterial siderophores that evade or overwhelm lipocalin 2 induce hypoxia inducible factor 1alpha and proinflammatory cytokine secretion in cultured respiratory epithelial cells. *Infection and immunity* 82(9):3826-3836.
51. McGill NW & Williams SJ (2009) 2,6-Disubstituted benzoates as neighboring groups for enhanced diastereoselectivity in beta-galactosylation reactions: synthesis of beta-1,3-linked oligogalactosides related to arabinogalactan proteins. *J. Org. Chem.* 74(24):9388-9398.
52. Scarrow RC, Ecker, D.J., Ng, C., Liu, S. & Raymond, K.N (1991) Iron(III) coordination chemistry of linear dihydroxyserine compounds derived from enterobactin. *Inorg. Chem.* 30:900-906
53. Singh KV, Kaur J, Varshney GC, Raje M, & Suri CR (2004) Synthesis and characterization of hapten-protein conjugates for antibody production against small molecules. *Bioconjug. Chem.* 15(1):168-173.
54. Schagger H (2006) Tricine-SDS-PAGE. *Nat. Protoc.* 1(1):16-22.

CHAPTER 4

Discussion and Future Directions

4.1 Summary and Conclusions

The mammalian gastrointestinal (GI) tract is colonized by trillions of microbes, which are essential to maintain the mammalian gut ecosystem. Obligate anaerobes belonging to the phyla of Bacteroidetes and Firmicutes dominate the normal gut flora during homeostatic conditions, and have been shown to be essential in keeping enteric pathogens at bay, a process known as colonization-resistance (1, 2). Disruption of this delicate microbe-host balance (dysbiosis) with the use of broad-spectrum antibiotics is linked with an expansion of the Proteobacteria phylum (3-5). This expansion of Proteobacteria is viewed as a "side-effect" during the treatment of enteric pathogen infections, or in conditions such as inflammatory bowel syndrome (IBD) (6, 7). By inducing host inflammation, microbes associated with dysbiosis dramatically reduce the availability of nutrients in the lower GI tract (8, 9). In contrast to most members of the microbiota, Proteobacteria including *Escherichia coli* spp. and pathogenic strains of the Enterobacteriaceae family (such as the pathogen *Salmonella enterica*) are well suited to benefit from the "nutritional challenge" posed by the host during inflammation (10). In an inflamed gut, acquisition of metal ions like iron, zinc and manganese is essential for these enteric microbes to sustain their replication and survival (11-13). Commensals

Enterobacteriaceae and *Salmonella enterica* serovar Typhimurium, like many other pathogenic bacteria, require micromolar (10^{-6} M) concentrations of iron (Fe) to successfully colonize the vertebrate host. Because Fe concentrations are tightly regulated in the vertebrate host, to scavenge Fe, Enterobacteriaceae such as *S*. Typhimurium biosynthesize and export small-molecule metal-ion chelators called "siderophores". Siderophores chelate ferric iron (FeIII) with high affinity (Kd 10^{-25} M). Bacteria biosynthesize siderophores through the expression of very large gene clusters encoding for the biosynthetic and export machinery, and for specific uptake complexes. *S*. Typhimurium and commensal Enterobacteriaceae produce the siderophore enterobactin, which is essential for bacterial Fe acquisition. In response to infection and during inflammation, the host secretes the antimicrobial protein lipocalin-2 (LCN2), which sequesters enterobactin in the extracellular environment and inhibits the growth of those commensals that rely only on enterobactin for Fe acquisition. To counteract the host nutritional immunity defense mediated by LCN2, pathogens like *S.* Typhimurium have adopted other mechanisms to acquire Fe. *S.* Typhimurium biosynthesize a C-glucosylated form of enterobactin, called salmochelin (**Chapter 3, Fig. 3.4 A**), which is too large to be bound by LCN2. Therefore, salmochelin confers an advantage to *S.* Typhimurium over other microbes for Fe acquisition in the inflamed gut, where LCN2 is abundant. Indeed, a *S.* Typhimurium isogenic mutant that cannot uptake salmochelin from the extracellular environment (*iroN* mutant), shows decreased gut colonization during acute infection compared to the wild-type strain (12).

Commensal and pathogenic bacteria have also evolved mechanisms to hinder the ability of competing bacteria to specifically acquire Fe; one of these mechanisms

involves the secretion of antimicrobial peptides (14, 15). As discussed extensively in chapters 1 and 2, one strain capable of secreting antimicrobial peptides to better compete for Fe is the probiotic strain *Escherichia coli* Nissle 1917 (EcN). *In vitro,* EcN produces and secretes two microcins that exhibit bactericidal activity towards phylogenetically-related strains, including some pathogenic bacteria (16). EcN microcins belong to the class IIb, and are characterized by the covalent link of the antimicrobial peptide to a siderophore-like platform trough post-translational modifications. Microcins can then access target bacteria through siderophore receptors via a "Trojan Horse" mechanism of action (17, 18).

Given the importance of Fe for bacterial survival, and because Gram-negative pathogens represent a major public health issue (19), with this work we aimed to develop two different approaches to reduce enteric pathogens growth by taking advantage of siderophore-mediated Fe acquisition. In particular, as ***long-term goals***, both strategies aim to solely target the siderophore producers within the Enterobacteriaceae family. This tactic could have major advantages compared to broad-spectrum antibiotic treatments. Importantly, other members of the resident microbiota will not be targeted by such selective strategies, and the efficacy will be much greater towards the targeted pathogen.

The following ***two hypotheses*** were investigated in this work:

1) The probiotic strain *Escherichia coli* Nissle 1917 (EcN) microcins inhibit the growth of related commensals and pathogens in an inflamed gut, but not in the absence of inflammation, and are essential for EcN survival in this environment

2) Boosting nutritional immunity by immunization against bacterial siderophores inhibits the growth of enteric pathogens

Major conclusions and future directions resulting from our work aimed to test these hypotheses will be discussed in the following paragraphs.

4.1.1 The probiotic strain *Escherichia coli* Nissle 1917 (EcN) microcins inhibit the growth of related commensals and pathogens in an inflamed gut and are essential for EcN survival

First, we explored the *in vivo* role of bacterial antimicrobial peptides, called microcins, expressed by the probiotic strains of *Escherichia coli* Nissle 1917 (EcN) during low iron conditions (**Chapter 2 and Fig. 2.3 H**). Although few reports highlighted the importance of other classes of antimicrobial peptides (e.g., bacteriocins and colicins) (20, 21) for bacterial competition in the gastrointestinal tract, whether microcins play a role in the gut remained undetermined (22). Investigating the function of microcins in bacterial competition can inform efforts aimed to develop therapeutic strategies to target pathogens that utilize siderophores to acquire iron and thrive during inflammation (23). Accordingly, we aimed to determine whether microcins are utilized by EcN to outgrow its closest competitors by mediating intra-species colonization resistance in the gut (22). We sought to investigate the role of microcins by generating isogenic mutants of EcN lacking either the microcins export machinery (*mchDEF*) or both structural genes (*mcmA* and *mchB*) encoding for microcins M and H47 (**Fig. 2.1 and Table 2.1**). In Chapter 2, we demonstrated that microcins are dispensable in the absence of intestinal inflammation (**Fig. 2.2 and Fig. 2.3**). These findings likely explain why, 50 years after their discovery (24, 25), a role for microcins during gut bacterial competition remained elusive. Because EcN microcins are expressed during iron starvation and utilize siderophore receptors to cross the outer membrane of their target competitors (24), we utilized an mouse colitis model to examine the role of EcN microcins during gut

colonization in competition with a mouse commensal *E. coli* strain (**Fig. 2.4 A**). Our data demonstrated that secretion of microcins by wild-type EcN reduced commensal *E. coli* colonization in the presence of intestinal inflammation (**Fig. 2.4 C**). Moreover, the importance of microcin secretion for EcN survival in the inflamed intestine was highlighted by the finding that isogenic mutants lacking *mchDEF* or *mcmA* and *mchB* exhibited lower levels of colonization at later time points (**Fig. 2.4 B, D and Fig. 2.6 B**). Because this strategy employed by EcN could be implemented as a therapeutic tool against siderophore-producing pathogens, we investigated EcN competition with the enteric pathogen *Salmonella enterica* serovar Typhimurium and the pathobiont adherent-invasive *E. coli* (AIEC). Similarly to what we found with commensal *E. coli*, EcN microcins reduced *S*. Typhimurium and AIEC burden in the mouse intestine (**Fig. 2.13 C and 2.15 C**). Moreover, our data also indicate that the strategy employed by EcN for intra-species competition contributes to survival of EcN in the inflamed gut only when very close competitors that also produce siderophores are present in the environment (**Fig. 2.4 E-F and Fig. 2.9**).

Collectively, our findings provide the first *in vivo* evidence that secretion of microcins is essential for intra-species and inter-species competition and, consequently, for the establishment of an ecological niche in the inflamed gut. As this strategy employed by EcN and other spp. is directed solely against competitors with related siderophore-dependent iron acquisition, this approach could be used to more specifically target enteric pathogens and pathobionts without affecting the surrounding beneficial microbiota (i.e., Bacteroidetes and Firmicutes) (**Fig. 2.18**) Sequencing of the microbial communities during DSS treatemnt and *E. coli* gut colonization, when in competition

with either EcN wild-type of mutants, further support the idea that this strategy solely target related siderophore-producers (**Fig. 2.18**). Moreover, strains of *S*. Typhimurium lacking the ability to acquire the siderophores enterobactin (*fepA* mutant) and salmochelin (*iroN* mutant) from the surrounding environment were insensitive to the effects of EcN microcins during *in vitro* co-culture (**Figure 2.19**). This latter data further highlight that microcins target only strains that express siderophores receptors. These receptors are normally expressed during iron starvation or in the presence of inflammation, and only pathogens capable of expressing them will survive in an inflamed environment. In conclusion, microcin-siderophore conjugates could be useful to overcome the challenging task of seeking targeted and efficacious ways to cross the gram-negative bacterial membrane of enteric pathogens and pathobionts to efficiently reduce their growth.

4.1.1.1 Future Directions

With the increase in antibiotic resistance and the limited availability of preventive strategies, new ways are needed to target enteric pathogens (19, 26). Moreover, because the use of antibiotics to treat certain enteric pathogenic infections (e.g. *Salmonella* spp.) or GI disorders has been shown to be detrimental for the host, there's a need for novel strategies to control Enterobacteriaceae spp. growth (27). These efforts have been hindered due to our limited understanding of the mechanisms promoting gut colonization by these bacterial species. Because bacterial species have lived in highly competitive ecosystems for millennia, they excel at identifying their enemies' weaknesses. Deciphering the mechanisms that other bacterial species have

acquired to limit colonization by pathogens and pathobionts can inform novel strategies to impair their growth in the host (2, 22). Our work demonstrates that bacterial antimicrobial peptides, called microcins, produced by the probiotic strain *E. coli* Nissle, inhibit the growth of closely related commensals and pathogens in the inflamed gut (**Chapter 2**). However, several questions remain unanswered.

Microcins produced by EcN belong to the class IIb, which include those microcins that are post-translationally modified and linked to a siderophore platform. Although, this modification was shown for microcin E492 produced by *Klebsiella*, still remain unclear whether this is also the case for EcN microcin and whether an unmodified peptides would still hold antimicrobial activity towards the target competitor. We hypothesized that microcins have a greater effect against the target competitor (e.g. *S.* Typhimurium) only when they are post-translationally modified and linked to a siderophore-like platform. Consistent with this idea, we found that a strain of EcN lacking the ability to generate an active C-glucosylated enterobactin (*iroBC* mutant) is unable to inhibit the growth of *S.* Typhimurium in an *in vitro* competition assay (**Fig. 4.1 A**), despite its normal replication rate (**Fig. 4.1 B**). However, we were surprised to find that an EcN strain unable to produce enterobactin is still able to inhibit *S*. Typhimurium growth (**Fig. 4.1 A**). We hypothesized that, as the EcN *entC* mutant still expresses the enterobactin receptor *fepA*, the strain can uptake enterobactin secreted by *S*. Typhimurium and post-translationally modify the microcins in its periplasm membrane (done by *iroBC* gene products) (28). As microcin secretion aims to target only the siderophore-producers, an important question that still needs to be addressed is whether unmodified microcins could target bacterial species that are not closely related. Further studies will elucidate

whether the most efficacious way to deliver a therapeutic strategy to fight enteric pathogen infections should rely on the synthesis of modified or unmodified microcins.

FIGURE 4.1

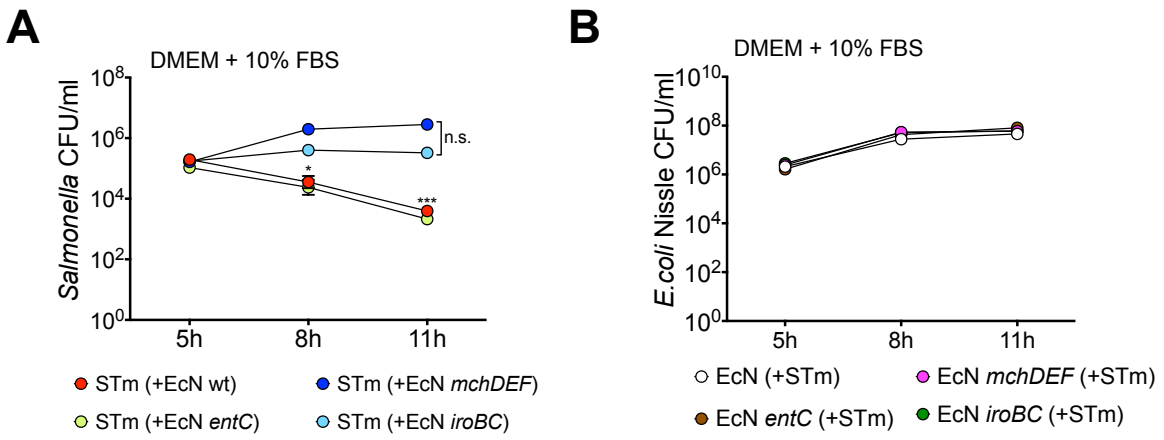


Figure 4.1. *In vitro* competition assay of EcN wild-type and mutants against *S*. Typhimurium. *In vitro* competition assays between wild-type EcN or microcin mutant (EcN *mchDEF*) or EcN lacking the ability to produce enterobactin (*entC*) or salmochelin (*iroBC)* against *Salmonella* Typhimurium (STm). All strains were grown overnight in nutrient broth + 0.2 mM 2,2'-dipyridyl prior to inoculation in DMEM/F12 + 10%FBS (iron-limiting media). **A** STm CFU/mL at 5, 8, and 11 hours post inoculation when alone or in competition with either wild-type EcN or the indicated EcN mutants in iron-limiting conditions. **B** CFU/ml of wild-type EcN or the indicated EcN mutants in competition with STm in iron-limiting conditions.

The possibility of using beneficial gut microbes to re-establish microbiota-mediated colonization resistance after antibiotic treatment was discussed in a recent issue of *Science* (27). Of great interest to the field is the identification of bacterial species that can be developed into next-generation probiotics, which can then be implemented to provide colonization resistance to pathogens (2). Along these lines, whether a strain of EcN engineered to over-express microcins would be more effective in inhibiting the growth of pathogens needs to be investigated.

Although our data suggest that microcins play a role during *in vivo* gut colonization, in particular during inflammation, whether diet composition may influence the observed phenotypes is not clear. Specifically, some reports have emphasized how dietary Fe levels have an impact in shaping the gut microbial communities, also during enteric pathogen infections (29, 30). Mice used in our studies were fed a normal chow diet, which contained about 200mg/Kg of iron (ferrous sulfate). However, for widely standardizes diets, the recommended normal Fe content is about 35mg/Kg (31). It would be important to investigate if microcin-mediated growth inhibition would be of even greater intensity if our mice were fed with a normal diet containing lower Fe concentrations (35 mg/Kg). Another related question is whether a Fe-rich diet can also differentially regulate the expression of microcins. Preliminary data suggest that in iron-rich environments microcins dot not play a role (**Fig. 2.11**). Additionally, some of our recent studies using germ-free mice indicate that the antimicrobial activity of microcins is not observed in the absence of a complex microbiota. These findings holds true whether inflammation is induced or not, however germ-free mice did not develop similar level of inflammation as SPF mice, which could also be a consequence of high iron

levels (**Fig. 2.2 B and data not shown**). Our hypothesis is that, in the absence other bacterial species that also consume iron, microcins are not essential for bacterial competition. These observations could also be justified as a result of the diet of germ-free mice, which contains higher Fe content (250 mg/Kg) than the diet for conventional animals (Specific Pathogen Free).

Another very important question is whether microcins produced by EcN could also have a role in shaping the human gut microbial communities. Indeed, EcN was first isolated during World War I from the gut of a soldier who did not develop diarrhea during a *Shigella* outbreak. Because we found that EcN microcins have inhibitory effect also against a human commensal *E. coli* (*E. coli* HS, **data not shown**), it would be informative to investigate the dynamics of these two strains in an *in vivo* setting and in the presence of inflammation.

As mentioned above, there is an increasing interest in developing next-generation probiotics with the potential to provide high colonization resistance to pathogens (2). For example, it may be feasible to design probiotics by engineering commensal strains to better compete with pathogens for nutrients in more hostile environments like the inflamed gut. The probiotic EcN exhibits several beneficial features, in addition to microcins, that could help to control growth of pathogens (11, 32). As discussed previously, probiotics can control pathogen growth by a direct mechanism (Chapter 1) as well as indirectly, by stimulating the innate and adaptive immune systems. To further investigate potential beneficial roles of EcN through stimulation of the immune system

and in the absence of other microbes, we employed germ-free mice. Our preliminary data indicate that EcN can induce immune responses that are potentially beneficial to the host. In particular, we found that mono-colonization of germ-free with EcN, but not with a mouse commensal *E.coli* (JB1), induced the migration of gut neutrophils, identified as Ly-6G$^+$ S100A9$^+$ (**Fig. 4.2 A and B**). S100A9 is one of the two subunits of calprotectin, a zinc- and manganese-binding protein secreted upon infection with *Salmonella* and other pathogens (13, 33). Further studies are warranted to determine the additional beneficial effects of EcN in promoting mucosal barrier functions, which could also contribute to impair the growth of pathogens. For example, some commensal microbes contribute to B cell development (34). In this regard, Segmented Filamentous Bacteria (SFB), but not commensal *E. coli,* was shown to contribute to the development of intestinal lymphoid tissue, including Peyer's patches, and also to the development of intestinal sIgA (35). Clinical studies have also reported that the microbiota contributes to B cell maturation in patients. Specifically, early-life colonization by *E. coli* and *Bifidobacterium longum* subspecies Infantis have been associated with higher numbers of mature CD20$^+$ B cells (36). Similarly, we found that after only 4 days of EcN mono-colonization, germ-free mice show development of Peyer's patches, lymphoid tissues localized to the small intestine. Our preliminary data show that EcN and a mouse commensal *E. coli* strain induced higher numbers of B cells (identified as B220$^+$CD19$^+$) in the small intestine and colon (**Fig. 4.2 A**). However, only mice colonized with EcN showed higher levels of regulatory B cells, identified as CD5$^+$ CD1d$^+$, in the Peyer's patches, suggesting an EcN-specific effect on the development of this B cell subset (**Fig. 4.2 B-D**). Further studies investigating the role of EcN in inducing

B cells migration and the development of regulatory B cells (37) could facilitate the development of new strategies to target enteric pathogens and boost the mucosal immune system. Such studies will be helpful to identify EcN features that, combined with microcins, would be of great efficacy to control growth of pathogens.

FIGURE 4.2

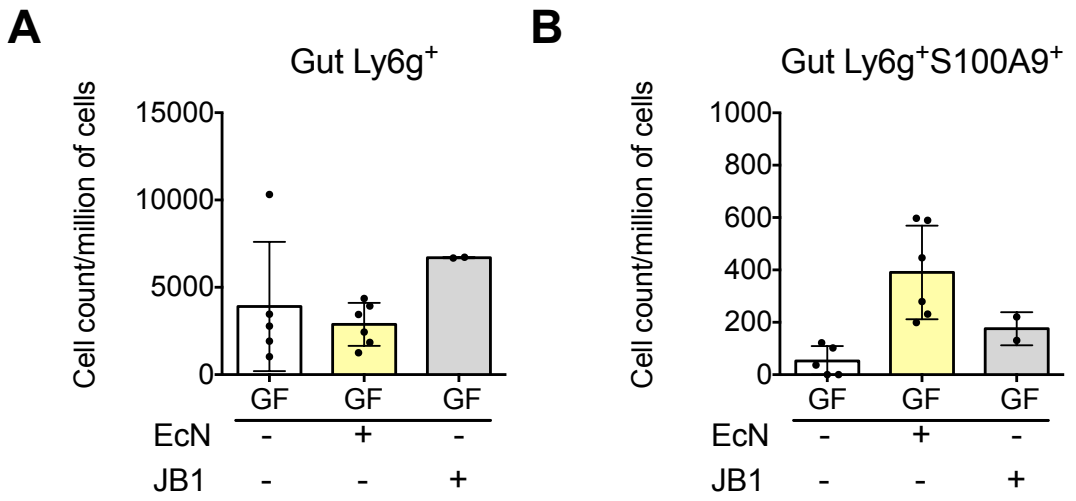


Figure 4.2. Effects of EcN mono-colonization of Germ-Free mice on the gut mucosal barrier. A. FACS analysis of gut neutrophils ($Ly6g^+$) from Germ-free or mono-colonized animals with EcN or a commensal *E. coli.* **B.** Intracellular staining of $Ly6G^+$ neutrophils for calprotectin subunit S100A9 from Germ-free or mono-colonized animals with EcN or a commensal *E. coli.*

FIGURE 4.3

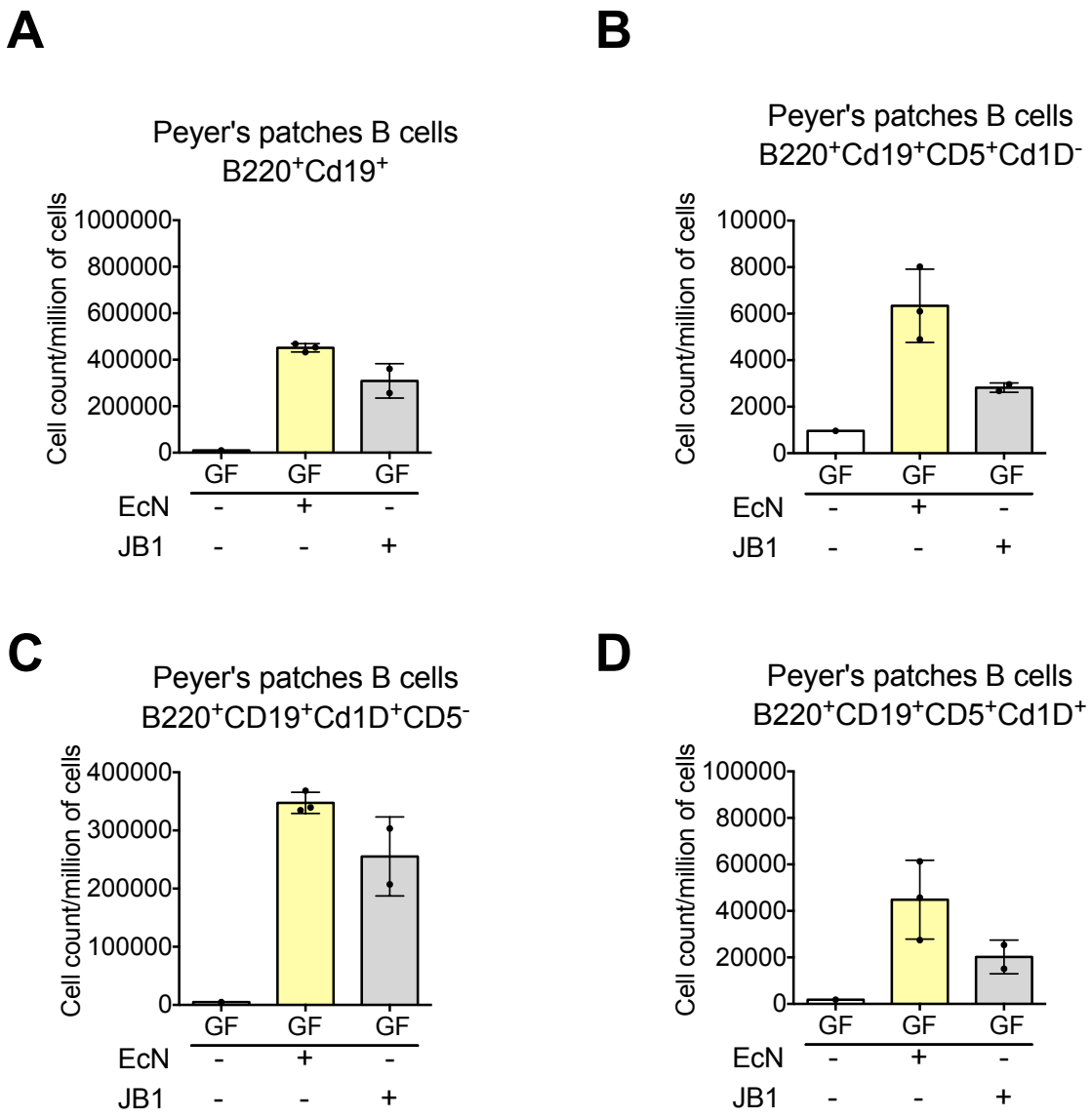


Figure 4.3. Effects of EcN mono-colonization of Germ-Free mice on adaptive immune system. A. FACS analysis of B cells isolated from Peyer's patches ($B220^+CD19^+$) from Germ-free or mono-colonized animals with EcN or a commensal *E. coli.* **B.** Identification with FACS of regulatory B cells ($CD5^+Cd1d^+$) in the Peyer's patches of Germ-free or mono-colonized animals with EcN and commensal *E.coli*.

4.1.2 Boosting nutritional immunity by immunization against bacterial siderophores inhibits the growth of enteric pathogens

As discussed extensively in previous paragraphs, there is a need to find alternative therapeutic strategies against enteric pathogen infections. To address this issue, we aimed to design and test a novel, narrow-spectrum, immunization strategy to block the ability of a gastrointestinal pathogen (in this case *S.* Typhimurium) to acquire the essential metal nutrient iron (Fe) (**Chapter 3**).

The ability to acquire Fe is a feature shared by many commensals and pathogens, including *Salmonella* (38). It has been shown the importance of Fe acquisition for *Salmonella* to establish gut colonization (12, 39). All enterobacteriace, including *Salmonella,* secrete the siderophore enterobactin (Ent) in order to sequester iron from the extracellular environment(40). However the host has evolved a mechanism to counteract enterobactin-mediated iron acquisition. Specifically, during gut inflammation the host secretes the antimicrobial protein lipocalin-2 (LCN2), which can bind and sequester the siderophore Ent (40). This allows the host to control the growth of commensal or pathogens that only rely on Ent for iron acquisition. However, Salmonella has acquired an additional locus (*iroA*), which encodes for an additional siderophore termed salmochelin (Glc-Ent) that cannot be bound by LCN2. Indeed, because of two glucosilation Glc-Ent is to big to fit in the LCN2 biding pocket (41). The secretion of Glc-Ent allows *Salmonella* to overcome this harm of nutritional immunity and to survive in the presence inflammation. Because *S.* Typhimurium evades LCN2 by secreting Glc-

Ent, we designed and employed a novel strategy to limit Glc-Ent-mediated Fe acquisition (12, 42). We hypothesized that, by blocking salmochelin with the generation of specific antibodies, we would be able to reduce *S.* Typhimurium replication and therefore ameliorate gastrointestinal disease caused by this pathogen. Due to the complex chemical structure of siderophores, bacteria cannot easily modify them. Hence, siderophores are attractive therapeutic targets to limit Fe acquisition by *Salmonella and* other pathogens (43). Our approach involved the chemical synthesis of siderophores (carried out by our collaborators Dr. Elisabeth Nolan and Dr. Phoom Charaitana at MIT), and their conjugation to immunogenic carrier proteins (in this work, the Cholera Toxin B subunit or CTB) (44). Once the synthesis of the siderophore enterobactin and the conjugation to CTB was established (**Fig. 3.2**), we performed animal immunization studies to test our hypothesis (**Fig. 3.1 A**).

By immunizing mice against *S.* Typhimurium siderophores, we detected the development of specific IgAs against both Ent and Glu-Ent (**Fig. 3.1 A**). Surprisingly, only IgA in the Peyer's patches, but not IgG in the spleen, were found to recognize both Ent and Glc-Ent, suggesting the development of a specific mucosal immune response to these siderophores (**Fig. 3.4 E**). We then used the colitis mouse model of *Salmonella* acute infection to investigate whether mice that develop specific anti-Glc-Ent IgA antibodies were better protected against *S.* Typhimurium gut colonization and infection of the gastrointestinal tract (45). We found that mice that were immunized with the CTB-Ent conjugate had a drastic and significant reduction of *S.* Typhimurium growth in the colonic lumen (**Fig 3.4 A**). Additionally, *S.* Typhimurium growth and levels of anti-Ent IgA, detected from stool samples of CTB-Ent mice, were inversely correlated (**Fig 3.4**

B). Also, we observed reduced *S.* Typhimurium dissemination to the spleen. Because we did not detect anti-siderophore IgG after immunization, the reduced dissemination could be due to the lower levels of *S.* Typhimurium in the gut. Moreover, as we found a lower competitive advantage of the wild-type *S.* Typhimurium over the *iroN* mutant, which is unable to acquire Glc-Ent, when mice were immunized with CTB-Ent, we reasoned that the observed phenotype was mediated specifically by the sequestration of salmochelin in the extracellular environment (12) (**Fig. 3.7 C**). Lastly, the lower colonization of *S.* Typhimurium in the colon of CTB-Ent immunized mice was accompanied by an expansion of *Lactobacilli* spp (**Fig. 3.9**). This outcome can be explained by previous observations that describe better survival of *Lactobacilli* in inflamed gut environments, where Fe is scarce (46).

Collectively, our data suggest that limiting Fe acquisition by exclusive targeting siderophore-mediated acquisition could be a useful strategy to reduce *S.* Typhimurium gut colonization. Additionally, our research provides the basis for the development of a vaccine against NTS and for the generation of therapeutic antibodies targeting *S.* Typhimurium siderophores. Broadly, our work indicates that new preventive and therapeutic strategies for microbial infections should target siderophore-mediated iron acquisition, a virulence trait shared by almost all bacterial and fungal pathogens (47). As recent studies demonstrate additional, non-classical roles for siderophores (48, 49), including protection from oxidative stress (50), inhibition of myeloperoxidase activity (51), and modulation of gene expression (52), antibody-mediated sequestration of siderophores may provide additional benefits to the host.

4.1.2.1 Future directions

With the increase in antibiotic resistance and the limited availability of preventive strategies, new ways are needed to target enteric pathogens (19, 26). Our work proposes a novel immunization strategy against bacterial siderophores that effectively reduced gut colonization by the pathogen *Salmonella* Typhimurium (**Chapter 3, Fig. 3.4**).

However, due to limitations of the current mouse models, we could investigate the efficacy on this strategy up to only eight days post *Salmonella*-infection (**Fig 3.7 F**). From a therapeutic point of view, it would be important to test whether our immunization can completely eradicate *S.* Typhimurium from the intestine in a long-term setting. Also similar to what we have proposed for the microcin studies, it would be informative to investigate the impact of diets with various Fe levels on this immunization approach, to determine whether differential Fe levels would impact our phenotypic outcome. As discussed previously, the normal diet that animals in this study received was high in Fe content.

Additionally, studies are warranted to determine whether siderophore immunization can be employed to other bacterial pathogens, as similar but distinct siderophores molecules are secreted by many bacterial and fungal pathogens to acquire Fe in the host (53, 54). As Proteobacteria utilize the same siderophore-based Fe acquisition strategy, we hypothesized that our immunization strategy could be useful at least during other types of gastrointestinal diseases associated with a bloom of Proteobacteria, such as commensals *E. coli.*

An important aspect that needs to be evaluated is whether our siderophore-conjugates can be used for the development of therapeutic antibodies targeting siderophores. Specifically, the purifications and isolation of these antibodies could be useful to further investigate with *in vitro* assays their ability to bind to Ent and Glc-Ent and importantly would be informative of which epitopes are recognized. Moreover, although we developed a new preventive strategy to ameliorate *S.* Typhimurium colonization, the most appealing question that remained to be addressed is whether we can generate large quantities of specific anti-siderophores antibodies to treat an ongoing infection. The generation of antibodies targeting bacterial Fe uptake systems was attempted in different settings, and only against siderophore receptors (55). Although these approaches were partly successful, only one aminoacid substitution in the siderophore receptor could render a bacterium resistant. Our view is that for a long-term and sustainable outcome it would be best to target the actual siderophore; to counteract a siderophore-immunization strategy, acquisition of a whole new siderophore gene cluster by horizontal gene transfer would be required, which is a possible but a rarer event than a point mutation in a single gene. In an attempt to isolate specific B cells clones that produced anti-Ent and Glc-Ent antibodies, we immunized mice with the CTB-Ent conjugate and we sorted B cells from the Peyer's patches. We employed flow cytometry to identify B cells that express anti-Ent antibodies by detecting them the use of an Ent-biotin conjugate (**Fig. 3.3**)**,** followed by detection with a streptavidin-PE conjugate (**Fig. 4.4 A**). Although we were able to identify anti-Ent-antibody-expressing B cells (identified as $B220^{+}CD19^{+}PE^{+}$; **Fig. 4.4 B and C**) from Peyer's patches of immunized animals, single cell sorting of specific clones proved to be more challenging than

anticipated. One major issue is that we could find specific B cells producing anti-Ent antibodies only at mucosal tissues (**Fig. 3.1 and 3.5**), particularly in Peyer's patches. Unfortunately, very few B cells are found in Peyer's patches, compared to other lymphoid tissues such as the spleen. Because the identification of such small cell populations from Peyer's patches is challenging, it would be important to develop different immunization approaches to raise specific antibodies also in the spleen. Moreover, these alternative approaches could also be informative for increasing the efficacy of a response against *Salmonella* infection at systemic sites.

FIGURE 4.4

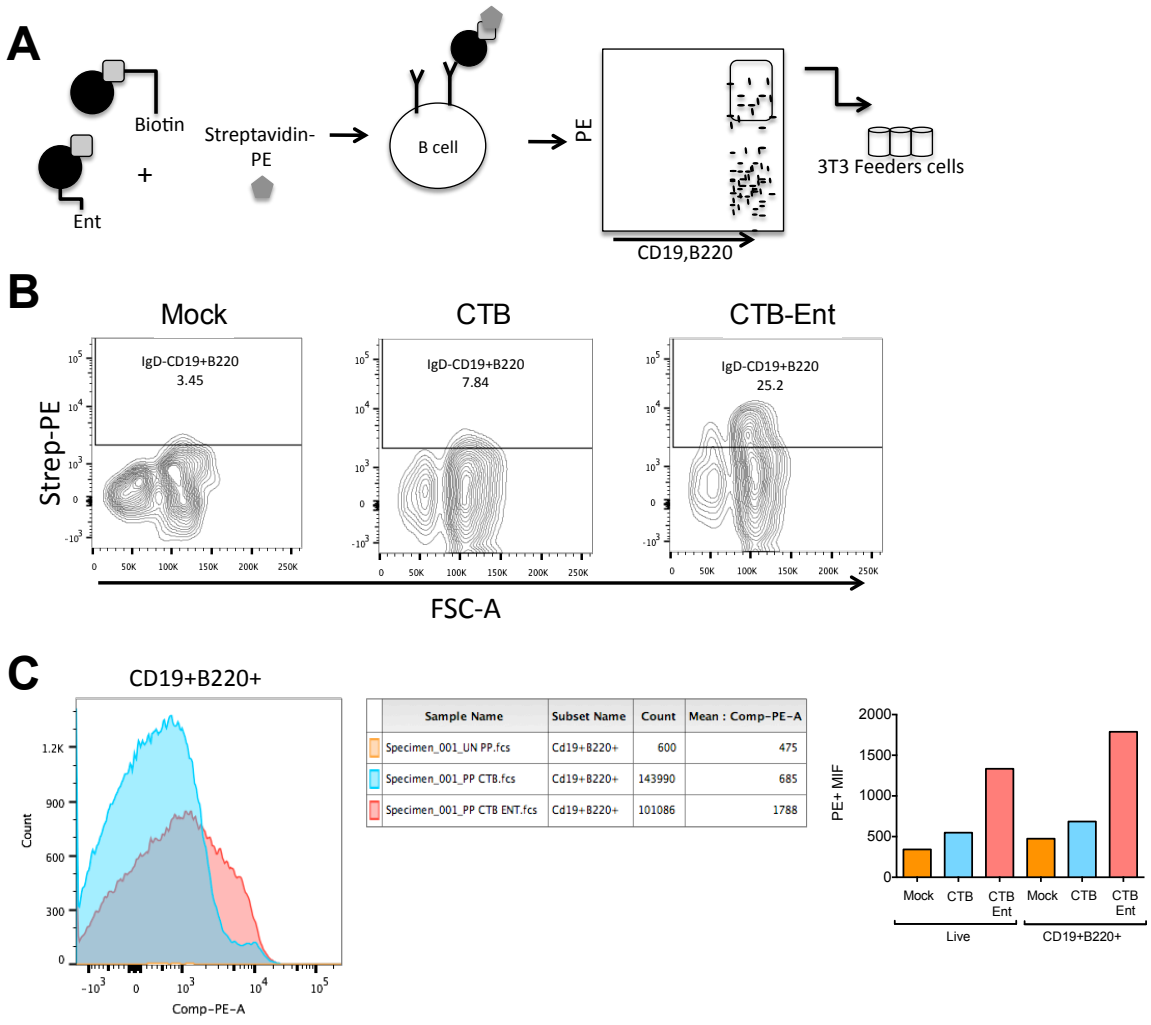


Figure 4.4. Flow cytometry analysis to detect B cells producing anti-Ent antibodies. A. Schematic representation of experimental setting. B cells isolated from Peyer's patches were strained with B cells markers CD19 and B220. Ent-Biotin was used to detect B cells expressing anti-Ent antibodies with streptavidin-PE fluorophore. **B**. Representative FACS plots from Mock, CTB and CTB-Ent immunized mice, of PE+ percentages of B cells gated on $B220^{+}CD19^{+}$. **C.** PE mean intensity of florescence (MIF) in mock, CTB and CTB-Ent immunized animals.

In summary, in this work we developed and tested new approaches to target enteric pathogen infections. In contrast to broad-spectrum antibiotics, we aimed to be selective against siderophore-producing pathogens, thereby avoiding or limiting the killing of beneficial gut microbes. Both antimicrobial strategies presented here elucidate new concepts of targeting a common but also specific bacterial virulence trait to fight bacterial infections.

4.2 References

1. Kamada N, Chen GY, Inohara N, & Nunez G (2013) Control of pathogens and pathobionts by the gut microbiota. *Nature immunology* 14(7):685-690.
2. Buffie CG & Pamer EG (2013) Microbiota-mediated colonization resistance against intestinal pathogens. *Nature reviews. Immunology* 13(11):790-801.
3. Spees AM*, et al.* (2013) Streptomycin-induced inflammation enhances *Escherichia coli* gut colonization through nitrate respiration. *mBio* 4(4).
4. Hill DA*, et al.* (2010) Metagenomic analyses reveal antibiotic-induced temporal and spatial changes in intestinal microbiota with associated alterations in immune cell homeostasis. *Mucosal immunology* 3(2):148-158.
5. Rivera-Chavez F*, et al.* (2016) Depletion of Butyrate-Producing Clostridia from the Gut Microbiota Drives an Aerobic Luminal Expansion of Salmonella. *Cell host & microbe* 19(4):443-454.
6. Winter SE & Bäumler AJ (2014) Why related bacterial species bloom simultaneously in the gut: principles underlying the 'Like will to like' concept. *Cellular microbiology* 16(2):179-184.
7. Cho I & Blaser MJ (2012) The human microbiome: at the interface of health and disease. *Nature reviews. Genetics* 13(4):260-270.
8. Winter SE & Bäumler AJ (2014) Dysbiosis in the inflamed intestine: Chance favors the prepared microbe. *Gut microbes* 5(1):71-73.
9. Stecher B, Maier L, & Hardt WD (2013) 'Blooming' in the gut: how dysbiosis might contribute to pathogen evolution. *Nature reviews. Microbiology* 11(4):277-284.
10. Winter SE*, et al.* (2013) Host-derived nitrate boosts growth of E. coli in the inflamed gut. *Science* 339(6120):708-711.
11. Deriu E*, et al.* (2013) Probiotic bacteria reduce salmonella typhimurium intestinal colonization by competing for iron. *Cell host & microbe* 14(1):26-37.
12. Raffatellu M*, et al.* (2009) Lipocalin-2 resistance confers an advantage to Salmonella enterica serotype Typhimurium for growth and survival in the inflamed intestine. *Cell host & microbe* 5(5):476-486.
13. Liu JZ*, et al.* (2012) Zinc sequestration by the neutrophil protein calprotectin enhances *Salmonella* growth in the inflamed gut. *Cell host & microbe* 11(3):227-239.
14. Duquesne S, Petit V, Peduzzi J, & Rebuffat S (2007) Structural and functional diversity of microcins, gene-encoded antibacterial peptides from enterobacteria. *Journal of molecular microbiology and biotechnology* 13(4):200-209.
15. Duquesne S, Destoumieux-Garzon D, Peduzzi J, & Rebuffat S (2007) Microcins, gene-encoded antibacterial peptides from enterobacteria. *Natural product reports* 24(4):708-734.
16. Patzer SI, Baquero MR, Bravo D, Moreno F, & Hantke K (2003) The colicin G, H and X determinants encode microcins M and H47, which might utilize the catecholate siderophore receptors FepA, Cir, Fiu and IroN. *Microbiology* 149(Pt 9):2557-2570.
17. Nolan EM & Walsh CT (2008) Investigations of the MceIJ-catalyzed posttranslational modification of the microcin E492 C-terminus: linkage of ribosomal and nonribosomal peptides to form "trojan horse" antibiotics. *Biochemistry* 47(35):9289-9299.

18. Nolan EM, Fischbach MA, Koglin A, & Walsh CT (2007) Biosynthetic tailoring of microcin E492m: post-translational modification affords an antibacterial siderophore-peptide conjugate. *Journal of the American Chemical Society* 129(46):14336-14347.
19. Anonymous (2013) The antibiotic alarm. *Nature* 495(7440):141.
20. Kommineni S*, et al.* (2015) Bacteriocin production augments niche competition by enterococci in the mammalian gastrointestinal tract. *Nature* 526(7575):719-722.
21. Nedialkova LP*, et al.* (2014) Inflammation fuels colicin Ib-dependent competition of *Salmonella* serovar Typhimurium and *E. coli* in enterobacterial blooms. *PLoS Pathog* 10(1):e1003844.
22. Sassone-Corsi M & Raffatellu M (2015) No vacancy: how beneficial microbes cooperate with immunity to provide colonization resistance to pathogens. *Journal of immunology* 194(9):4081-4087.
23. Ferreira D, Seca AM, C GAD, & Silva AM (2016) Targeting human pathogenic bacteria by siderophores: A proteomics review. *Journal of proteomics*.
24. Asensio C & Perez-Diaz JC (1976) A new family of low molecular weight antibiotics from enterobacteria. *Biochemical and biophysical research communications* 69(1):7-14.
25. F. Baquero FM (1978) The microcins. *FEMS Microbiology Letters* 23(2-3):117-124.
26. Anonymous (2014) Antimicrobial resistance: global report on surveillance. *World Health Organization*.
27. Pamer EG (2016) Resurrecting the intestinal microbiota to combat antibiotic-resistant pathogens. *Science* 352(6285):535-538.
28. Valdebenito M, Crumbliss AL, Winkelmann G, & Hantke K (2006) Environmental factors influence the production of enterobactin, salmochelin, aerobactin, and yersiniabactin in *Escherichia coli* strain Nissle 1917. *International journal of medical microbiology : IJMM* 296(8):513-520.
29. Kortman GA, Raffatellu M, Swinkels DW, & Tjalsma H (2014) Nutritional iron turned inside out: intestinal stress from a gut microbial perspective. *FEMS microbiology reviews* 38(6):1202-1234.
30. Kortman GA*, et al.* (2015) Low dietary iron intake restrains the intestinal inflammatory response and pathology of enteric infection by food-borne bacterial pathogens. *European journal of immunology* 45(9):2553-2567.
31. Anonymous (1995) Subcommitee on Laboratory Animal Nutrition *Nutrient requirements of laboratory animals: fourth revised edition* National academy press Washington, DC.
32. Behnsen J, Deriu E, Sassone-Corsi M, & Raffatellu M (2013) Probiotics: properties, examples, and specific applications. *Cold Spring Harbor perspectives in medicine* 3(3):a010074.
33. Diaz-Ochoa VE, Jellbauer S, Klaus S, & Raffatellu M (2014) Transition metal ions at the crossroads of mucosal immunity and microbial pathogenesis. *Frontiers in cellular and infection microbiology* 4:2.
34. Min YW & Rhee PL (2015) The Role of Microbiota on the Gut Immunology. *Clinical therapeutics* 37(5):968-975.

35. Lecuyer E, *et al.* (2014) Segmented filamentous bacterium uses secondary and tertiary lymphoid tissues to induce gut IgA and specific T helper 17 cell responses. *Immunity* 40(4):608-620.
36. Lundell AC, *et al.* (2012) Infant B cell memory differentiation and early gut bacterial colonization. *Journal of immunology* 188(9):4315-4322.
37. Rosser EC, *et al.* (2014) Regulatory B cells are induced by gut microbiota-driven interleukin-1beta and interleukin-6 production. *Nature medicine* 20(11):1334-1339.
38. Cassat JE & Skaar EP (2013) Iron in infection and immunity. *Cell host & microbe* 13(5):509-519.
39. Rohmer L, Hocquet D, & Miller SI (2011) Are pathogenic bacteria just looking for food? Metabolism and microbial pathogenesis. *Trends in microbiology* 19(7):341-348.
40. Skaar EP & Raffatellu M (2015) Metals in infectious diseases and nutritional immunity. *Metallomics : integrated biometal science* 7(6):926-928.
41. Raffatellu M & Bäumler AJ (2010) *Salmonella*'s iron armor for battling the host and its microbiota. *Gut microbes* 1(1):70-72.
42. Weinberg ED (1975) Nutritional immunity. Host's attempt to withold iron from microbial invaders. *Jama* 231(1):39-41.
43. Ji C, Juarez-Hernandez RE, & Miller MJ (2012) Exploiting bacterial iron acquisition: siderophore conjugates. *Future medicinal chemistry* 4(3):297-313.
44. Sanchez J & Holmgren J (2011) Cholera toxin - a foe & a friend. *The Indian journal of medical research* 133:153-163.
45. Hapfelmeier S & Hardt WD (2005) A mouse model for *S*. typhimurium-induced enterocolitis. *Trends Microbiol.* 13(10):497-503.
46. Ilott NE, *et al.* (2016) Defining the microbial transcriptional response to colitis through integrated host and microbiome profiling. *The ISME journal*.
47. Crump JA, Luby SP, & Mintz ED (2004) The global burden of typhoid fever. *Bull World Health Organ* 82(5):346-353.
48. Holden VI & Bachman MA (2015) Diverging roles of bacterial siderophores during infection. *Metallomics : integrated biometal science* 7(6):986-995.
49. Johnstone TC & Nolan EM (2015) Beyond iron: non-classical biological functions of bacterial siderophores. *Dalton transactions* 44(14):6320-6339.
50. Adler C, *et al.* (2014) The alternative role of enterobactin as an oxidative stress protector allows *Escherichia coli* colony development. *PloS one* 9(1):e84734.
51. Singh V, *et al.* (2015) Interplay between enterobactin, myeloperoxidase and lipocalin 2 regulates *E. coli* survival in the inflamed gut. *Nature communications* 6:7113.
52. Holden VI, *et al.* (2014) Bacterial siderophores that evade or overwhelm lipocalin 2 induce hypoxia inducible factor 1alpha and proinflammatory cytokine secretion in cultured respiratory epithelial cells. *Infection and immunity* 82(9):3826-3836.
53. Bachman MA, *et al.* (2011) *Klebsiella pneumoniae* yersiniabactin promotes respiratory tract infection through evasion of lipocalin 2. *Infect. Immun.* 79(8):3309-3316.
54. Fischbach MA, Lin H, Liu DR, & Walsh CT (2006) How pathogenic bacteria evade mammalian sabotage in the battle for iron. *Nature chemical biology* 2(3):132-138.

55. Bolin CA & Jensen AE (1987) Passive immunization with antibodies against iron-regulated outer membrane proteins protects turkeys from *Escherichia coli* septicemia. *Infection and immunity* 55(5):1239-1242.